

Characterization of the atypical NF- $\kappa$ B-inhibitory protein I $\kappa$ B<sub>NS</sub> in  
natural killer cells and T cells

**Dissertation**

zur Erlangung des akademischen Grades

**doctor rerum naturalium (Dr. rer. nat.)**

genehmigt durch die Fakultät für Naturwissenschaften der Otto-von-  
Guericke-Universität Magdeburg

**von MRes, Konstantinos Katsoulis-Dimitriou**

geb. am 16 Juni 1989 in Athen

Gutachter:

Prof. Dr. rer. nat. Ingo Schmitz

Prof. Dr. rer. nat. Carsten Watzl

eingereicht am: 19.02.2019   verteidigt am: 08.10.2019

# Table of Contents

<b>1. Abstract</b>	<b>5</b>
<b>2. Introduction</b>	<b>7</b>
2.1 Innate and adaptive immunity	7
2.2 Natural killer cells (NK)	9
2.3 T helper cell subsets	10
2.4 Regulatory T cells (Tregs)	14
2.5 The NF- $\kappa$ B transcription pathway	14
2.6 NK cells and NF- $\kappa$ B	16
2.7 T <sub>H</sub> 1 differentiation and NF- $\kappa$ B	17
2.8 Tregs cells and NF- $\kappa$ B	17
2.9 Regulation of NF- $\kappa$ B transcription	18
2.10 The atypical NF- $\kappa$ B regulator I $\kappa$ B <sub>NS</sub>	21
2.11 The <i>Leishmania major</i> infection model	22
2.12 Aim of the thesis	23
<b>3. Materials and methods</b>	<b>25</b>
3.1 Mouse lines	25
3.2 Surgical methods and murine cell isolation	28
3.2.1 Spleen, thymus and pLNs	28
3.2.2 Ear	28
3.2.3 Bone marrow	28
3.3 Flow cytometry	29
3.3.1 Extracellular staining	29
3.3.2 Intracellular staining	29
3.3.3 iNos staining	30
3.3.4 $\beta$ -galactosidase activity	30
3.3.5 Staining for cell sorting	30
3.3.6 Measurement and sorting	31
3.4 T cell differentiations	34
3.4.1 T <sub>H</sub> 1	34
3.4.2 iTreg	35
3.5 Yac-1 Cell line	36
3.6 Natural Killer cell in vitro functional assays	36
3.6.1 Proliferation assay	36
3.6.2 Degranulation assay	37
3.6.3 Cytotoxicity assay	37
3.7 <i>Leishmania major</i> infections	37
3.7.1 Infection	37

3.7.2 Limiting dilution	37
3.7.3 Preparation of soluble <i>Leishmania major</i> antigen (SLA)	38
<b>3.8 Western blotting</b>	<b>38</b>
3.8.1 Cell lysis	38
3.8.2 Bicinchoninic Acid Assay (BCA)	38
3.8.3 Polyacrylamide gel electrophoresis	39
3.8.4 Protein transfer and visualization	39
<b>3.9 Enzyme Linked Immunosorbent Assay (ELISA)</b>	<b>41</b>
<b>3.10 Immunohistological analysis</b>	<b>42</b>
<b>3.11 PCR and agarose gel electrophoresis</b>	<b>42</b>
3.11.1 Extraction of Eucaryotic RNA or DNA	42
3.11.2 Genotyping PCR	43
3.11.3 Agarose gel electrophoresis	43
3.11.4 First strand cDNA synthesis	43
3.11.5 Quantitative real time PCR (qRT-PCR)	43
<b>3.12 RNA sequencing</b>	<b>46</b>
<b>3.13 Statistics</b>	<b>47</b>
<b>4. Results</b>	<b>48</b>
<b>4.1 The role of I<math>\kappa</math>B<sub>NS</sub> in Natural killer cells</b>	<b>48</b>
4.1.1: Screening with a novel LacZ reporter mouse for I $\kappa$ B <sub>NS</sub> expresion reveals high promoter activity in natural killer cells	48
4.1.2: I $\kappa$ B <sub>NS</sub> -deficient natural killer cells show no defect during IL-2-mediated proliferation and I $\kappa$ B <sub>NS</sub> -deficient mice do not have altered NK cell numbers	52
4.1.3: Natural killer cells from I $\kappa$ B <sub>NS</sub> -deficient mice have <i>in vitro</i> a degranulation defect compared to wild type, but do not show a cytotoxicity defect	56
4.1.4: Nfkbid <sup><math>\Delta</math>Ncr1</sup> mice show a CD4+ and CD8+ T cell inflation in the spleen at 22 weeks of age, but not high activation of those cells	59
4.1.5: Differential expression analysis of NK cells from Nfkbid <sup><math>\Delta</math>Ncr1</sup> and Nfkbid <sup>fl/fl</sup> mice, shows that I $\kappa$ B <sub>NS</sub> suppresses B cell genes and downregulates vesicle transport genes in the steady state	62
<b>4.2 The role of I<math>\kappa</math>B<sub>NS</sub> in T cells</b>	<b>64</b>
4.2.1: I $\kappa$ B <sub>NS</sub> is important for the early phase of T <sub>H</sub> 1 differentiation	64
4.2.2: Nfkbid <sup><math>\Delta</math>CD4</sup> mice have a reduced regulatory T cell compartment and show impaired T <sub>H</sub> 1 differentiation and iTreg generation <i>in vitro</i>	67
4.2.3: Nfkbid <sup><math>\Delta</math>CD4</sup> mice cope better with <i>Leishmania major</i> infection and have lower parasite numbers, compared to control mice	73
4.2.3: Nfkbid <sup><math>\Delta</math>CD4</sup> mice have reduced inflammation 18 weeks post <i>L. major</i> infection, compared to control mice	77
4.2.4: Nfkbid <sup><math>\Delta</math>CD4</sup> mice have reduced Treg percentages in the spleen and draining lymph node during <i>L. major</i> infection, but higher Treg percentages at the site of infection, compared to control mice	81
4.2.5: Nfkbid <sup><math>\Delta</math>CD4</sup> mice show signs of an earlier starting immune response to <i>L. major</i> , compared to control mice	84
4.2.6: Nfkbid <sup><math>\Delta</math>Foxp3</sup> mice have a normal regulatory T cell compartment and do not develop spontaneous autoimmunity by 8-11 weeks of age	86
<b>5. Discussion</b>	<b>95</b>
<b>5.1 I<math>\kappa</math>B<sub>NS</sub> in NK cells is responsible for maintaining T cell homeostasis</b>	<b>95</b>
<b>5.2 I<math>\kappa</math>B<sub>NS</sub> may be suppressing B cell developmental pathways in NK cells</b>	<b>97</b>

5.3 $\text{I}\kappa\text{B}_{\text{NS}}$ is necessary for the early stages of $\text{T}_{\text{H}1}$ differentiation -----	98
5.4 $\text{I}\kappa\text{B}_{\text{NS}}$ deficiency in T cells leads to better disease outcome of <i>Leishmania major</i> infection in a Treg-related manner -----	99
5.5 Differential expression analysis of naïve and effector Tregs from $\text{Nfkbid}^{\Delta\text{Foxp3}}$ mice reveals a more active cell cycle profile, but also functional deficiency -----	102
5.5 Conclusion -----	103
<b>7. Table of abbreviations -----</b>	<b>105</b>
<b>8. Bibliography -----</b>	<b>108</b>
<b>9. Declaration of originality -----</b>	<b>120</b>

## 1. Abstract

The NF- $\kappa$ B transcription pathway is extremely important for immune responses and homeostasis. Therefore, strong regulation of it is absolutely necessary. One of these regulatory mechanisms is the existence of nuclear I $\kappa$ B proteins. Although good progress has been made in elucidating their role, there is still a lot to be discovered about their function in the immune system. This is even more important, since the characteristic of nuclear I $\kappa$ Bs to act either as enhancers or suppressors of NF- $\kappa$ B, depending on the cell type, grants them the ability to fine tune the immune response. Thus, the nuclear I $\kappa$ Bs possess interest as pharmacological targets.

During this thesis, the expression of the nuclear NF- $\kappa$ B regulator I $\kappa$ B<sub>NS</sub> in several types of immune cells was measured and its role in NK, T<sub>H</sub>1 and Treg cells was investigated by the use of novel conditional deletion mouse models. I $\kappa$ B<sub>NS</sub> in NK cells, was found to be important in regulating T cell homeostasis. Also, it was found to suppress a B cell developmental pathway. In T cells, I $\kappa$ B<sub>NS</sub> was shown to be crucial for the early stages of T<sub>H</sub>1 differentiation. Also, mice where I $\kappa$ B<sub>NS</sub> was missing in T cells, were less susceptible to *Leishmania major* infection. They showed a faster and earlier immune response and had reduced numbers of regulatory T cells in the periphery. In contrast to control mice, the I $\kappa$ B<sub>NS</sub>-deficient animals were able to better eliminate *Leishmania* and prevent persistent infection. Moreover, differential-expression analysis showed that I $\kappa$ B<sub>NS</sub>-deficient effector and naive Tregs had impaired calcium signalling and an elevated WNT pathway, which would lead to impaired Treg function.

Overall, this thesis demonstrated that I $\kappa$ B<sub>NS</sub> is crucial for a number of effector cells of the immune system, such as NK cells, T<sub>H</sub>1 cells and regulatory T cells. This was confirmed in an in vivo model of *Leishmania infection* by the use of novel conditional knock out mice. The fact that I $\kappa$ B<sub>NS</sub> deletion in T cells does not cause any autoimmunity, but is beneficial in the context of *Leishmania major* infection, emphasizes the possibility that I $\kappa$ B<sub>NS</sub> is an interesting drug target.

## 1. Zusammenfassung

Der Transkriptionsfaktor NF- $\kappa$ B spielt eine wichtige Rolle bei Immunantworten und der Zellhomöostase. Deshalb ist eine strikte Regulation von NF- $\kappa$ B entscheidend. Einer dieser Regulationsmechanismen basiert auf nukleären I $\kappa$ B Proteinen. Obwohl die nukleären I $\kappa$ B Proteine schon geraume Zeit untersucht werden, ist noch vieles über deren Funktion im Immunsystem unbekannt. Da sie als Aktivator oder Suppressor in Abhängigkeit des Zelltyps wirken, regulieren sie Immunantworten sehr genau. Deswegen sind sie auch für pharmakologische Fragestellungen interessant.

Im Rahmen dieser Doktorarbeit wurde die Expression des nukleären NF- $\kappa$ B Regulators I $\kappa$ B<sub>NS</sub> in verschiedenen Immunzellen bestimmt, und dessen Rolle in natürlichen Killerzellen, Th1 Zellen und regulatorischen T-Zellen unter Nutzung von neuen konditionalen Mausmodellen analysiert. Es stellte sich heraus, dass I $\kappa$ B<sub>NS</sub> in natürlichen Killerzellen bei der Regulierung von T-Zellhomöostase entscheidend ist. Außerdem unterdrückt I $\kappa$ B<sub>NS</sub> bestimmte Transkriptionsfaktoren in natürlichen Killerzellen, die ein B-Zell-spezifisches Differenzierungsprogramm in Lymphozyten induzieren. In T-Zellen hat I $\kappa$ B<sub>NS</sub> eine wichtige Bedeutung in der frühen Phase der Th1 Differenzierung. Mäuse, bei denen I $\kappa$ B<sub>NS</sub> in T-Zellen fehlt, waren weniger anfällig für *Leishmania major* Infektionen. Sie zeigten eine schnellere und frühere Immunantwort und hatten eine reduzierte Anzahl an regulatorischen T-Zellen in der Peripherie. Im Gegensatz zu den Kontrollmäusen, waren die I $\kappa$ B<sub>NS</sub>-defizienten Tiere in der Lage, die Leishmanien zu eliminieren und eine persistierende Infektion zu verhindern. Die Mäuse RNA-Sequenzierung ergab, dass I $\kappa$ B<sub>NS</sub>-defiziente regulatorische T-Zellen einen verminderten Calcium-Signalweg und einen erhöhten WNT-Signalweg aufwiesen, was auf eine verschlechterte Funktion der regulatorischen T-Zellen hindeutet.

Somit zeigte diese Doktorarbeit, dass I $\kappa$ B<sub>NS</sub> eine wichtige Rolle für eine Anzahl von Effektor-Immunzellen wie etwa natürliche Killerzellen, Th1 Zellen und regulatorische T-Zellen spielt. Dies wurde auch im *in vivo* Modell mittels Leishmanien Infektion in konditionalen Knock-out Mäusen bestätigt. Da I $\kappa$ B<sub>NS</sub> Deletion in T-Zellen keine Autoimmunität verursachte, aber hilfreich bei der Bekämpfung von *Leishmania major* Infektionen war, kann geschlossen werden, dass I $\kappa$ B<sub>NS</sub> eine potentielle pharmakologische Zielstruktur darstellt.

## 2. Introduction

### 2.1 Innate and adaptive immunity

In a simplified view, the immune system is the sum of the cellular and humoral components and physical barriers, which aim to protect the organism from external and internal factors, such as infectious bacteria, cancer cells or toxins that can disrupt homeostasis of important systems<sup>1</sup>. Taking into account that failure of the immune system to fulfil its role can lead to incurable infections, cancer or even autoimmunity, it becomes clear that understanding its function is of utmost importance<sup>1,2</sup>. If we exclude physiological barriers that protect us from pathogen invasion, a large part of the immune system is the cell-driven immune response, which can be separated into two facets, what we call the innate and adaptive immunity<sup>1,3,4</sup>.

The innate immune response is a rapid process that aims to counter foreign pathogens as soon as they are discovered. It is thus the innate part of the immune system that reacts first to an invading pathogen or newly generated cancer cell<sup>1,3</sup>. Because the innate immune response needs to take place quickly and efficiently, the cell types involved have the ability to recognize pathogens and abnormal cells, such as cancer, without the need for antigen presentation. This is for example achieved with the recognition of pathogen-associated molecular patterns (PAMPs) such as lipopolysaccharides (LPS) and double stranded RNA<sup>5,6</sup>. This is made possible by pattern recognition receptors that can be located on the plasma membrane, like Toll-like receptors (TLRs), or the cytosol, like retinoic acid-inducible gene I-like receptors (RLRs)<sup>7</sup>. Another important role of innate immunity is to rapidly recruit immune cells to sites of infection or inflammation through the release of cytokines, such as TNF- $\alpha$ <sup>8</sup>. The main cell types that are considered as part of the innate immune system are phagocytes, such as macrophages and neutrophils, natural killer cells (NK), dendritic cells, mast cells, basophils, eosinophils, and innate lymphoid cells (ILCs)<sup>1,7,9</sup>.

Adaptive immunity is an evolutionarily later addition that is a characteristic of vertebrates. Whereas innate immunity recognizes pathogens by generic receptors that detect conserved pathogen-associated molecular patterns, adaptive immunity has cells that can elicit a response against a single antigen<sup>4,10</sup>. This extremely specific immune response is possible, because the cells of the adaptive immune system use variant recognition receptors, which

are not encoded in the germline, but are generated de novo. More specifically, cells of the adaptive immune response can recognize antigen and generate high affinity molecules that act against it. An example of this, are the variable regions of immunoglobulin (Ig) that is produced by B cells and of the T cell receptor, which are assembled from germline variable (V), diversity (D) and joining (J) segments<sup>7,11-13</sup>. Another important feature of adaptive immunity is the ability to remember antigen from previous exposure, termed immunological memory. This can manifest in the form of constant alert, by retaining circulating antibody when the antigen is not present, or in the form of a rapid, stronger response upon re-exposure<sup>14,15</sup>. The importance of immunological memory is obvious when we take into account that this is the basis upon vaccination is built. With vaccination being the only medical intervention that has so far eradicated a disease (smallpox)<sup>14,16</sup>.

Although the adaptive and innate responses were originally considered two divergent strands of immunology, we can see from the 2011 Nobel prize in physiology and medicine, awarded to Jules Hoffmann, Bruce Beutler, and Ralph Steinman, that science has acknowledged them as equally important and intertwined parts of immunity<sup>16</sup>. Evolutionarily this makes complete sense, since the adaptive part of the immune system was not manifested spontaneously but was built upon the innate part<sup>10</sup>. For example, cytokines and chemokines released by innate immune cells, such as macrophages and neutrophils, early during an infection, can recruit and activate T cells to mount adaptive immune responses<sup>7,9</sup>. Also, antigen presentation, a process mainly instigated by innate immune cells, is crucial for T-cell activation and initiation of an adaptive immune response. Arguably, the most potent antigen presenter is the dendritic cell, which is able to recognize antigen at the site of infection, for example through TLRs, migrate to the lymph node and present it to naïve T cells, as a complex with a major histocompatibility class II (MHC class II) molecule<sup>17</sup>. This, along with co-stimulation through CD80-CD86 receptors on the dendritic cell and CD28 on the T cell, leads to naïve T-cell differentiation and initiation of the adaptive immune response<sup>17-19</sup>. Moreover, in recent years, the line between innate and adaptive immunity has grown blurrier, since one of the main characteristics of adaptive immunity, immunological memory, was found in innate immune cells, such as NK cells and ILCs<sup>20,21</sup>.

## 2.2 Natural killer cells (NK)

Although being lymphocytes, natural killer cells are considered as a part of innate immunity but, in recent years, it has been shown that they have the ability to mount memory recall responses, referred to as immunological training. This underlines their importance as a cell type in the interface between innate and adaptive immunity<sup>20,22</sup>.

One of the main functions of natural killer cells is to act as the sentinels of the immune system against emerging cancer cells and newly infected cells. They can thus survey other cells and at target recognition display very potent cytotoxic abilities without the need for priming<sup>23</sup>. However, in order to showcase their full effector activity, stimulation by cytokines, either in soluble form or trans-presented for example by dendritic cells, is necessary<sup>24</sup>. This vigilance of NK cells in the steady state is possible because, instead of generating receptor diversity by DNA rearrangement, they possess a plethora of germ line encoded activating or inhibitory receptors<sup>25</sup>. Activating receptors on NK cells have more similarity to adhesion and co-stimulatory receptors in T cells. They are mostly C-type lectin receptors, such as NKG2D, SLAM family receptors, such as CD244 and immunoreceptor tyrosine-based activation motif (ITAM) bearing NK receptor complexes, such as FcεR1γ and DAP12<sup>26</sup>. On the other hand, the NK cell inhibitory receptors act mainly by recognizing main histocompatibility class I complexes (MHC class I)<sup>26</sup>.

When a mature NK cell comes into contact with a sensitive target cell, the two cells form a highly organized intercellular junction termed the immunological synapse<sup>27,28</sup>. Initiation of synapse formation is mediated by the β2-integrin LFA-1, but this alone is not sufficient to initiate cytotoxicity<sup>29</sup>. This happens because at the synapse, both activating and inhibitory receptors are recruited and interact with their target ligands. Then, the outcome of synapse formation is determined by the collective of these interactions<sup>27,28</sup>. When the signal is sufficient to induce cytotoxicity, the lytic granules, containing molecules such as perforin and granzyme B, in the NK cells converge onto the microtubule-organizing centre (MTOC), get polarized towards the synapse and with dramatic cytoskeletal rearrangements are eventually exocytosed<sup>30,31</sup>. This process leads to cell killing similarly to cytotoxic T cells<sup>32</sup>.

Despite being well known for their cytotoxic ability, NK cells are also able to relay and amplify cytokine signals, mainly secreting interferon  $\gamma$  (IFN $\gamma$ ) and tumor necrosis factor  $\alpha$  (TNF- $\alpha$ )<sup>33</sup>. This underlines their importance, since as innate immune cells, they are the earliest IFN $\gamma$  producers during infection<sup>34</sup>. It is of interest that the mechanism of cytokine secretion by NK cells appear to be independent to their cytotoxic ability, since cytokines and lytic enzymes do not share granules, and at least one secretion mechanism (mediated by the adaptor protein ADAP) can induce cytokine secretion but not cytotoxicity<sup>35,36</sup>.

NK cells are mainly produced in the bone marrow, although it has been proposed that a fraction of them develops in organs such as the liver and thymus<sup>37,38</sup>. Like all lymphocytes from the bone marrow, NK cells start from a common lymphoid progenitor (CLP), which becomes committed to the NK cell lineage, by becoming a natural killer precursor (NKP)<sup>38</sup>. In the mouse, the characteristic of the NKP is the expression of the IL-15 receptor  $\beta$  chain (CD122) and a lack of common lineage markers, including NK1.1 and DX5 (CD49b)<sup>37</sup>. In the next step, NKPs develop further into immature NK cells (iNK), which do not longer express IL-7R $\alpha$  and start expressing NK1.1<sup>37</sup>. Finally, as iNK cells start expressing CD43, CD11b, Ly49 receptors and CD49b, they become mature NK cells by acquiring competence in cytotoxicity and cytokine production<sup>39</sup>.

### **2.3 T helper cell subsets**

The identification and characterization of different T cell subsets has greatly advanced our understanding of adaptive immune responses in infection and inflammation<sup>40</sup>. Effector T helper cells are the coordinators of the immune response. They normally begin as a naïve T cell and are able to differentiate into a diverse repertoire of subsets, which by the secretion of specific cytokines can modulate tailored responses against pathogens and inflammatory processes<sup>41</sup>. They can help B cells to undergo class switching, affinity maturation and differentiation, control the recruitment and function of innate immune cells and drive perpetual cytotoxic T cell responses<sup>41</sup>.

The great variety of effector T helper cells and plasticity of naïve T cells is achieved by a similar number of subset-specific transcription factors. These act by inducing subset-specific transcriptional pathways, while simultaneously suppressing alternative cell fates<sup>42</sup>. Induction

of these transcriptional pathways is achieved by stimulation by innate immune cytokines during antigen presentation, for example by dendritic cells<sup>43</sup>. The main T helper cell subsets known to date are T<sub>H</sub>1, T<sub>H</sub>2, T<sub>H</sub>9, T<sub>H</sub>17, T<sub>H</sub>22, regulatory T cells (Tregs) and T follicular helper cells (Tfh)<sup>44</sup> (Figure 2).

A T<sub>H</sub>1 immune response is usually induced against intracellular pathogens, such as viruses or *Mycobacterium tuberculosis*, which induce the secretion of IL-12 and type I interferons from innate immune cells. This cytokine environment, in conjunction with antigen presentation, leads to the production of the transcription factor T-bet by naïve T cells<sup>45</sup>. In turn, T-bet binds to the promoter regions and regulates genes responsible for Th1 lineage commitment<sup>46</sup>. The main cytokines produced by T<sub>H</sub>1 cells are considered to be IFN $\gamma$  and TNF- $\alpha$ , which are able to further activate cells like macrophages and also induce neighbouring cells to downregulate cellular mechanism components commonly hijacked by viruses<sup>47</sup>.

On the contrary to T<sub>H</sub>1, which are generated against intracellular pathogens, T<sub>H</sub>2 cells have been associated with fighting against extracellular parasites<sup>48</sup>. T<sub>H</sub>2 cells are produced when naïve T cells are activated in the presence of IL-4 and are able to produce big amounts of IL-4, IL-5 and IL-13, which in turn activate immune cells specialized in parasite killing, such as eosinophils, mast cells and basophils<sup>49</sup>. These cytokines also stimulate B cells to produce IgE and IgA antibodies that travel to mucosal surfaces and impede future parasite establishment<sup>47</sup>. The main transcription factor of T<sub>H</sub>2 cells is GATA3<sup>50</sup>.

Another T helper subtype that deals with parasite infection are T<sub>H</sub>9 cells<sup>51,52</sup>. These are produced in the presence of IL-4 and TGF- $\beta$ , and act similarly to T<sub>H</sub>2 cells by producing IL-4 and IL-13 but additionally IL-9. This cytokine promotes CD4<sup>+</sup> and mast cell expansion and survival, but the full range of its effects has not been fully studied yet<sup>53</sup>. Because, T<sub>H</sub>9 cells have been shown to possess high plasticity, there is debate over whether they comprise a separate T cell subset<sup>54,55</sup>.

T<sub>H</sub>17 cells are produced to fight against extracellular fungi and bacteria and their differentiation is driven by TGF- $\beta$  and IL-6, under the influence of IL-23 and IL-1 $\beta$ <sup>56-58</sup>. The main transcription factor associated with this subset is ROR $\gamma$ t<sup>59</sup>. The signature cytokine of T<sub>H</sub>17 cells, IL-17, can strongly activate neutrophils and drive their recruitment to the site of infection and thus aid the clearance of bacterial and fungal infections. The importance of

T<sub>H</sub>17 cells becomes clear when we take into consideration that individuals with IL-17 defects suffer from recurring, severe bacterial and fungal infections<sup>60</sup>.

T follicular helper (T<sub>fh</sub>) cells are not generated in response to a specific type of pathogen, but their differentiation is induced by IL-21 and IL-27, which promote the production of the transcription factor Bcl-6, leading to homing to B cell follicles in secondary lymphoid organs<sup>61</sup>. Once T<sub>fh</sub> cells are located in the follicles, they produce cytokines and co-stimulatory molecules that aid high affinity antibody generation<sup>62</sup>. The importance of T<sub>fh</sub> cells is made clear, when we take into account that mice deficient in their generation cannot produce high affinity antibodies, thus becoming susceptible to a wide range of infectious agents<sup>14</sup>.

T<sub>H</sub>22 appears to be a novel human T helper cell subset, since production of IL-22 in mice seems to be restricted in T<sub>H</sub>17 cells<sup>63</sup>. Generation of T<sub>H</sub>22 cells has been reported to be IL-6 and TNF- $\alpha$  dependent and the transcription factor aryl-hydrocarbon receptor (AhR) has been associated with regulating their lineage commitment<sup>64,65</sup>. The role of IL-22 in fighting infections is foggy, since it depends on the pathogen and the type of infection, but it is reported to promote communication between the immune system and other types of cells, such as stromal cells, and numerous studies have shown that it is not implicated with fighting intracellular pathogens<sup>41</sup>.

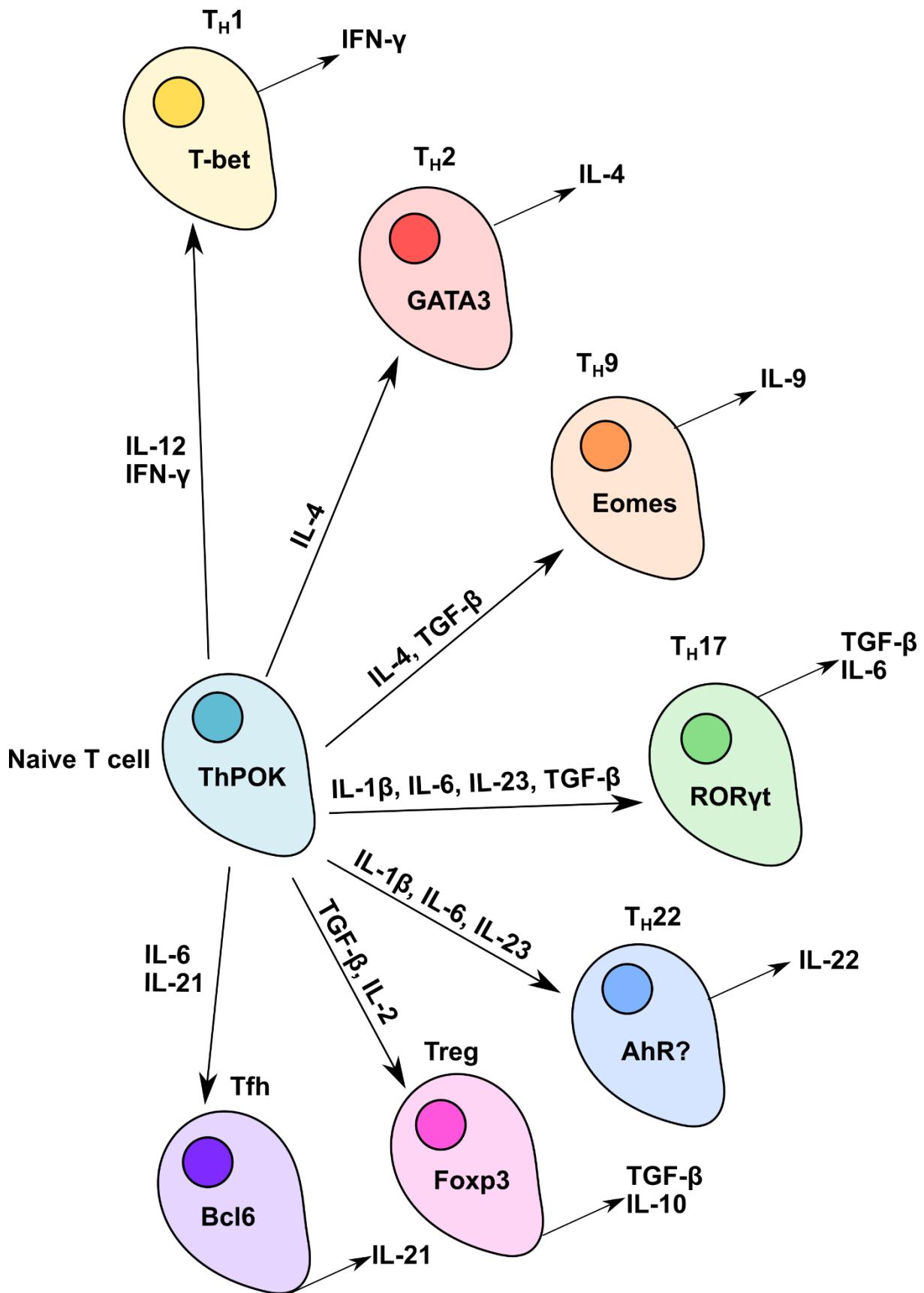


**Figure 2:** Polarizing cytokines and TCR stimulation of Naïve T cells, lead to activation of subset-specific transcription factors. These transcription factors drive the effector function of the different subsets by regulating the secretion of subset-specific cytokines. Modified from Kara et. al. 2014<sup>41</sup>.

## 2.4 Regulatory T cells (Tregs)

The immune system has the power to efficiently and quickly kill invading microorganisms and aberrant cells, but this ability can be very dangerous when it turns against healthy tissue. For this reason self-tolerance is achieved at several levels, the first being thymic selection of T cell populations, but also through several regulatory cell types in the periphery<sup>66</sup>.

The main group of regulatory T cells are ones that, in the steady state, express surface markers such as CD25 and their lineage is governed by the transcription factor Foxp3<sup>67-70</sup>. This T cell subset can be divided in thymic derived Tregs (tTregs) and peripherally induced Tregs (iTregs)<sup>71</sup>. An important characteristic of Tregs is their ability to suppress effector T cells in a TCR independent way, meaning that a regulatory T cell with one antigen specificity can suppress T cells with different antigen specificities (bystander suppression)<sup>66</sup>. The important role of regulatory T cells in immune homeostasis becomes evident when we take into account that mice and humans with Foxp3 defects develop severe autoimmune phenotypes, such as Scurfy in mice and IPEX syndrome in humans<sup>72,73</sup>.

In order to achieve their immune suppressive effects, Tregs employ a plethora of mechanisms. One of them is to block T cell activation by interfering with T cell priming, for example by using the surface molecule CTLA-4 to inhibit CD28 mediated co-stimulation of naïve T cells by APCs<sup>74</sup>. There have also been a lot of reports that Tregs can lyse immune cells by using a perforin and Granzyme B pathway, similarly to cytotoxic T cells<sup>75</sup>. Moreover, regulatory T cells are able to secrete a wide range of immune suppressive molecules, such as IL-10, TGF- $\beta$ , CTLA-4, IL-9, heme oxygenase-1 (HO-1), cAMP, galectins and IL-3<sup>66</sup>.

## 2.5 The NF- $\kappa$ B transcription pathway

The NF- $\kappa$ B transcription pathway was discovered more than 30 year ago, when Sen and Baltimore identified a nuclear factor, binding to the  $\kappa$  light-chain gene in B cells (NF- $\kappa$ B)<sup>76</sup>. Initially, because the affected gene was found in activated B cells and was induced during B cell maturation, it was thought that its function was related to B cell development. But after 30 years of research it is clear that the pathway is extremely important for biological systems in general<sup>77</sup>.

Since its discovery, NF- $\kappa$ B has played a prominent role as a model of inducible transcription factors. Thus, It has greatly contributed to our understanding of such systems and to how signaling affects gene expression and cell function<sup>78</sup>. Up to now, most of our knowledge about the pathway originates from two major fields of research, immunology and cancer biology. However, although knowledge from cancer research is rapidly expanding, historically a lot of current understanding originated from investigating the role of NF- $\kappa$ B in regulating the immune response<sup>79</sup>. It is indeed established that the NF- $\kappa$ B transcription family is controlling both the innate and adaptive immune response, as well as the development and maintenance of tissues and cells comprising the immune system<sup>79,80</sup>. Additionally, NF- $\kappa$ B regulates various pro-inflammatory genes, such as genes encoding cytokines and chemokines and genes governing innate immune cell activation, T-cell differentiation and the inflammasome<sup>79,80</sup>.

The NF- $\kappa$ B family of proteins consists of five members, RelA (p65), RelB, c-Rel, p50 and p52<sup>81</sup>. They are often referred to as Rel proteins, due to their common characteristic, which is a 300 aminoacid Rel homology domain (RHD) at their N-terminus<sup>81</sup>. This domain has three main functions, the first of which is the ability to bind DNA at a specific, nearly palindromic DNA sequence in target genes, termed a  $\kappa$ B site<sup>76,78,82</sup>. The second function of the RHD is that it grants Rel proteins the ability to form homodimers and heterodimers, which are the functional units of the pathway. Lastly, the domain contains a binding site for inhibitory proteins (see 2.6)<sup>78,81,82</sup>.

Despite having the common RHD, Rel proteins can be further subdivided according to the existence of an additional transcriptional activation domain (TAD) at the C-terminus<sup>78,82,83</sup>. This domain exists in RelA (p65), RelB and c-Rel, conferring their dimers the ability to enhance transcription of their target genes<sup>78,79,82</sup>. However, the last two proteins, p50 and p52, are generated after cleavage of their precursor forms, p105 and p100, respectively and lack the TAD. Thus they are able to drive gene transcription when paired with RelA (p65), RelB or c-Rel, but as homodimers they act as repressors<sup>78,79,81,82</sup>.

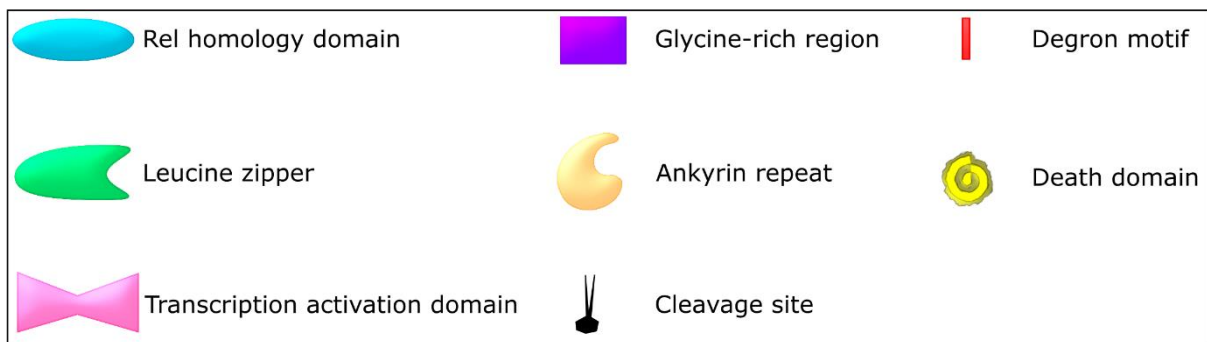
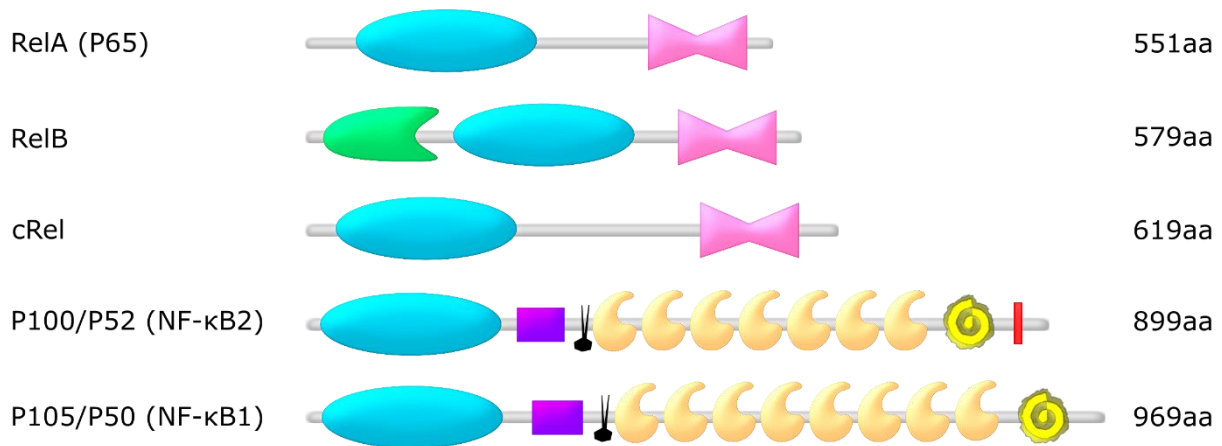


**Figure 1:** RelA (p65), RelB, c-Rel, p50 and p52 are the five Rel-homology domain (RHD) proteins that comprise the NF- $\kappa$ B transcription family. The RHD is located at the N-terminus and contains a nuclear localization signal (NLS) that allows NF- $\kappa$ B dimers to enter the nucleus. RelA (p65), RelB and c-Rel contain in their C-terminus a transcriptional activation domain (TAD), which allows them to enhance target gene transcription. p50 and p52, come from the precursor forms p105 and p100, after cleavage at a glycine-rich region between the REL and ankyrin repeat domain. The ankyrin repeat domain is a characteristic of I $\kappa$ B inhibitor proteins, which allows them to mask the NLS and restrain NF- $\kappa$ B dimers in the cytoplasm. Adapted from Hayden and Ghosh 2008<sup>81</sup>.

## 2.6 NK cells and NF- $\kappa$ B

The NF- $\kappa$ B transcription pathway plays an important role in signaling downstream of NK receptors. This becomes clear when we take into account that NK cells from patients deficient for pathway machinery, such as NF- $\kappa$ B essential modulator (NEMO) and inhibitor of  $\kappa$ B kinase  $\beta$  (IKK $\beta$ ), are defective in IFN $\gamma$  production and cytotoxicity<sup>84,85</sup>. To this date, only a few studies have taken place, usually focusing at a single ITAM activating receptor each<sup>86,87</sup>. However, since the NK cell requires so many different receptors for activation, investigating a receptor in a vacuum, may not give dependable information. This is further supported by a recent study, showing that sole engagement of NKG2D, 2B4 and DNAM-1 is not sufficient for NF- $\kappa$ B activation, but synergistic signalling of all three is necessary<sup>88</sup>.

## 2.7 T<sub>H</sub>1 differentiation and NF-κB

A general introduction into the role and characteristics of T<sub>H</sub>1 effector T cells was given in 2.3. To get into more detail in the transcriptional pathways that govern T<sub>H</sub>1 cells, their differentiation must be more thoroughly discussed.

The first signal leading a naïve CD4<sup>+</sup> T cell into differentiating to the T<sub>H</sub>1 lineage is T cell receptor stimulation by antigen presentation, as well as the induction of the transcription factor STAT1 by IFN $\gamma$ , type 1 interferons and IL-27<sup>89,90</sup>. Subsequently, STAT1 induces T-bet expression and the upregulation of the IL-12 receptor beta-2 chain, which has high affinity for IL-12, thus sensitizing the cells to this essential T<sub>H</sub>1 promoting cytokine<sup>91,92</sup>. In turn, IL-12 signalling leads to production of the transcription factor STAT4, which in conjunction with T-bet activates the *Ifng* gene, leading to an autoregulatory feedback loop that further promotes T<sub>H</sub>1 differentiation via STAT1<sup>46,93</sup>. IL-2 signalling has also been shown to be important for this process<sup>94</sup>.

NF-κB signaling has been found to be induced downstream of TCR stimulation, showing its importance from the first stages of T helper differentiation<sup>95</sup>. It is therefore important for T<sub>H</sub>1 differentiation. This is also supported by the fact that when the pathway is blocked in mice, T<sub>H</sub>1 responses are strongly dampened<sup>96</sup>. Nevertheless, not all NF-κB members affect T<sub>H</sub>1 polarization in the same way, showing that NF-κB regulates T<sub>H</sub>1 in multiple levels. For example although both c-Rel-deficient mice and RelB deficient T cells show a defect in T<sub>H</sub>1 responses and IFN $\gamma$  production, only RelB achieves this by reducing expression of the master transcription factor T-bet<sup>97,98</sup>. Also RelA has been shown to bind to highly conserved non-coding sequences (CNS) of the *Ifng* gene and in the case of RelA deficiency IFN $\gamma$  production is greatly impaired<sup>99</sup>.

## 2.8 Tregs cells and NF-κB

The NF-κB member c-Rel has been implicated with Treg development through its ability to transactivate the *Foxp3* gene. Deficiency of c-Rel causes impairment in tTreg generation and

studies report that its action has to do with binding and demethylating CNS2 of the Foxp3 locus, binding to the promoter and forming a c-Rel-enhansosome, and binding to the CNS3 and inducing Foxp3 via acting downstream of TCR signalling<sup>100-103</sup>. It has also been shown that constant NF- $\kappa$ B activation, through the NF- $\kappa$ B inducing kinase (NIK), specifically in Foxp3<sup>+</sup> cells in mice, leads to Tregs losing suppressing function and an autoimmune phenotype, which underlines the importance of NF- $\kappa$ B for Treg homeostasis<sup>104</sup>. Moreover, it has been reported that p65 and c-Rel are crucial for Treg cell development, suppressive function and molecular identity and that NF- $\kappa$ B/RelA in conjunction with TNFRSF is required for the differentiation and maintenance of effector Tregs<sup>105,106</sup>.

## 2.9 Regulation of NF- $\kappa$ B transcription

As was described through this introduction, the NF- $\kappa$ B transcription pathway is extremely important for Immune responses and homeostasis. But although NF- $\kappa$ B dimers are able to regulate themselves through the existence of the TAD, more layers of regulation are in place (see 2.5)<sup>78</sup>.

A second layer of regulation is the existence of the cytoplasmic I $\kappa$ B proteins, namely I $\kappa$ B $\alpha$ , I $\kappa$ B $\beta$ , I $\kappa$ B $\epsilon$ , p100 and p105 (Figure 4). These proteins act as inhibitors of NF- $\kappa$ B signalling, by masking the nuclear localisation signal on the Rel homology domain of NF- $\kappa$ B dimers and thus, restraining the dimers in the cytoplasm<sup>78</sup>. When an activation signal arrives, for example TNF-receptor signalling, TLR engagement or TCR stimulation, cytoplasmic I $\kappa$ Bs, are phosphorylated by the I $\kappa$ B kinase complex, consisting of IKK $\alpha$ , IKK $\beta$  and NEMO (IKK $\gamma$ ). A process that leads to their polyubiquitinylation and proteasomal degradation<sup>81</sup>. Then, the NF- $\kappa$ B dimers are free to translocate into the nucleus and interact with  $\kappa$ B sites on the DNA (Figure 3). The characteristic domain of all I $\kappa$ B proteins is the ankyrin repeat domain (ARD), composed of 6 to 8 ankyrin repeats (ANK). This domain gives them the ability to bind and mask the NLS on the RHD<sup>79</sup>.

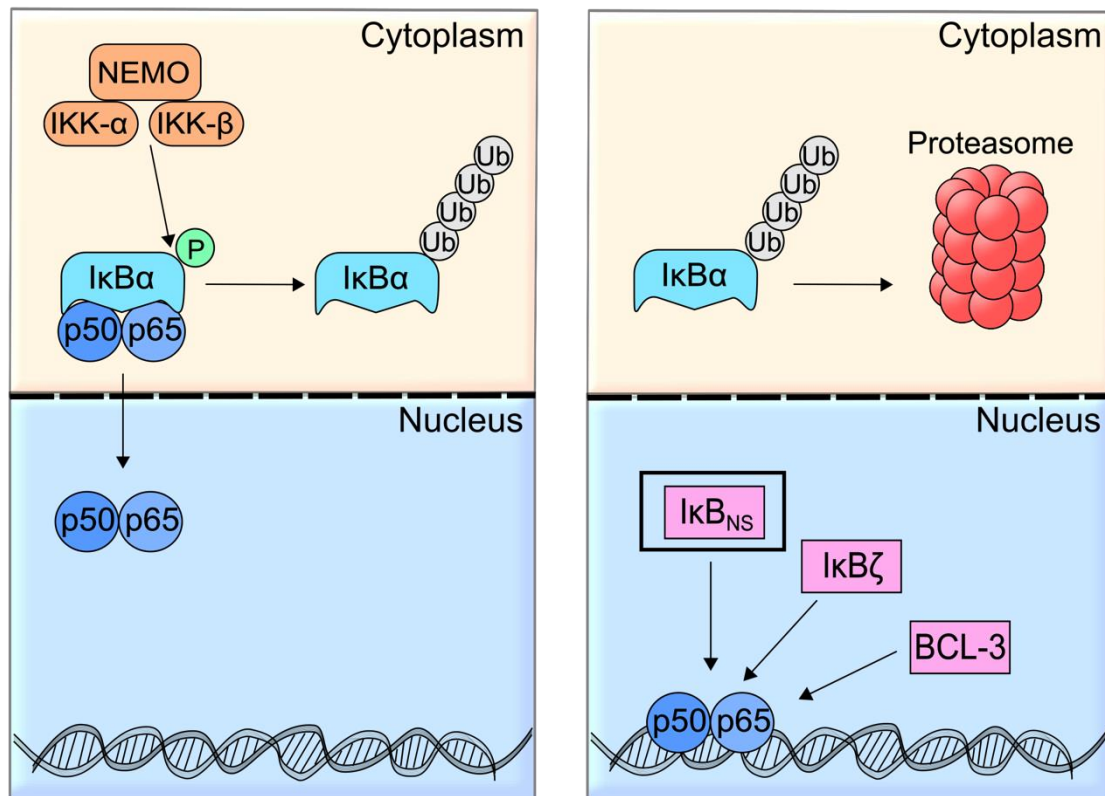


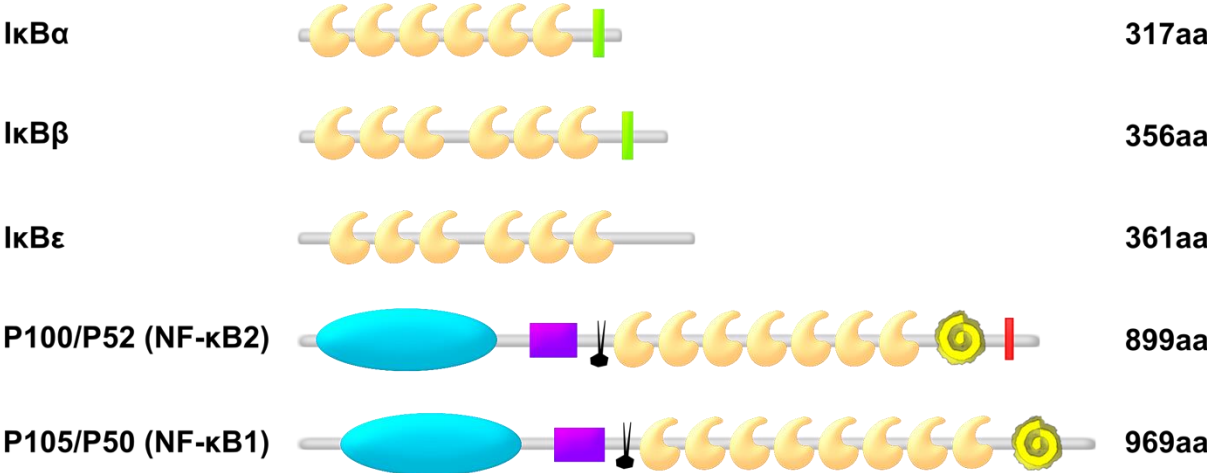
**Figure 3:** Graphical representation of the canonical regulation of the NF- $\kappa$ B pathway. The common signalling event in NF- $\kappa$ B induction is the activation of the I $\kappa$ B kinase complex, which consists of IKK $\alpha$ , IKK $\beta$  and NEMO (IKK $\gamma$ ). When an NF- $\kappa$ B activation signal arrives, for example TNF-receptor signalling, TLR engagement or TCR stimulation, cytoplasmic I $\kappa$ Bs (such as I $\kappa$ B $\alpha$ ) are phosphorylated by the I $\kappa$ B kinase complex and marked for proteasomal degradation. Subsequently the transcription factor, here indicated as a p50/p65 heterodimer, is free to translocate into the nucleus and interact with  $\kappa$ B sites on the DNA (left panel). Once in the nucleus, NF- $\kappa$ B can be targeted by atypical I $\kappa$ B proteins such as Bcl-3, I $\kappa$ B $\zeta$  and I $\kappa$ B $_{NS}$ . (right panel). Modified from Annemann et. al. 2016<sup>107</sup>

Although the mechanism described above is common for all cytoplasmic I $\kappa$ B proteins and is termed canonical activation of the pathway, a second non-canonical way exists that involves p100 and p105<sup>108</sup>. These proteins are special in that, although they have the ankyrin repeat domain they also possess a Rel homology domain. In the non-canonical activation of the pathway, p100 and p105 are phosphorylated directly by IKK $\alpha$ , which leads to their processing to p52 and p50 respectively<sup>109</sup>.

Regardless of whether the NF- $\kappa$ B dimers enter the nucleus through canonical or non-canonical activation, another layer of regulation takes place by the nuclear or atypical I $\kappa$ B proteins. The first of these proteins to be discovered was Bcl3, followed by I $\kappa$ B $_{NS}$ , I $\kappa$ B $\zeta$  and I $\kappa$ B $\eta$  (Figure 4)<sup>107</sup>. The atypical I $\kappa$ B proteins have been reported to act by regulating dimer

exchange, stabilizing NF- $\kappa$ B dimers on the DNA and recruiting histone modifying enzymes<sup>108</sup>. Their most interesting characteristic, however, is that they do not act solely as inhibitors of NF- $\kappa$ B signalling, but can also be enhancers depending on the cell type, signalling conditions and regulated gene<sup>107,108</sup>.

**Cytoplasmic I $\kappa$ Bs**



**Nuclear I $\kappa$ Bs**



	Rel homology domain		Glycine-rich region		Degron motif
	PEST		Ankyrin repeat		Death domain
	Transcription activation domain		Cleavage site		

**Figure 2:** Graphical representation of the I $\kappa$ B proteins, subdivided into cytoplasmic and nuclear according to their localization. The typical domain of the I $\kappa$ B proteins is the ankyrin repeat domain (ARD), composed of 6 to 8 ankyrin repeats (ANK). Modified from Annemann et. al. 2016<sup>107</sup>.

## 2.10 The atypical NF- $\kappa$ B regulator I $\kappa$ B<sub>NS</sub>

I $\kappa$ B<sub>NS</sub>, which is produced by the gene *Nfkbid*, is the smallest member of the atypical I $\kappa$ B family, consisting of only 327 amino-acids<sup>110</sup>. It was first discovered in an investigation of genes that are induced during clonal selection of T cells in the thymus, and was found to bind to all members of the NF- $\kappa$ B family in vitro<sup>110</sup>. Another study has shown that I $\kappa$ B<sub>NS</sub> interacts mainly with p50 and not p65 in RAW macrophages<sup>111</sup>. Also a weak interaction with c-Rel in stimulated T cells has been reported<sup>112</sup>. I $\kappa$ B<sub>NS</sub> is an inducible molecule that acts downstream of TCR stimulation, LPS stimulation of macrophages, CD40 and IL-10 signalling<sup>111-115</sup>.

I $\kappa$ B<sub>NS</sub> is expressed in effector T cell subsets, as well as regulatory T cells<sup>112,114,116</sup>. CD4<sup>+</sup> and CD8<sup>+</sup> T cells deficient in I $\kappa$ B<sub>NS</sub> have an in vitro proliferation defect compared to wild type cells, but the addition of IL-2 or IL-7 in culture has been shown to rescue the phenotype<sup>113,114</sup>. Also, a proliferation defect has been reported in T<sub>H</sub>1 and T<sub>H</sub>17 cells during in vitro differentiation, as well as reduction in the expression of their signature cytokines, IFN $\gamma$  and IL-17 respectively<sup>112</sup>. But during two different models of induced colitis in mice, IFN $\gamma$  production was found to be increased instead<sup>112,113</sup>. Also, after *Citrobacter rodentium* infection T<sub>H</sub>17 cells were severely reduced in I $\kappa$ B<sub>NS</sub> knock out mice and IL-10, IL-17 and GM-CSF production by T<sub>H</sub>17 was significantly reduced<sup>116,117</sup>. But although direct regulation of IL-17 production by I $\kappa$ B<sub>NS</sub> was excluded<sup>117</sup>, chromatin immunoprecipitation showed binding of I $\kappa$ B<sub>NS</sub> in the *Il10* gene locus<sup>116</sup>. Moreover, in another study, I $\kappa$ B<sub>NS</sub> has been shown to regulate IL-2 expression via the NF- $\kappa$ B site in the IL-2 locus<sup>114</sup>. In the case of regulatory T cells, I $\kappa$ B<sub>NS</sub> has been found to regulate Foxp3 expression by binding with p50 and c-Rel in the CNS3 region of the gene promoter<sup>112</sup>. This leads to a 50% reduction of peripheral Tregs in I $\kappa$ B<sub>NS</sub> knockout mice, due to Tregs being retained at the precursor stage during thymic maturation<sup>112</sup>. A role for I $\kappa$ B<sub>NS</sub> in CXCR5 expression during T follicular helper cell development has also been reported, as a result of I $\kappa$ B<sub>NS</sub> binding to Bcl6<sup>118</sup>.

Besides its important role in T cells, I $\kappa$ B<sub>NS</sub> is also regulating genes in B cells and macrophages. This is made clear when we take into account that mice, which are deficient in I $\kappa$ B<sub>NS</sub>, do not form marginal zone B cells and B1 cells, and also they have impaired plasma cell

formation<sup>115,119</sup>. Moreover, these mice have problems in producing specific antibodies and make the IgG3 class switch<sup>115</sup>. Also, I $\kappa$ B<sub>NS</sub> knock out B cell proliferation was impaired upon LPS or anti-CD40 stimulation<sup>119</sup>. Furthermore, in macrophages and dendritic cells, I $\kappa$ B<sub>NS</sub> has been shown to inhibit IL-6 and IL-12 expression upon LPS-treatment and I $\kappa$ B<sub>NS</sub>-deficient mice are highly susceptible to LPS-induced endotoxic shock<sup>111,113</sup>.

## 2.11 The *Leishmania major* infection model

Normally, cutaneous leishmaniasis, caused by *Leishmania major*, happens when the sandfly vector, *Phlebotomus papatasi*, bites the host, transferring a small number of *Leishmania major* promastigotes into the skin feeding site<sup>120</sup>. This is followed by infection of the main target cell type, which is macrophages, but also neutrophils, monocytes and dendritic cells<sup>121</sup>. Inside the infected cells, *Leishmania major* promastigotes transform into the replicating form of the amastigote<sup>122</sup>. The life cycle of the parasite is complete when a sandfly bites the infected host, ingesting amastigotes in the process, which leads to more promastigote production in the gut of the fly<sup>122</sup>. In rodents and humans, a cutaneous lesion is formed at the site of infection, that heals over time leaving a small number of active parasites behind<sup>123</sup>. But in some cases, and because of other *Leishmania* species, more serious, non-healing forms of the disease can develop, such as kala-azar and diffuse cutaneous leishmaniasis<sup>121</sup>. More than 1 million cases of leishmaniasis arise world-wide each year and the outcome of the disease is of great interest to immunologists, since it depends on the type and the intensity of the immune response<sup>123</sup>.

The *Leishmania major* infection model was the first case where the relevance of the balance between T<sub>H</sub>1 and T<sub>H</sub>2 immune responses was investigated<sup>121</sup>. In the model, a T<sub>H</sub>1 response is associated with clearing the infection and a T<sub>H</sub>2 response with susceptibility. This is because IFN $\gamma$  activated macrophages are responsible for clearing the infection by producing nitric oxide<sup>123</sup>. Something seen not only in mice, where C57BL/6 have a T<sub>H</sub>1 healing phenotype and BALB/c mice a T<sub>H</sub>2 response that leads to uncontrollable systemic disease, but also in humans, where some patients, infected with *Leishmania* species, develop a healing T<sub>H</sub>1 response and some a humoral response with bad prognosis<sup>123</sup>. Although recent developments have revealed that a more complex interplay of cytokine and cell interactions

are responsible for the outcome of infection, this model remains a great tool for investigating T<sub>H</sub>1 and T<sub>H</sub>2 responses<sup>121–123</sup>.

In *Leishmania major*, regulatory T cells have been associated with parasite persistence, and seem to promote a chronic version of the disease, where a small parasite number remains in the lesion<sup>124</sup>. Induction of Tregs can make immune competent mice susceptible to infection and it can also reactivate a secondary infection, showing that Tregs are important both for the early and late stages of the infection<sup>125,126</sup>.

## 2.12 Aim of the thesis

I $\kappa$ B proteins can determine the course of immune responses via regulating the NF- $\kappa$ B pathway<sup>78</sup>. Among them are the nuclear I $\kappa$ Bs, holding the most interest as potential drug targets, due to their ability to fine tune immune responses by acting as enhancers or inhibitors of the pathway<sup>107,108</sup>. In the past years a lot of important roles have been illuminated for I $\kappa$ B<sub>NS</sub> in T cells, B cells and macrophages (see 2.8), but little is known about its function in other immune cell types. Also, all studies to date have taken place in mouse models in which I $\kappa$ B<sub>NS</sub> is deleted in all cells, making it unclear whether observed effects are direct or a result of cross-play between cell types.

Therefore, the first aim of this thesis was to use a novel reporter mouse model to investigate the expression of I $\kappa$ B<sub>NS</sub> in a range of immune cells. Then proceed to investigate the function of I $\kappa$ B<sub>NS</sub> in potentially interesting and novel targets by using conventional, as well as conditional knock out mice and modern cellular and molecular techniques. Thus, the first part of the thesis is about the role of I $\kappa$ B<sub>NS</sub> in natural killer cells.

The second aim of the thesis is to expand our understanding of the role of I $\kappa$ B<sub>NS</sub> during T<sub>H</sub>1 differentiation. It has been shown that I $\kappa$ B<sub>NS</sub> deficient T<sub>H</sub>1 cells are deficient in proliferation and IFN $\gamma$  production in vitro, and that although I $\kappa$ B<sub>NS</sub> knock out mice have a reduced regulatory T cell compartment they do not develop spontaneous autoimmunity<sup>112,116</sup>. Thus it was hypothesized that I $\kappa$ B<sub>NS</sub> plays an important role in T<sub>H</sub>1. This was investigated by using a novel inducible knock out mouse model, as well as T cell specific knock out mouse models. Moreover the in vivo relevance of I $\kappa$ B<sub>NS</sub> was investigated in a relevant T<sub>H</sub>1 infection model.

Lastly, the role of I $\kappa$ B<sub>NS</sub> in regulatory T cells was further investigated. Using, conditional knock out mice, RNA sequencing was performed in an attempt to shed light to how important I $\kappa$ B<sub>NS</sub> is for effector and naïve regulatory T cells.

### 3. Materials and methods

#### 3.1 Mouse lines

All mice were bred in specific pathogen free (SPF) conditions at the animal facility of the Helmholtz Centre for Infection Research (Braunschweig, Germany). All animal infection experiments were approved by the relevant authority of Sachsen Anhalt (Landesamt für Verbraucherschutz) and were performed in collaboration with the lab of Prof. Dr. Andreas Müller in the Otto von Guericke University of Magdeburg, at the animal facility of the University.

Nfkbid<sup>tm1a(EUCOMM)Wtsi</sup> reporter mice, here referred to as Nfkbid<sup>lacZ</sup>, were purchased from the EUCOMM consortium. Nfkbid<sup>Fl</sup> mice were generated by crossing Nfkbid<sup>lacZ</sup> with FLP recombinase expressing mice, which led to the excision of the LacZ cassette. The resulting mouse line was subsequently crossed to B6.129-Gt(ROSA)26Sor<sup>tm1(cre/ERT2)Tyj/J</sup> mice in order to create an inducible knock out mouse line<sup>127</sup>.

B6.129/SV-NFKBID<sup>(tm1Clay)</sup> mice, which will be referred to as Nfkbid<sup>-/-</sup> were kindly provided by Prof. Dr. Linda Clayton from the Harvard medical school (Boston, USA)<sup>112,114</sup>.

Tg(Ncr1-iCre)265 mice were generated by the group of Prof. Dr. Veronika Sexl from the University of Veterinary Medicine of Vienna (Austria), but were kindly provided to us by Prof. Dr. Ulrich Kalinke from the Medical University of Hannover (Germany)<sup>128</sup>. These mice were crossed to the Nfkbid<sup>Fl</sup> line in order to generate a natural killer cell specific knockout mouse. Knockout mice of this line will in this thesis be referred to as Nfkbid<sup>ΔNcr1</sup>.

B6.129(Cg)-Foxp3<sup>tm4(YFP/cre)Ayr/J</sup> mice were generated by Prof. Dr. Alexander Rudensky from the Memorial Sloan Kettering Cancer cancer center, but were kindly provided to us by Prof. Dr. Tim Sparwasser from the Medical University of Hannover (Germany)<sup>129</sup>. These mice were crossed to the Nfkbid<sup>Fl</sup> line in order to generate a Foxp3 specific knockout mouse. Knockout mice of this line will in this thesis be referred to as Nfkbid<sup>ΔFoxp3</sup>.

CD4<sup>cre</sup> mice were generated by the group of Prof. Dr. Dan Littmann at the University of California, but were kindly provided to us by Prof. Dr. Ulrich Kalinke from the Medical University of Hannover (Germany)<sup>130</sup>. These mice were crossed to the Nfkbid<sup>Fl</sup> line in order

to generate a T cell specific knockout mouse<sup>131</sup>. Knockout mice of this line will in this thesis be referred to as Nfkbid<sup>ΔCD4</sup>.

**Table 1: Commonly used buffers and solutions.**

Buffer	Company	Ingredients
<b>Cell culture</b>		
PBS	Gibco <sup>R</sup> Paisley UK	
IMDM	Gibco <sup>R</sup> Paisley UK	
RPMI 1640	Gibco <sup>R</sup> Paisley UK	
HEPES	Biochrom-Merck	
Fetal Calf Serum (FCS)	Biochrom	
Sodium-Pyruvate	Gibco <sup>R</sup> Paisley UK	
Non-essential amino acids	Gibco <sup>R</sup> Paisley UK	
β-Mercaptoethanol	Gibco <sup>R</sup> Paisley UK	
Pen/Strep	Gibco <sup>R</sup> Paisley UK	
<b>Cell lysis</b>		
TPNE Lysis buffer	Self made	1x PBS 2 mM EDTA 300mM NaCl (total) 1% Triton X-100 Added before lysis: 0.01 mM PMSF 10 ng/ml SPI 0.8 μM Na <sub>3</sub> VO <sub>4</sub>
<b>Genotyping PCR</b>		

Biopsy lysis buffer	Self made	MilliQ H <sub>2</sub> O 0.45% Nonidet P40 0.45% Tween 20 0.1% Gelatine 50 mM KCl 1.5 MgCl <sub>2</sub> * 6H <sub>2</sub> O 10 mM Tris HCl 20 mg/ml Proteinase K (Roche)
<b>Western blotting</b>		
TBS	Self made	13.7 mM NaCl 0.268 mM KCl 24.76 mM TRIS
1x Running buffer	Self made	25 mM Tris, pH 8.0 192 mM glycerol 1% SDS
1x Transfer buffer	Self made	25 mM Tris, pH 8.0 192 mM glycerol 20% methanol
5x RSB	Self made	50 mM Tris, pH6.8 50% glycerol 10% SDS 25% β-mercaptoethanol 0.25 mg/ml bromphenol blue
SPI	Self made	100 µg/ml aptinin 100 µg/ml leupeptin 100 µg/ml pepstatin A 100 µg/ml chymostatin

## **3.2 Surgical methods and murine cell isolation**

### **3.2.1 Spleen, thymus and pLNs**

Mice were culled by CO<sub>2</sub> suffocation, with utmost attention so that the least amount of stress was induced. After that, the mice were placed in the surgical area and the fur wetted with ethanol. The organs were isolated by the use of surgical scissors and forceps and mashed through a 70 µM cell strainer in a petri dish containing 2 ml of 1x PBS. The flow-through was collected in a 15 ml falcon tube and the process was repeated two more times, with addition of fresh PBS. Subsequently the cells were centrifuged at 300 g, 4 °C for 5 min in an Eppendorf centrifuge 5840R and the supernatant was discarded. Then red blood cells were lysed by incubating for 2 min at room temperature in ACK buffer (0.15 M NH<sub>4</sub>CL, 1 mM KHCO<sub>3</sub>, 0.1 mM EDTA, pH 7.3). When the incubation was over the ACK buffer was quenched by addition of 10 times the volume 1x PBS, and the centrifugation step was repeated. Then the cells were re-suspended in PBS and used for further experiments.

### **3.2.2 Ear**

For isolation of lymphocytes from the ear pinna, the ear was dissected by cutting at the base, carefully to not damage the tissue. Subsequently the two ventral sheets were torn apart by using jagged forceps and incubated for 1 h in lysis medium RPMI 1640 (GlutaMAX<sup>TM</sup>) 50 µg/mL Pen/Strep, 1 mg/ml Collagenase A (Sigma Aldrich), 0.5 mg/ml DNase I (Sigma Aldrich). After the digestion, the solution was filtered through a 70 µM cell strainer by flushing with 4 ml of 1x PBS. Then, the cells were centrifuged at 300 g, 4 °C for 10 min and the supernatant was discarded, before they were re-suspended in PBS and used for further experiments. The lymphocyte isolation from the ear pinna was performed in collaboration with the group of Prof. Dr. Andreas Müller at the Otto von Guericke University of Magdeburg.

### **3.2.3 Bone marrow**

The tibia was removed from the hind leg of mice, using surgical scissors and forceps, after which the ends were cut and the bone placed in a 500 µL Eppendorf tube with a hole at the bottom. This tube was placed in a 1.5 mL Eppendorf without a lid, containing 100µL 1x PBS. Subsequently the tubes were centrifuged at 300 g, 4 °C for 30 seconds in an Eppendorf

centrifuge 5417R and the bone marrow was re-suspended in 1 ml 1x PBS, before it was used for further experiments.

### **3.3 Flow cytometry**

For all antibodies and staining reagents used in FACS see table 2. All analysis of FACS data was performed with FlowJoV10 software.

#### **3.3.1 Extracellular staining**

Unless stated otherwise, cell staining took place in round bottom 1.4 ml matrix black tubes (Thermofisher scientific, USA). Normally, cells were washed with 500 µl PBS pH 7.4 (Gibco<sup>R</sup> Life technologies, Paisley UK) by centrifuging at 300 g, 4 °C for 5 min in an Eppendorf centrifuge 5810R, and discarding the supernatant. Then, cells were stained, where appropriate, with the LIVE/DEAD™ Fixable Blue Dead Cell Stain Kit, (Life technologies, USA) for 30 mins in the dark, according to manufacturer's instructions, after which a washing step was repeated with PBS. Then the samples were incubated with FcBlock (anti-CD16/32, BD) for 15 mins at 4 °C. Extracellular antibody staining took place for 15 mins at 4 °C in FACS buffer (2% BSA, PBS pH 7.4, 0.1% NaN<sub>3</sub>). In the case of CXCR5, the staining was performed for 20 mins at room temperature before the live dead stain.

#### **3.3.2 Intracellular staining**

For Intracellular staining, the Foxp3 staining buffer set was used, (130-093-142, Miltenyi Biotec GmbH, Bergish Gladbach, Germany). The staining was performed according to manufacturer's instructions. Cells were fixed in 1% formaldehyde for 30 mins in 4 °C, after which the cells were washed with 500 µL Fixation/Permeabilization buffer by centrifuging at 300 g, 4 °C for 5 mins. Then the cells were incubated in 100 µl of antibody working solution for another 30 mins at 4 °C in the dark. After a last wash with 500 µl Fix/Perm buffer, cells were re-suspended in Fix/Perm buffer.

### 3.3.3 iNos staining

After cells were isolated from the ear, as described in 3.2.2, they were re-suspended in 450  $\mu$ L of PBS and fixed by adding 450  $\mu$ L of 4% Formaldehyde (BD) solution and incubated for 1 h at 4 °C. Then they were centrifuged for 5 min at 900 g and 4 °C, the supernatant discarded and re-suspended in 500  $\mu$ L Perm/Wash Buffer (BD), of which 400  $\mu$ L were collected for staining. Subsequently, the cells were centrifuged again, washed twice with Perm/Wash buffer (BD) and incubated with FcBlock anti-CD16/32 (BD) for 15 mins at RT. This step is necessary for preventing unspecific staining due to Fc receptor binding. When the incubation was over, the washing step was repeated and the cell suspension was incubated with anti-NOS2 (Santa Cruz) primary antibody for 30 mins at RT. Then the washing process was repeated and the cells incubated in secondary antibody for 30 mins at RT. Lastly, a 1x wash with PBS was performed and an incubation with extracellular antibodies for 20 mins at RT followed. After a final wash with PBS the cells were taken to the flow cytometer. The iNos staining was performed by the group of Prof. Dr. Andreas Müller at the Otto von Guericke University of Magdeburg.

### 3.3.4 $\beta$ -galactosidase activity

The activity of the  $I\kappa B_{NS}$  promotor was visualized in single cells by use of the FluoReporter<sup>®</sup> *lacZ* Flow Cytometry Kit, (F-1930, Molecular Probes Inc, USA), according to manufacturer's instructions. In more detail, cells were loaded with the FDG reagent by the process of osmotic shock. For the FDG loading at least  $5 \times 10^5$  cells per sample in 100  $\mu$ L FACS staining medium (PBS, 4% v/v FCS, 10 mM HEPES, pH 7.2), as well as the FDG solution were incubated for 10 minutes at 37 °C with light stirring (400 rpm). Subsequently 100  $\mu$ L of FDG solution were added per sample, followed by an incubation of 2 mins, 37 °C. Then the loading was stopped by addition of 1.8 ml of FACS staining medium per sample, after which extracellular staining was performed (as described in 3.3.1). The entire extracellular staining procedure took place on ice. When inside the cell, FDG is cleaved by  $\beta$ -galactosidase and fluorescein (FITC) is produced. Which can be visualized by a flow-cytometer.

### 3.3.5 Staining for cell sorting

For sorting particular populations of cells from a single cell suspension, a single 15 min, 4 °C incubation in 1 ml of antibody mix per 10<sup>7</sup> total cells was performed in a 15 ml falcon tube. Then, cells were washed and re-suspended in PBS and passed through a 40 µm strainer, before the sorting took place.

### 3.3.6 Measurement and sorting

All measurements were performed either in a BD LSR-Fortessa (BD Bioscience), or a BD LSR-II (BD Bioscience) flow cytometer. Cell sorting was performed either in a BD FACS Aria (BD bioscience) or a Moflo II (Beckmann Coulter).

**Table 2: Antibodies and reagents for flow cytometry**

	Chromophore	Clone	Isotype	Company
<b>Fluorescent Assays</b>				
Annexin 5	APC	-	-	BDpharmigen
Annexin 5	FITC	-	-	Biolegend
Blue fluorescent Reactive Dye	Emmision 450nm	-	-	Life technologies
Cell Trace Violet	Emmision 450nm	-	-	Life technologies
LacZ fluorescence Staining kit (M1930)	FITC	-	-	Molecular probes
<b>Antibodies</b>				
B220	PercP Cy5.5	RA3-6B2	Rat IgG2a,κ	Biolegend
CD3	PE	500A2	Hamster IgG2, κ	BDpharmigen
CD3	FITC	145-2C11	Hamster IgG1, κ	BDpharmigen
CD3	PE-Cy7	145-2C11	Hamster IgG1, κ	eBioscience
CD4	Pacific Blue	RMA4-5	Rat IgG2a,κ	Biolegend

CD4	PercP Cy5.5	RMA4-5	Rat IgG2a,κ	Biolegend
CD4	FITC	RMA4-5	Rat IgG2a,κ	eBioscience
CD8a	APC	53-6.7	Rat IgG2a,κ	Biolegend
CD8a	PercP Cy5.5	53-6.7	Rat IgG2a,κ	Biolegend
CD8a	FITC	53-6.7	Rat IgG2a,κ	BDpharmigen
CD11b	Pacific Blue	M1/70	Rat IgG2b,κ	Biolegend
CD11b	PE	M1/70	Rat IgG2b,κ	BDpharmigen
CD11c	APC-eFluor780	N418	Hamster, IgG	eBioscience
Fc Block (CD16/CD32)	-	2.4G2	Rat, Ugg2b	BDPharmigen
CD19	PercP Cy5.5	eBio1D3	Rat IgG2a,κ	eBioscience
CD19	APC-Cy7	6D5	Rat IgG2a,κ	Biolegend
CD19	FITC	eBio1D3	Rat IgG2a,κ	eBioscience
CD25	FITC	PC61	Rat IgG1,λ	Biolegend
CD25	PercP Cy5.5	PC61.5	Rat IgG1,λ	eBioscience
CD27	APC	LG.3A10	Armenian Hamster IgG	Biolegend
CD44	PE	IM7	Rat IgG2b,κ	eBioscience
CD44	APC	IM7	Rat IgG2b,κ	Biolegend
CD44	PE-Cy7	IM7	Rat IgG2b,κ	Biolegend

CD49b	FITC	Dx5	Rat Lewis IgM, $\kappa$	BDpharmigen
CD62L	PercP-Cy5.5	MEL-14	Rat IgG2a, $\kappa$	eBioscience
CD107a (LAMP-1)	Brilliant Violet 421	1D4B	Rat IgG2a, $\kappa$	Biolegend
CD122	APC	TM- $\beta$ 1	Rat IgG2b, $\kappa$	Biolegend
CD127	PE	SB/199	Rat IgG2b, $\kappa$	BDpharmigen
CXCR5	APC	REA215	Recombinant Human IgG1	Miltenyi Biotec
F4-80	PE	BM8	Rat IgG2a, $\kappa$	Biolegend
Foxp3	Alexafluor488	FJK-16s	Rat IgG2a, $\kappa$	eBioscience
GR1	FITC	RB6-8C5	Rat IgG2b, $\kappa$	Biolegend
GITR	PE Cy7	DTA-1	Rat IgG2b, $\kappa$	eBioscience
Granzyme B	Pacific Blue	GB11	Mouse IgG1, $\kappa$	Biolegend
IFN $\gamma$	APC	XMG1.2	Rat IgG1, $\kappa$	Biolegend
IFN $\gamma$	PE	XMG1.2	Rat IgG1, $\kappa$	Biolegend
IL-10	Brilliant violet 421	JES5-16E3	Rat IgG2b, $\kappa$	Biolegend
IL-4	PE	11B11	Rat IgG1, $\kappa$	Biolegend
Ly49A	APC	A1	Mouse IgG2a, $\kappa$	Miltenyi Biotec
Ly49C/I	APC	REA253	Recombinant Human IgG1	Miltenyi Biotec
Ly49C/I	PE	REA253	Recombinant Human IgG1	Miltenyi Biotec

Ly6G	PE-Cy7	1A8	Rat IgG2a, $\kappa$	Biolegend
NK1.1	Brilliant Violet 421	PK136	Mouse IgG2a, $\kappa$	Biolegend
NK1.1	PE	PK136	Mouse IgG2a, $\kappa$	BDPharmigen
NKp46	Efluor660	29A1.4	Rat IgG2a, $\kappa$	eBioscience
NKp46	PE-Cy7	29A1.4	Rat IgG2a, $\kappa$	Biolegend
PD1	PE	J43	Armenian Hamster IgG2, $\kappa$	BDpharmigen
Perforin	FITC	eBioOMAK-D	Rat IgG2a, $\kappa$	eBioscience
Tbet	FITC	4B10	Mouse IgG1, $\kappa$	Biolegend
Ter119	FITC	TER-110	Rat IgG2b, $\kappa$	Biolegend

### 3.4 T cell differentiations

#### 3.4.1 T<sub>H</sub>1

CD4<sup>+</sup> CD62L<sup>+</sup> CD25<sup>-</sup> naïve T cells were isolated from mouse spleen and peripheral lymph nodes by cell sorting. Then T<sub>H</sub>1 differentiation was performed as described before<sup>116</sup>. In more detail, 1 x 10<sup>6</sup> naïve CD4<sup>+</sup> T cells were plated per well in a 24-well-plate in IMDM culture medium (supplemented with 10% (v/v) fetal calf serum, 50  $\mu$ g/mL Penicillin/Streptomycin, 1% (v/v) non-essential amino acids, 1 mM sodium pyruvate, 25 mM HEPES, 0.05 mM  $\beta$ -mercaptoethanol). On plating, the cells were provided with a Th1 polarizing signal (Table 3). Then, the cells were cultured for 4 and up to 6 days in 37 °C, 5% CO<sub>2</sub>, 99% humidity. On day 3, the cells were split 1:1 and new medium was added. For

measuring IFN $\gamma$  production by differentiated cells, a re-stimulation with PMA (10 ng/mL, Sigma Aldrich) and ionomycin (1  $\mu$ g/mL, Sigma Aldrich) for 4 hours was performed. 2 hours after stimulation, brefeldin A (10  $\mu$ g/mL, Sigma Aldrich) was also added. Then the cells were stained for FACS. In the case of inducible I $\kappa$ B<sub>NS</sub> deletions, 1  $\mu$ M of 4-hydroxytamoxifen was added to the culture, either on day 2 or day 4. During splitting on day 3, the Tamoxifen concentration was renewed.

### 3.4.2 iTreg

Similarly to the T<sub>H</sub>1 differentiation protocol, CD4<sup>+</sup> CD62L<sup>+</sup> CD25<sup>-</sup> naïve T cells were isolated from spleen and peripheral lymph nodes. Then, 200,000 were plated per well on a 96-well-plate in RPMI 1640 complete (10% (v/v) fetal calf serum, 50  $\mu$ g/mL Penicillin/Streptomycin, 1% (v/v) non-essential amino acids, 1 mM sodium pyruvate) medium. Upon plating the cells were provided with iTreg differentiation signal as described below (Table 3)<sup>112</sup>. After 5 days of incubation in 37 °C, 5% CO<sub>2</sub>, 99% humidity the cells were harvested and prepared for FACS. Foxp3 was used as a marker to quantify iTreg generation.

**Table 3: Signals for in vitro naive T cell differentiation**

Name	Concentration	Clone	Company
<b>Into T<sub>H</sub>1</b>			
Leaf purified anti-CD3	2 $\mu$ g/ml	145-2C11	Biologend
Leaf purified anti-CD28	2 $\mu$ g/ml	37.51	Biologend
anti-IL4	10 $\mu$ g/ml	11B11	Self-made
IL12	10 ng/ml	Recombinant	R&D Systems
<b>Into iTregs</b>			
Leaf purified anti-CD3	2 $\mu$ g/ml	145-2C11	Biologend
Leaf purified anti-CD28	2 $\mu$ g/ml	37.51	Biologend

anti-IL4	10 µg/ml	11B11	Self-made
Porcine TGF-β	(2.5, 1.5, 0.5) ng/ml	Recombinant	R&D Systems
IL2	50 ng/ml	Recombinant	R&D Systems
anti-IFNγ	10 µg/ml	XMG1.2	Self-made

### 3.5 Yac-1 Cell line

Yac-1 cells were kindly provided by the group of Prof. Dr. Lothar Jänsch at the Helmholtz Centre for Infection Research. Yac-1 is a mouse T cell lymphoma line that was produced by injection of the Moloney leukemia virus into newborn mice and can induce a response from murine NK cells, leading to lysis of the Yac-1 cells<sup>132</sup>.

### 3.6 Natural Killer cell in vitro functional assays

For all assays, NK cells were sorted by gating on CD3<sup>-</sup> CD19<sup>-</sup> NK1.1<sup>+</sup> Dx5<sup>+</sup> cells from the spleen. The culture medium used is always RPMI 1640 complete (10% (v/v) fetal calf serum, 50 µg/mL Penicillin/Streptomycin, 1% (v/v) non-essential amino acids, 1 mM sodium pyruvate, 0.05 mM β-mercaptoethanol)

#### 3.6.1 Proliferation assay

NK cells were sorted, stained with a 1:1000 dilution of Cell Trace Violet (Life Technologies) in PBS, according to manufacturer's protocol and plated at 500,000 cells per well in a 96-well-plate. Subsequently, they were stimulated with 50 ng/ml IL-2 (R&D systems) and incubated in 37 °C, 5% CO<sub>2</sub>, 99% humidity for up to 4 days. Each day, proliferation through cell trace violet was measured by flow cytometry. For this, the loss of fluorescence in the pacific blue channel was used as an indicator of proliferation<sup>133</sup>.

### **3.6.2 Degranulation assay**

NK cells were sorted and co-incubated with Yac-1 cells in a 1:1 ratio. More specifically, 200,000 NK and 200,000 Yac-1 cells were plated per well on a round bottom 96-well-plate. 5 µg/ml Monensin (Sigma Aldrich) and CD107a FACS antibody were added directly into the culture, in order to stop the CD107a epitope (Lamp-1) from rapidly internalizing. After a period of 3 hours, the cells were harvested and CD107a expression was measured by flow cytometry. Yac-1 and NK cells were separated by the use of the NK1.1 marker and a sample without Yac-1 cells was used as a negative control.

### **3.6.3 Cytotoxicity assay**

NK cells were sorted and were used right away for the resting cell assay or were incubated for 3 days with 50 ng/ml IL-2 (R&D systems) for the activated cell assay. Then, they were co-incubated with Yac-1 cells in the desired ratios, for a period of 16 hours for the resting cell assay and 5 hours for the activated cell assay. A sample treated with 10 µM staurosporin (Sigma Aldrich) was used as a positive control and a sample without NK cells as a negative control. After the co-incubation, the cells were harvested and stained with Annexin V, NK1.1 and Blue fluorescent reactive dye (table 2), for determination of Yac-1 killing by the NK cells.

## **3.7 *Leishmania major* infections**

### **3.7.1 Infection**

All infections were performed by Dr. Fu Yan from the group of Prof. Dr. Andreas Müller at the Otto von Guericke University of Magdeburg. Mice were infected with  $2 \times 10^6$  *Leishmania Major* DsRed, or Wt promastigotes. The infection was achieved by intradermal injection in the ear pinna.

### **3.7.2 Limiting dilution**

After isolation of cells from the ear, as described in 3.2.2, serial dilutions were performed in M119 medium (Sigma Aldrich) supplemented with 10% heat inactivated fetal bovine serum (FCS, Sigma Aldrich), 0.1 mM adenine (Sigma Aldrich), 1 mg/ml biotin (Sigma Aldrich), 5

mg/ml hemin (Sigma Aldrich) and 2 mg/ml biopterin (Sigma Aldrich). The limiting dilutions were performed by the group of Prof. Dr. Andreas Müller at the Otto von Guericke University of Magdeburg.

### **3.7.3 Preparation of soluble *Leishmania major* antigen (SLA)**

The soluble Leishmania antigen was kindly prepared by the group of Prof. Dr. Andreas Müller at the Otto von Guericke University of Magdeburg as has been described in the literature<sup>134</sup>. In more detail, antigen extracts were prepared from promastigote stationary phase parasite cultures. The parasites were lysed in 50 mM Tris (Carl Roth), 5 mM EDTA (Carl Roth), HCl buffer with pH 7. The lysis buffer and parasite solution was subjected to three rapid freeze-thaw cycles and three pulses of 20 seconds and 40 W at a BRANSON 1200 sonicator. Then, the sample was centrifuged at 5000 g for 20 min at 4 °C to remove debris left from the lysis. Protein concentration was determined with the BCA assay (Thermo Fisher Scientific) and aliquots were stored in the -80 °C before further use.

## **3.8 Western blotting**

### **3.8.1 Cell lysis**

For the cell lysis and protein isolation, cells were initially moved into 1.5ml Eppendorf tubes, after which they were washed once with PBS by centrifuging at 300 g, 4 °C for 5 min in an Eppendorf centrifuge 5417R, and discarding the supernatant. Then they were re-suspended in 10 µL TPNE lysis buffer per million cells, by mixing thoroughly with the pipette. Afterwards the cell suspension was incubated on ice for 25 mins, followed by centrifugation at max speed for 15 mins at 4 °C. Subsequently, the supernatants were transferred to a new tube and the pellet was discarded.

### **3.8.2 Bicinchoninic Acid Assay (BCA)**

To determine protein concentrations a Pierce™ BCA Protein Assay Kit (Thermo Fischer Scientific) was used, according to manufacturer's instructions. Absorption at 562 nm was

measured with a M200 microplate reader (TECAN) to determine protein concentration, after which the samples were incubated at 95 °C for 5 mins in 1x reducing sample buffer (RSB, Table 1).

### 3.8.3 Polyacrylamide gel electrophoresis

For protein separation, a 12% polyacrylamide gel (Table 4) was run in 1x running buffer (Table 1) at 80-100V, using the BioRad Tetra Cell machine. The protein ladder, used for determining protein size, was the PageRuler™ (Thermo Scientific).

### 3.8.4 Protein transfer and visualization

After the gel was run, protein was transferred onto a PVDF membrane (GE Healthcare) using a BioRad Criterion Blotter and 1x Transfer buffer (Table 1). Subsequently, the membrane was blocked for at least 1 h in block buffer (1xTBS, 5% milk 0.05% v/v Tween20). After the blocking step, the membrane was incubated overnight at 4 °C and with constant stirring, in blocking buffer containing primary antibody. On the next day, the membrane was washed 6 times, for 10 minutes each, with wash buffer (1xTBS, 0.05% v/v Tween20), then incubated with horse radish peroxidase (HRP) conjugated antibody in block buffer for 1 h. After that, the washing process was repeated and the membrane was developed using ECL Select™ western blotting detection reagent (GE Healthcare). The developing took place either in a Fusion FX-7 camera (Vilber Lourmat) or with Amersham Hyperfilm™ ECL (GE Healthcare).

**Table 4: 12% Polyacrylamide gel recipe**

Name	Volume for 10 ml
<b>Running gel</b>	
dH <sub>2</sub> O	3.3 ml
30% acrylamide mix (Rotiphorese <sup>R</sup> Gel 30)	4.0 ml
1.5 M Tris (pH 8.8)	2.5 ml

10% SDS	0.1 ml
10% APS	0.1 ml
TEMED (99% p.a.)	0.004 ml
<b>Stacking gel</b>	
dH <sub>2</sub> O	6.8 ml
30% acrylamide mix (Rotiphorese <sup>R</sup> Gel 30)	1.7 ml
1.0 M Tris (pH 6.8)	1.25 ml
10% SDS	0.1 ml
10% APS	0.1 ml
TEMED (99% p.a.)	0.01 ml

**Table 5: Western blot antibodies.**

Target	Species	Clone	Isotype	Company
<b>Primary antibodies</b>				
I $\kappa$ B <sub>NS</sub>	rabbit	-	Rabbit IgG	Self made
$\beta$ -actin	mouse	AC-74	IgG2a	Sigma Aldrich
$\alpha$ -tubulin	mouse	DM-1A	IgG1	Sigma Aldrich
GAPDH	mouse	-	IgG2b	Protein Tech
BCL-X	mouse	7B2.5	IgG1	Merck

Horse radish peroxidase-conjugated secondary antibodies				
Anti-rabbit IgG	goat	-	-	Dianova
Anti-mouse IgG2a	goat	-	-	Biozol
Anti-mouse IgG1	goat	-	-	Biozol
Anti-mouse IgG2b	goat	-	-	Biozol

### 3.9 Enzyme Linked Immunosorbent Assay (ELISA)

For IL-10 and IFN $\gamma$  ELISAs, the corresponding Duoset<sup>R</sup> ELISA development system kits were bought from R&D systems and the experiments performed according to manufacturer's instructions. Reagent diluent (0,1% BSA, 0.05% Tween<sup>R</sup>20 in Tris-buffered saline: 20 mM Trizma base & 150 mM NaCl, pH 7.2-7.4, 0.2  $\mu$ m filtered) blocking (1% BSA in PBS, pH 7.2-7.4, 0.2  $\mu$ m filtered), stop (2 N H<sub>2</sub>SO<sub>4</sub>) and wash (0.05% Tween<sup>R</sup>20 in PBS, pH 7.2-7.4) buffers were prepared in house and the assay run in F96 Maxisorp immunoplates (Nunc<sup>TM</sup>). For the IL-10 ELISA, the Blocking buffer is also the reagent diluent. All antibodies, standards and streptavidin HRP were included in the kit. In more detail on the procedure, the wells were initially coated with capture antibody by adding 100  $\mu$ l of antibody in reagent diluent, using the working dilution suggested by the kit, and incubating overnight at room temperature. On the next day, the wells were washed 3 times with ELISA wash buffer and were incubated with 300  $\mu$ l of blocking buffer for 2 hours at room temperature. Subsequently, the washing step was repeated, and a 2 h incubation in RT, with 100  $\mu$ l of sample and standards took place. Then, another wash was performed, followed by another 2 hour incubation with detection antibody, after which the wash was repeated and the wells were incubated for 20 minutes at room temperature with Streptavidin-HRP. After that, 100  $\mu$ l of substrate solution, consisting of 1:1 of color reagent A (H<sub>2</sub>O<sub>2</sub>, R&D Systems) and color reagent B (Tetramethylbenzidine, R&D Systems), were added in each well. After another 20 min incubation at room temperature, the color reaction was stopped with 50  $\mu$ l of stop solution and absorbance at 450 nm, with plate correction at 570 nm, was measured at an M200

microplate reader (TECAN). Standard curves and protein concentration were calculated in Microsoft Excel™.

### **3.10 Immunohistological analysis**

Immunohistological staining of Foxp3 expressing cells in the mouse ear and draining lymph nodes, during *Leishmania major* infections was performed by Dr. Marina Pils from the histology unit of the Helmholtz Centre for Infection Research (Braunschweig). In more detail, Paraffin sections were deparaffinized in xylene and rehydrated in graded ethanol series. For antigen retrieval, slides were placed in a pressure cooker in citratebuffer (pH 7.6). Endogenous Peroxidase was blocked with 3% H<sub>2</sub>O<sub>2</sub>. Subsequently, slides were blocked with ready to use blocking solution (Zytomed Systems).

Rat anti-Foxp3 monoclonal antibody (eBioscience, clone FJK-16s, order information: 14-5773-82), diluted 1:50 in antibody diluent from Zytomed Systems was used as first antibody. As secondary antibody, Goat anti-rat IgG H+L (KPL, Gaithersburg, Maryland, USA, order information: 16-16-12) was applied. Subsequently, Streptavidin-HRP-Conjugate (Zytomed Systems), 3,3' diaminobenzidine (DAB) Chromogen and substrate buffer (Zytomed Systems) were added. Counterstaining was performed with hematoxylin (Merck).

### **3. 11 PCR and agarose gel electrophoresis**

Most of the DNA isolation, genotyping PCR and agarose gel electrophoresis for genotyping was performed by our technician Sabrina Schumann.

#### **3.11.1 Extraction of Eucaryotic RNA or DNA**

To extract total RNA from eukaryotic cells, the RNeasy<sup>R</sup> Mini Kit (Qiagen) was used according to manufacturer's instructions. Then RNA concentration was measured by absorption at 260 nm with a Nanodrop 1000 spectrophotometer (peqlab). For isolation of DNA from tail biopsies and ear clippings, in order to perform genotyping PCR, the samples were incubated in 500 µl biopsy lysis buffer (table 1) at 56 °C with 800 rpm stirring, for approximately 7

hours. After that, the lysis reaction was stopped by incubating at 95 °C for 5 minutes, followed by storing of samples in 4 °C.

### **3.11.2 Genotyping PCR**

After PCR-ready DNA was isolated from tail biopsies or ear clippings, a 25 µl genotyping PCR reaction was performed according to the recipe shown on table 6. The primer sequences (Table 7) were designed in house or, in case of mouse lines provided by our collaborators, received together with the mouse line. Then, the oligos were bought in a salt free solution from Eurofins MWG Operon. The PCR reactions were run on a peqSTAR 96 Universal thermocycler (peqLab). For an example of a PCR program, see Table 8.

### **3.11.3 Agarose gel electrophoresis**

Size separation of PCR products was performed by electrophoresis of a 2% agarose gel, containing 10 µl midori green (Biozym) per 100 ml TAE buffer (40 mM Tris Base, 20 mM acetic acid, 1 mM EDTA, pH 8.5). For running the gel, the electrophoresis chamber perfectBlue™ (peqlab) and the power supply EPS 301 (Amersham Bioscience) were used. The gel was developed in the Intas gel documentation system and PCR amplicon size was determined by addition of the GeneRuler™ Low range DNA ladder (Thermo scientific).

### **3.11.4 First strand cDNA synthesis**

cDNA synthesis was performed with 100 ng of isolated total RNA by using the RevertAid™ Premium First strand cDNA Syntesis Kit (Thermo Scientific), according to manufacturer's instructions. The oligo-dT primers were used and not the random primer. After the cDNA synthesis mix was made, by following the protocol, the reaction was run in a peqSTAR 96 Universal thermocycler (peqLab).

### **3.11.5 Quantitative real time PCR (qRT-PCR)**

The cDNA produced in the previous step was normally used in 1:5 dilution for the qRT-PCR reaction. To visualize gene DNA amplification in real time the cyanine dye Sybr Green

(Roche) was used. This dye is a DNA intercalator that binds double stranded DNA and the resulting complex can be stimulated at 494 nm, to emit light that can be measured after each cycle. For the experiments in this thesis, 45 amplification cycles were run in a LightCycler 96<sup>R</sup> system (Roche), using the saved “Sybr Green amp melt” program, as provided by the manufacturer. All primers (Table 7) were designed in house, with the primer designer software that can be found on the Roche website ([https://lifescience.roche.com/en\\_de/brands/universal-probe-library.html#assay-design-center](https://lifescience.roche.com/en_de/brands/universal-probe-library.html#assay-design-center)) and were made to span introns so that amplification of genomic DNA is avoided. All qRT-PCR reactions were 20 µL.

**Table 6: Reagents for genotyping PCR**

Name	Volume	Company
DNA template	2 µL	Kapa biosystems
2x Kapa2G Fast ready mix	12.5 µL	
Forward Primer	1.25 µL	
Reverse primer	1.25 µL	
MilliQ water	at 25µL total	
		-

**Table 7: PCR Primers**

Name	Sequence
<b>Genotyping PCR</b>	
Nfkbid <sup>F1</sup>	Fwd: TCC ATG AGG TAG GGA TGG AGA GTA Rev: CTC CCA GTG CTG ATA TTA CAG GCA Rev2: TCA AAT AAT GAT GCT CTT GTC TCC

Nfkbid <sup>LacZ</sup>	Fwd: TCC ATG AGG TAG GGA TGG AGA GTA Rev: CTC CCA GTG CTG ATA TTA CAG GCA Rev1: CCT TCC TCC TAC ATA GTT GGC AGT
Foxp3 wt	Fwd: CCT AGC CCC TAG TTC CAA CC Rev: AAG GTT CCA GTG CTG TTG CT
Foxp3 Cre	Fwd: AGG ATG TGA GGG ACT ACC TCC TGT A Rev: TCC TTC ACT CTG ATT CTG GCA ATT T
CD4 Cre	Fwd: ACG ACC AAG TGA CAG CAA TG Rev: CTC GAC CAG TTT AGT TAC CC
Ncr1 Cre	Fwd: GAC CAT GAT GCT GGG TTT GGC CCA GAT G Rev: ATG CGG TGG GCT CTA TGG CTT CTG
<b>qRT-PCR</b>	
Ebf1	Fwd: CAG GAA ACC CAC GTG ACA T Rev: CCA CGT TGA CTG TGG TAG ACA
Pax5	Fwd: GAC GCT GAC AGG GAT GGT Rev: GGG GAA CCT CCA AGA ATC AT
Snx1	Fwd: GCC AAC AAG CCT GAC AAA C Rev: GTC ACC CGA GAT TCC CAC T
Rab8b	Fwd: ACG ACA AAA GAC AAG TGT CGA A Rev: TCC AAA AAT TTA ATC CCA TAG TCA A
Nfkbid	Fwd: GGG CTC TTTT CCC ATT CTC T Rev: GGA CAC AAT CCA GCC TGT CT
UBC	Fwd: AAG AGA ATC CAC AAG GAA TTG AAT G Rev: CAA CAG GAC CTG CTG AAC ACT G
IL-10	Fwd: TGC CAA GCC TTA TCG GAA ATG Rev: CCC AGG GAA TTC AAA TGC TCC
IFN $\gamma$	Fwd: ATC TGG AGG AAC TGG CAA AA Rev: TTC AAG ACT TCA AAG AGT CTG AGG TA

**Table 8: Programs for PCR**

Time	Temperature	Function	Cycles
<b>Genotyping PCR</b>			

5 min	95 °C	Initial denaturation	
30 sec	95 °C	Denaturation	
30 sec	* °C	Annealing	25-32
30 sec	72 °C	Elongation	
10 min	72 °C	Terminal elongation	-
<b>qRT-PCR</b>			
1 minute	95 °C	Preincubation	1
10 seconds	95 °C		
10 seconds	60 °C	Single acquisition	45
10 seconds	72 °C		
10 seconds	95 °C		
60 seconds	65 °C	Continuous acquisition	1
1 second	97 °C		
MilliQ water		Until 25µL total	-

\*Annealing temperature was always the average of the primers.

### 3.12 RNA sequencing

RNA isolation was performed with the RNeasy+ Mini Kit (Qiagen) according to manufacturing instructions. All other steps were performed by the GMAK facility of the Helmholtz Centre for Infection Research and bioinformatics analysis by Dr. Robert Geffers. In more detail, RNA integrity was determined by running the sample on the 2100 Bioanalyzer, (Agilent Technologies). Then, RNA sequencing libraries were generated from 500 ng total RNA by

using the Dynabeads<sup>R</sup> mRNA DIRECT<sup>TM</sup> Micro Purification Kit (Thermo Fisher) to purify the mRNA, and the ScriptSeq v2 RNA-Seq Library Preparation Kit (Epicentre), everything according to manufacturer's instructions. Subsequently, the libraries were sequenced on an Illumina HiSeq2500 using the TruSeq SBS Kit v3-HS with an average of  $6 \times 10^7$  reads per sample. FASTQC (babraham) was used to check the quality of the FASTQ files, after which Trim Galore (babraham) was used to trim sequencing adapter contamination by removing reads shorter than 20bp from the FASTQ file. Trimmed reads were aligned to the reference genome using the open source short read aligner STAR with settings according to log file<sup>135</sup>. Feature counts were determined using the R package Rsubread and data was cleaned by considering for further analysis only genes that showed counts greater than 5 at least two times across all samples. Gene annotation was done by the R package bioMart and before starting the statistical analysis, expression data was log<sub>2</sub> transformed and normalized to the 50<sup>th</sup> percentile<sup>136,137</sup>. In the end, differential gene expression analysis was calculated by the R package edgeR and clusterProfiler was used for functional analysis.

### **3.13 Statistics**

All statistics were performed with GraphPad Prism version 5.04. In the case of statistical significance, with one star is signified a p value smaller than 0.05, two stars mean a p value smaller than 0.01, three stars a p value smaller than 0.001 and four stars a p value smaller than 0.0001. The statistical method used was two tailed Mann Whitney test, unless stated otherwise in the Figure legend.

## 4. Results

### 4.1 The role of I $\kappa$ B<sub>NS</sub> in Natural killer cells

#### 4.1.1: Screening with a novel LacZ reporter mouse for I $\kappa$ B<sub>NS</sub> expression reveals high promoter activity in natural killer cells

As was discussed in chapter 2.9. a lot of studies have shed light to the role of I $\kappa$ B<sub>NS</sub> in T cells, B cells and macrophages but its role in other immune cell types remains largely unknown<sup>107</sup>. In order to identify other immune cell subsets where I $\kappa$ B<sub>NS</sub> could potentially have an important role, a newly generated reporter mouse was used. The *Nfkbid*<sup>lacZ</sup> mouse contains a LacZ cassette, which is inserted inside the I $\kappa$ B<sub>NS</sub>-encoding *Nfkbid* gene and expresses  $\beta$ -galactosidase under the control of the *Nfkbid* promoter (*Nfkbid* being the gene of I $\kappa$ B<sub>NS</sub>). *Nfkbid* promoter activity can thus be quantified through the usage of the substrate fluorescein di-d-galactopyranosidase (FDG) that is cleaved by  $\beta$ -galactosidase, leading to the release of fluorescein (FITC), which can be measured by flow cytometry.

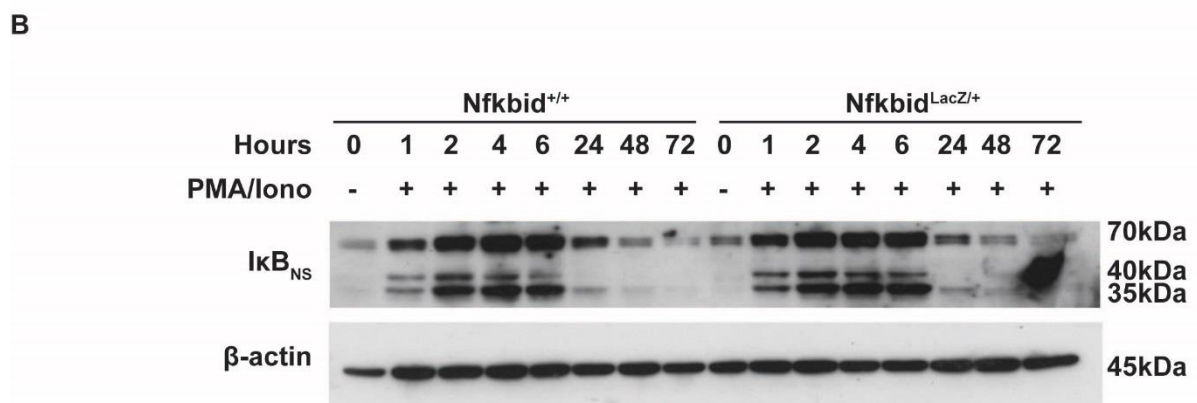
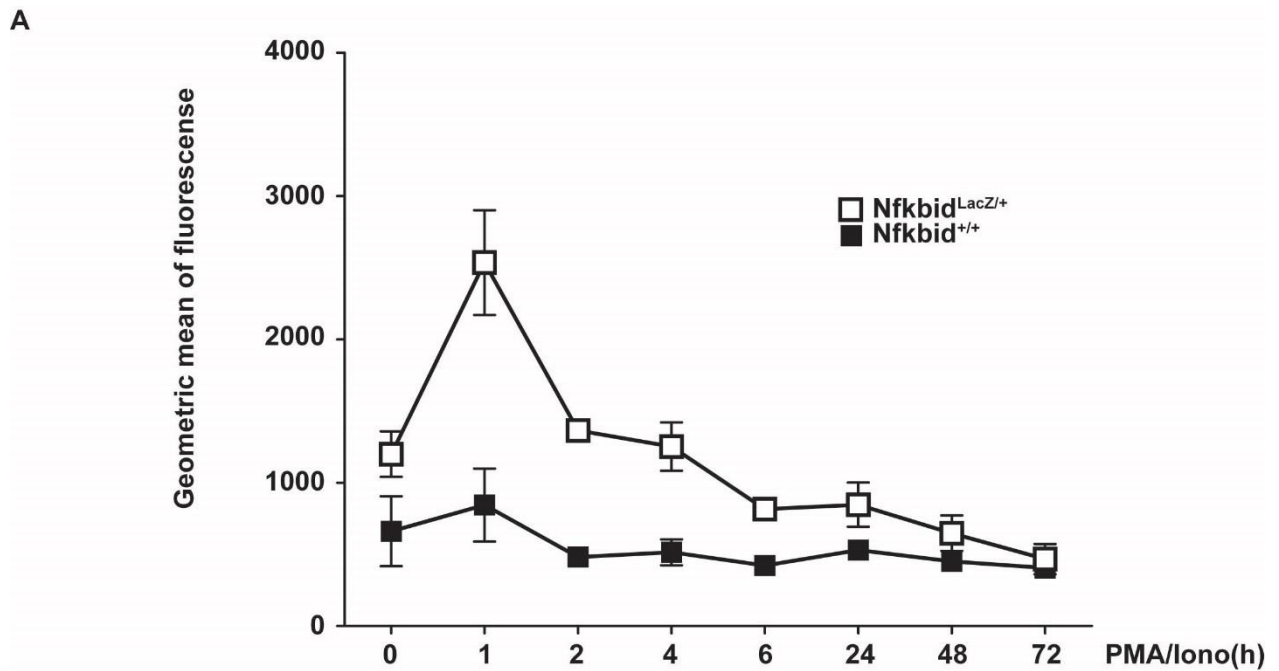


**Figure 5: IκB<sub>NS</sub> promoter activity, visualized by using Nfkbid<sup>LacZ</sup> mice, correlates with protein expression. A.** Kinetic of Nfkbid promoter activity in total lymphocytes from peripheral lymph nodes, visualized through FDG staining in flow cytometry after PMA (10μg/ml) and Ionomycin (1μM) stimulation. Two independent experiments with n=1 mouse per experiment are shown as mean ±SEM. **B.** Kinetic of IκB<sub>NS</sub> protein expression during the experiments shown in A. Of the two independent experiments performed a representative western blot is shown.

But before the new reporter mouse could be used, it was important to test whether the FITC signal in FACS correlates with protein production of IκB<sub>NS</sub>, which would show that the mouse model is a good reporter. To check if this was true, lymphocytes from Nfkbid<sup>LacZ</sup> and wild type littermates were isolated and stimulated with PMA and ionomycin for a period of 72 h (Figure 5). At each time point, some cells were used for flow cytometric analysis of Nfkbid promoter activity (Figure 5A) and some for IκB<sub>NS</sub> protein expression (Figure 5B). It was found

that *Nfkbid* promoter activity peaks 1 h after stimulation (Figure 5A), which correlates with the appearance of the inducible 35 kDa and 40 kDa bands of the I $\kappa$ B<sub>NS</sub> protein (Figure 5B). It is of note that I $\kappa$ B<sub>NS</sub> protein expression peaks at the 4 h timepoint (Figure 5B). But from these results, promoter activity, as visualized by the LacZ reporter, seems to correlate with the I $\kappa$ B<sub>NS</sub> protein.

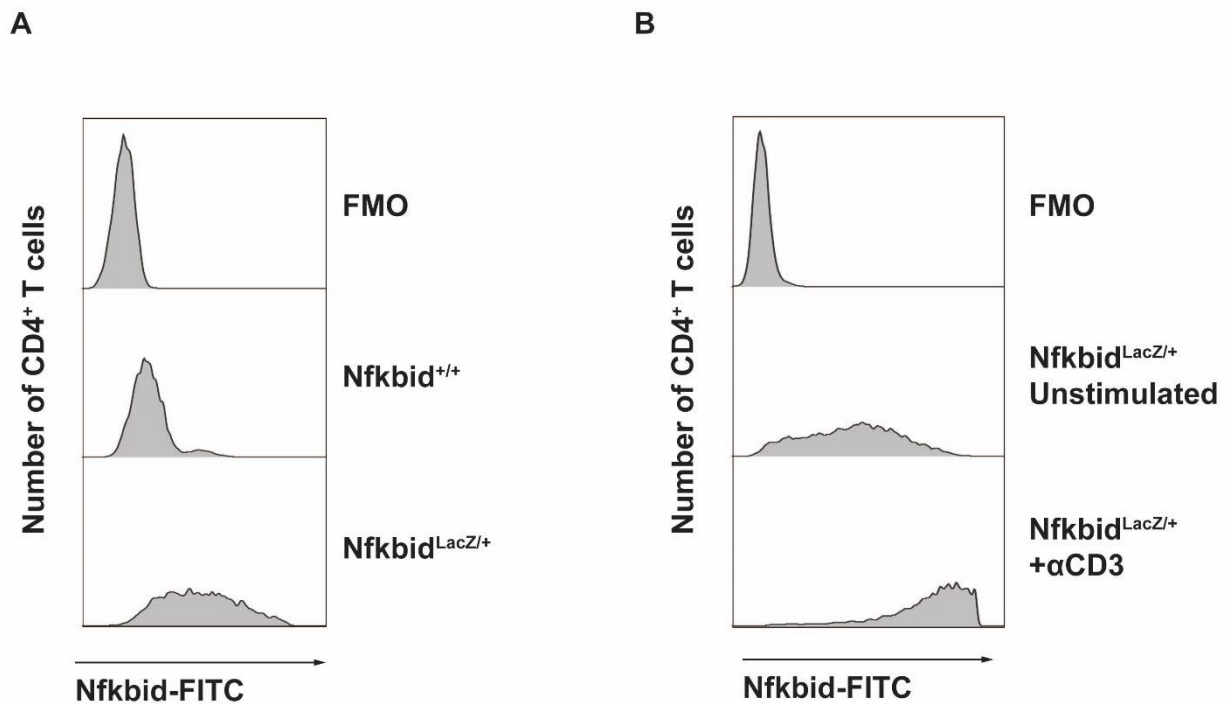


**Figure 6: Basal and induced *Nfkbid* promoter activity can be visualized in CD4<sup>+</sup> T cells by FACS using the *Nfkbid*<sup>LacZ</sup> mice. A.** Basal expression of *Nfkbid* promoter activity in CD4<sup>+</sup> T cells from peripheral lymph nodes, as visualized by flow cytometry. A representative FACS plot is shown of 2 independent experiments with n=1 mouse per experiment. **B.** Induction of *Nfkbid* promoter activity in CD4<sup>+</sup> T cells from peripheral lymph nodes, after stimulation with plate bound αCD3 (10 μg/ml), as visualized by flow cytometry. A representative FACS plot is shown of 2 independent experiments with n=1 mouse per experiment.

I $\kappa$ B<sub>NS</sub> in T cells is basally expressed in the steady state and is induced after T cell receptor stimulation<sup>107,112,114</sup>. It was therefore logical to investigate whether it would be possible to reproduce those results by using the *Nfkbid*<sup>LacZ</sup> reporter mouse. Indeed, basal *Nfkbid* promoter activity could be seen in CD4<sup>+</sup> T cells of the reporter mouse, while background from the staining was very low in the wild type control (Figure 6A). Moreover, when an *in vitro* plate-bound αCD3 stimulation took place, a clear induction of promoter activity could

be seen (Figure 6B). This further confirms that the *Nfkbid*<sup>LacZ</sup> mouse line is a good tool for visualizing *Nfkbid* activity.

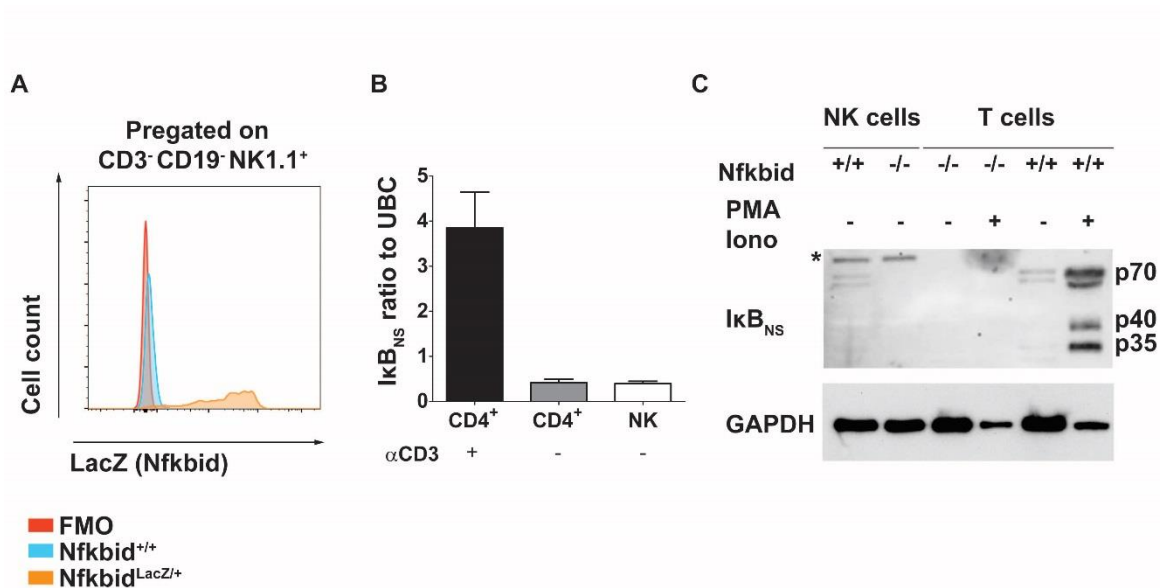


**Figure 7: *Nfkbid* promoter activity and expression in the mRNA and protein level was detected in natural killer cells.** **A.** *Nfkbid* promoter activity in steady state natural killer cells from the spleen. The graph depicted is representative of two independent experiments with n=1 mouse per experiment. **B.** Expression of *IkB<sub>NS</sub>* mRNA, relative to the housekeeping gene UBC, in FACS sorted natural killer cells, CD4<sup>+</sup> T cells and CD4<sup>+</sup> T cells stimulated with plate bound  $\alpha$ CD3 (4  $\mu$ g/ml, 3 h). The measurement method was real time qPCR. The graph shows 3 independent experiments with n=4 pooled mice per experiment as mean  $\pm$ SEM. **C.** *IkB<sub>NS</sub>* protein expression in FACS sorted NK cells and T cells from spleens of wild type and *Nfkbid*<sup>-/-</sup> mice. T cells were in steady state condition or stimulated with PMA (10  $\mu$ g/ml) and Ionomycin (1  $\mu$ M) for 3h. This western blot is representative of 3 independent experiments with n=10 pooled mice per experiment.

Since the *Nfkbid*<sup>LacZ</sup> mice were used to confirm existing literature, the next logical step was to look for basal *Nfkbid* promoter activity in immune cell subsets. After a screening, performed through FACS in immune cell populations from the mouse spleen, high promoter activity was detected in CD3<sup>-</sup> CD19<sup>-</sup> NK1.1<sup>+</sup> natural killer cells (Figure 7A). In order to confirm that this finding was translated in all levels, mRNA expression of *IkB<sub>NS</sub>* was measured, in sorted cells from wild type mice, by real time qPCR.  $\alpha$ CD3 stimulated and resting CD4<sup>+</sup> T cells were used as controls (Figure 7B). Interestingly, the ratio of *IkB<sub>NS</sub>* mRNA copies to UBC was similar in NK cells and resting CD4<sup>+</sup> T cells. Additionally, *IkB<sub>NS</sub>* protein expression was measured in NK cells from wild type mice by western. CD4<sup>+</sup> T cells were once more used as a positive control and NK cells and T cells from *Nfkbid*<sup>-/-</sup> mice were used as a negative control (Figure 7C). From this experiment it was shown that basal expression of *IkB<sub>NS</sub>* protein exists in NK cells and is expressed at similar level to resting T cells. The band marked with \* that appears only in NK

cells was considered a background band, since it was also seen in the I $\kappa$ B<sub>NS</sub> knockout NK cells (Figure 7C).

#### **4.1.2: I $\kappa$ B<sub>NS</sub>-deficient natural killer cells show no defect during IL-2-mediated proliferation and I $\kappa$ B<sub>NS</sub>-deficient mice do not have altered NK cell numbers**

I $\kappa$ B<sub>NS</sub> has been associated with T cell and plasma B cell proliferation and marginal zone B cell development<sup>114,116,138</sup>. It was therefore logical to investigate whether I $\kappa$ B<sub>NS</sub>-deficient NK cells show a defect in proliferation, compared to wild type cells. IL-2 has been shown to mediate NK cell proliferation<sup>139</sup>. Therefore an IL-2-mediated proliferation assay was used. NK cells were sorted and incubated with IL-2, then proliferation was measured through cell trace violet. No differences between I $\kappa$ B<sub>NS</sub>-deficient and wild type NK cells were found (Figure 8A). There was also no difference on day 3, which is when proliferation of NK cells first starts (Figure 8B). Therefore, there was no proliferation defect for I $\kappa$ B<sub>NS</sub>-deficient NK cells in this *in vitro* setting.

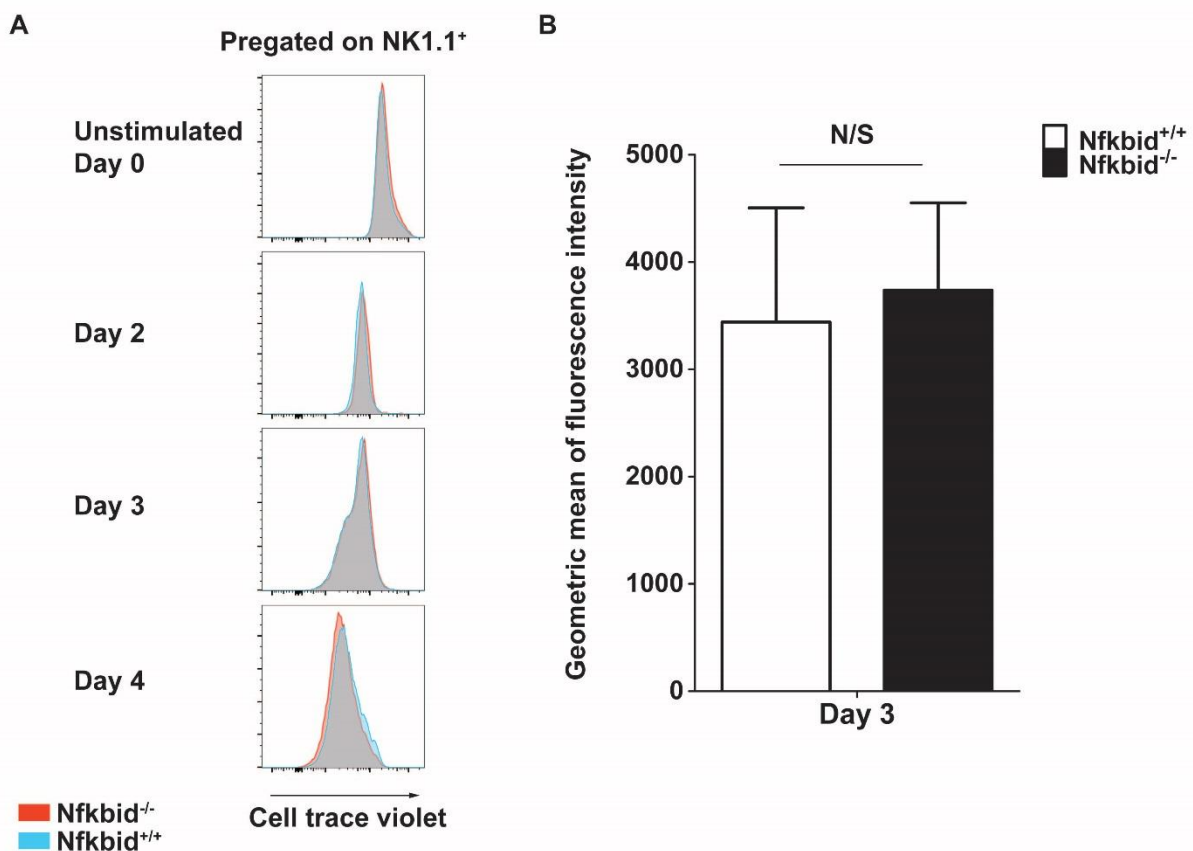


**Figure 8:  $I\kappa B_{NS}$ -deficient NK cells do not have a proliferation defect after IL-2 stimulation, compared to wild type NK cells.** **A.** Natural killer cells were FACS sorted from the spleens of *Nfkbid*<sup>-/-</sup> and wild type mice, stained with cell trace violet as a proliferation marker and stimulated with IL-2 (50 ng/ml) for a period up to 4 days. Proliferation was measured through flow cytometry. The histograms shown are representative of 3 independent experiments with n=8 pooled mice per experiment. **B.** Cumulative data on day 3 of A. The graphs shown representative of 3 independent experiments with n=8 pooled mice per experiment as mean  $\pm$ SEM.

After investigating proliferation, NK cell percentages and numbers were measured in spleen, peripheral lymph nodes and mesenteric lymph nodes of  $I\kappa B_{NS}$ -deficient mice. Percentages of CD3<sup>-</sup> CD19<sup>-</sup> NK1.1<sup>+</sup> CD49b<sup>+</sup> were not found to differ in *Nfkbid*<sup>-/-</sup> mice (Figure 9A and 9B upper panel), compared to wild type and also NK cell numbers were not altered (Figure 9B lower panel). This agrees with existing reports<sup>114</sup>.

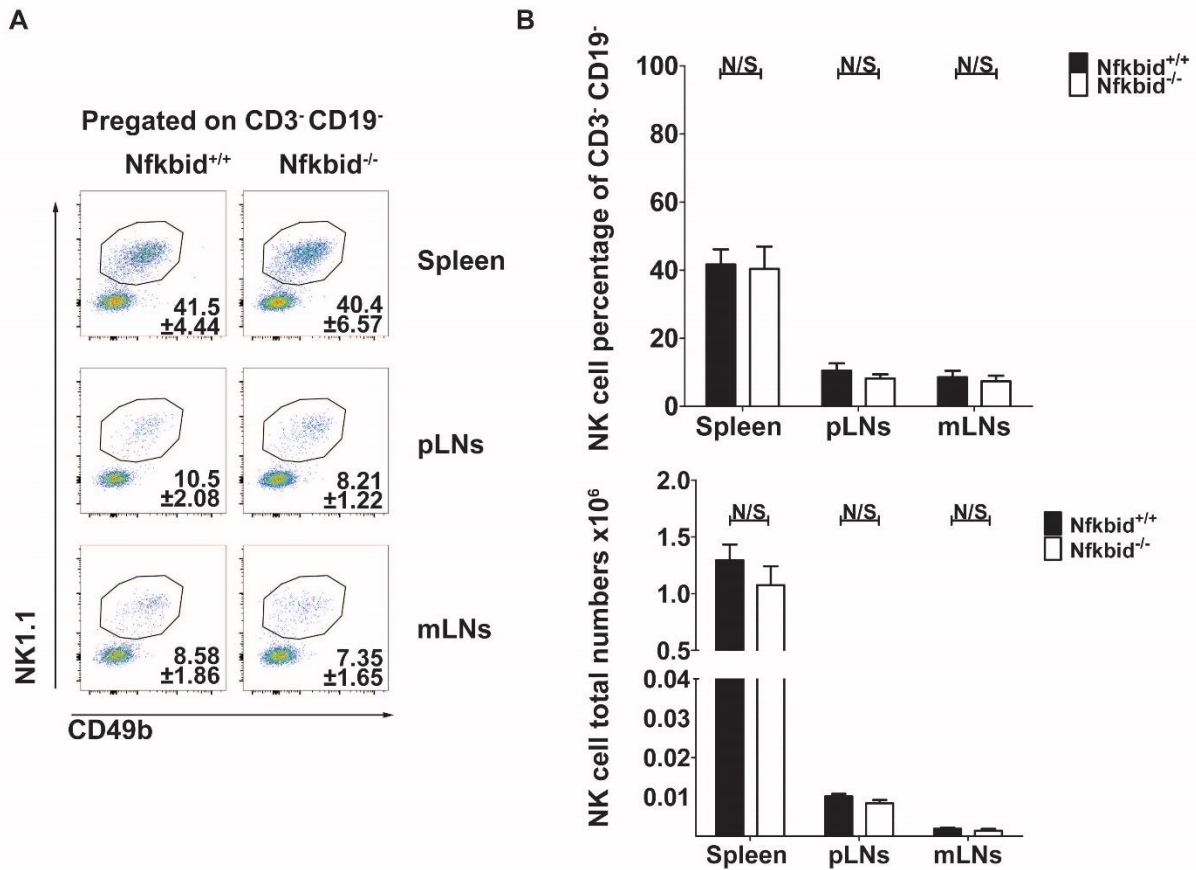


**Figure 9: Nfkbid<sup>-/-</sup> mice have similar NK cell percentages and numbers to wild type mice. A.** Representative FACS plots *ex vivo* flow cytometric analysis of NK cells in Nfkbid<sup>-/-</sup> and wild type mice. The percentages shown are median and standard error of graphs depicted on B (upper panel). The plots are representative of 5 independent experiments with n=2 Nfkbid<sup>-/-</sup> and n=2 Nfkbid<sup>+/+</sup> mice per experiment and shown as mean ±SEM. **B.** Cumulative graphs of NK cell percentages and total number of the same experiments depicted on A. The graphs are representative of 5 independent experiments with n=2 Nfkbid<sup>-/-</sup> and n=2 Nfkbid<sup>+/+</sup> mice per experiment and shown as mean ±SEM.

I $\kappa$ B<sub>NS</sub> has been implicated with Treg and marginal zone B cell development and T cell differentiation<sup>107</sup>. Therefore, it made sense to look into different NK cell development stages in the bone marrow. More specifically, the CD122<sup>+</sup> NK1.1<sup>+</sup> CD11b<sup>-</sup> Nkp46<sup>+</sup> more mature population and the CD122<sup>+</sup> NK1.1<sup>+</sup> CD11b<sup>-</sup> Nkp46<sup>-</sup> precursor cells<sup>140</sup> were measured by flow cytometry. Once again no differences were observed between I $\kappa$ B<sub>NS</sub>-deficient and wild type mice, showing that I $\kappa$ B<sub>NS</sub> is not regulating this phase of NK cell maturation.

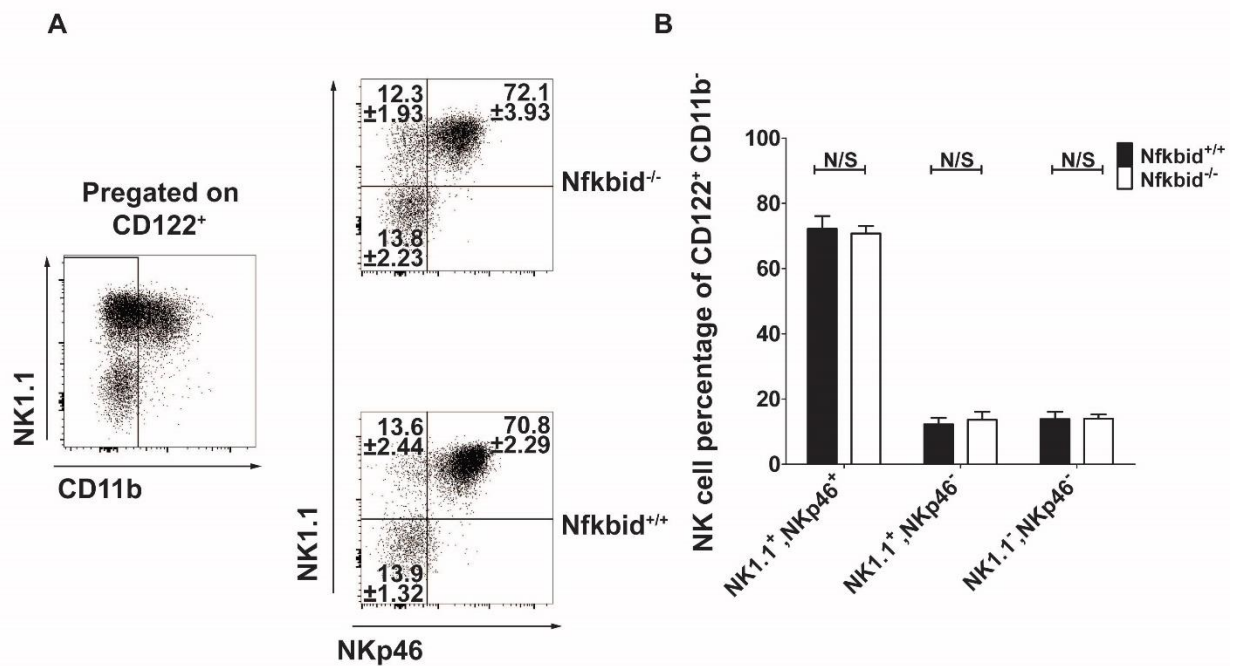


**Figure 10: Nfkbid<sup>-/-</sup> mice have similar percentages of NK cell developmental stages in the bone marrow to wild type mice.** **A.** Representative FACS plots of *ex vivo* flow cytometric analysis of NK cell developmental stages in the bone marrow in Nfkbid<sup>-/-</sup> and wild type mice. The percentages shown are mean ±SEM of graphs depicted on B. The plots are representative of 3 independent experiments with n=2 Nfkbid<sup>-/-</sup> and n=2 Nfkbid<sup>+/+</sup> mice per experiment. **B.** Cumulative graph of percentages of NK cell developmental stages of the same experiments depicted on A. The graphs are representative of 3 independent experiments with n=2 Nfkbid<sup>-/-</sup> and n=2 Nfkbid<sup>+/+</sup> mice per experiment and are shown as mean ±SEM.

#### 4.1.3: Natural killer cells from $I\kappa B_{NS}$ -deficient mice have *in vitro* a degranulation defect compared to wild type, but do not show a cytotoxicity defect

Yac-1 cells can activate NK cells through NKG2D stimulating receptors and are a sensitive target for NK cell-mediated cell lysis<sup>141</sup>. Thus, the Yac-1 cell line was used to determine whether  $I\kappa B_{NS}$ -deficient NK cells are impaired in degranulation and cytotoxicity. For the degranulation assay, the CD107a (Lamp-1) molecule was measured through FACS. This molecule is translocated to the membrane during target cell killing and it has been shown to be a good measure for degranulation and cytotoxicity<sup>142</sup>. During the experiment, co-incubation of *ex vivo* isolated NK cells with equal numbers of Yac-1 cells was able to induce CD107a, while the lack of Yac-1 lead to no induction of CD107a (Figure 11A). When  $I\kappa B_{NS}$ -deficient NK cells were compared to wild type controls, a significant reduction of CD107a on the surface of the knock out cells was observed, both in steady state and in IL-2 matured NK cells (Figure 11B). This shows that  $I\kappa B_{NS}$ -deficient NK cells have a degranulation defect.

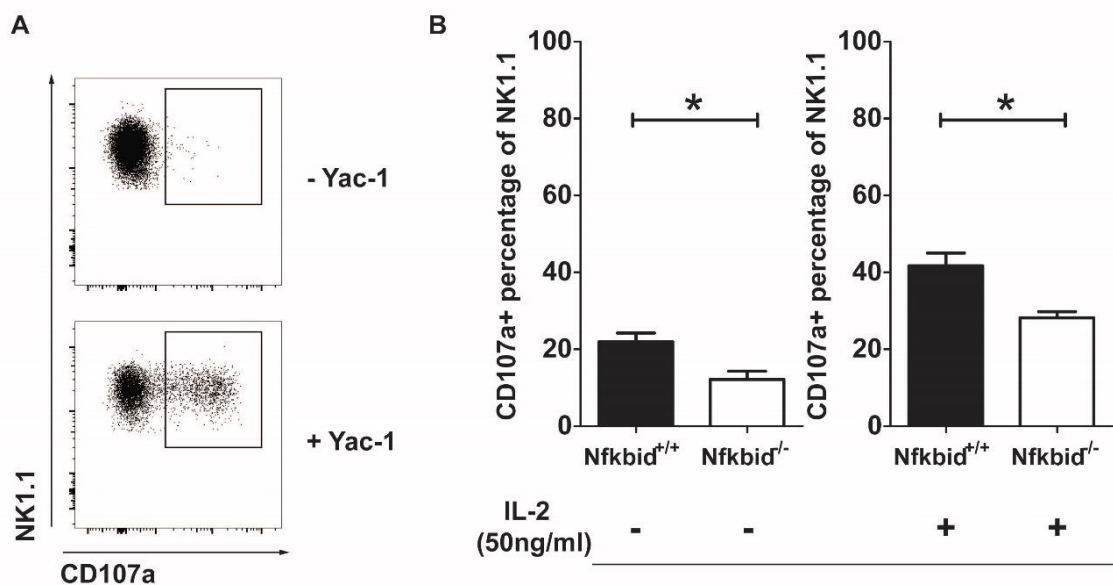


**Figure 11:  $I\kappa B_{NS}$ -deficient NK cells have a degranulation defect compared to wild type. A.** representative FACS plots of CD107a staining in NK cells in co-culture with Yac-1 target cells or in culture without Yac-1. **B.** Cumulative graphs of CD107a expression of NK cells, FACS sorted from spleens of  $Nfkbid^{-/-}$  and wild type mice, in co-culture with Yac-1 target cells. Before starting the co-culture, NK cells were in the steady state, or pre-cultured in IL-2 (50 ng/ml) for 3 days. Results are depicted as mean  $\pm$ SEM and are from 3 independent experiments with  $n=4$   $Nfkbid^{-/-}$  and  $n=4$   $Nfkbid^{+/+}$  pooled mice per experiment.

Since CD107a (Lamp-1) has been associated with autophagy and shown to have a role in lysosome biogenesis<sup>143</sup>, and autophagy has been shown to be crucial for NK cell development and memory formation<sup>20,144</sup>, it made sense to check if there is a difference at acidic granules in I $\kappa$ B<sub>NS</sub>-deficient NK cells. For this assay, lymphocytes from mouse spleens were either stimulated for 3 h with the autophagy inducer rapamycin, the autophagy suppressor bafilomycin, or not and the amount of acidic granules in the cells was measured with lysotracker deep red through flow cytometry. As expected, rapamycin treated cells had a higher than basal (non-treated) mean fluorescence in the lysotracker channel and bafilomycin treated cell had lower (Figure 12A). When I $\kappa$ B<sub>NS</sub>-deficient NK cells were compared to wild type, no significant differences were found (Figure 12B).

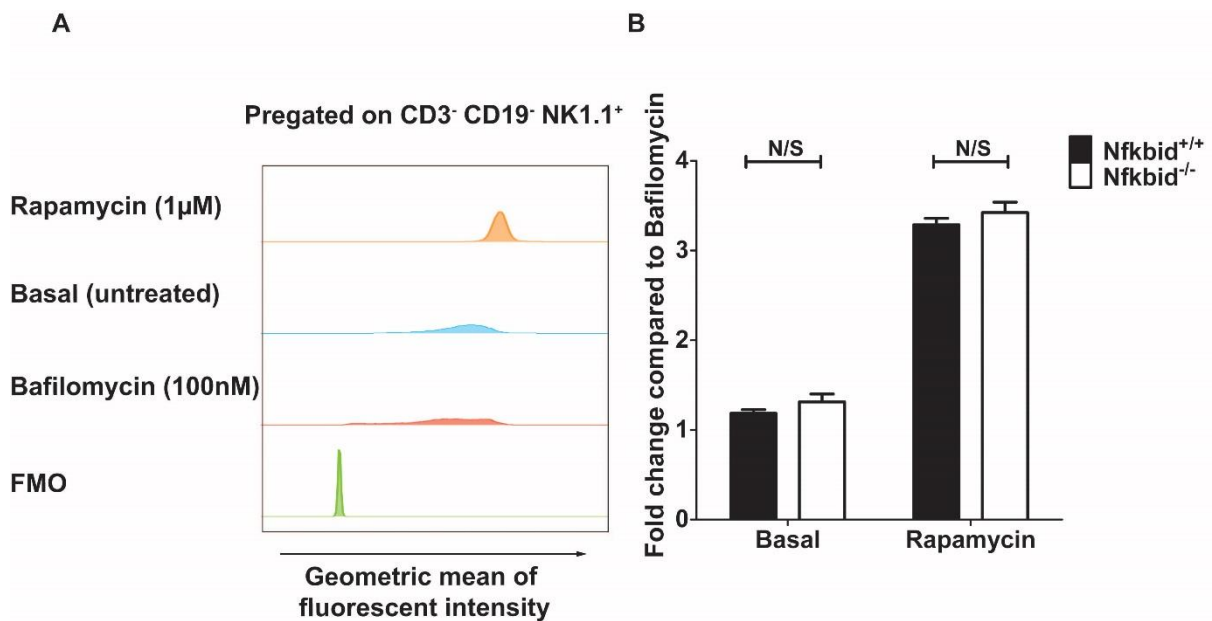


**Figure 12: I $\kappa$ B<sub>NS</sub>-deficient NK cells have a similar number of acidic granules compared to wild type.**

**A.** Representative plot of LysoTracker deep red fluorescence in NK cells from spleen of Nfkbid<sup>-/-</sup> and wild type mice, after a 3 h treatment with autophagy inducer Rapamycin (1  $\mu$ M), autophagy suppressor Bafilomycin (100 nM) or no treatment. The plot is representative of two independent experiments with n=1 mouse per experiment. **B.** Cumulative results of experiments depicted in A. The plot is shown as mean  $\pm$ SEM and is representative of two independent experiments with n=1 mouse per experiment. Results are normalized to Bafilomycin.

Since a degranulation defect was discovered in NK cells from Nfkbid<sup>-/-</sup> mice, the next step was to investigate if this was translated into a cytotoxicity defect. To achieve this, NK cells

from *Nfkbid*<sup>-/-</sup> and *Nfkbid*<sup>+/+</sup> mice were co-incubated for 16 h with Yac-1 cells at varying ratios. Subsequently, Yac-1 cell survival was measured through flow cytometry. The NK cells were either used straight away after sorting or matured for 3 days in IL-2. Regardless of whether the NK cells were steady state (Figure 13A) or IL-2 matured (Figure 13B) no significant differences were observed between *I $\kappa$ B<sub>NS</sub>*-deficient and wild type NK cells. Only a small trend of slightly lower cytotoxicity in *I $\kappa$ B<sub>NS</sub>*-deficient NK cells was seen.

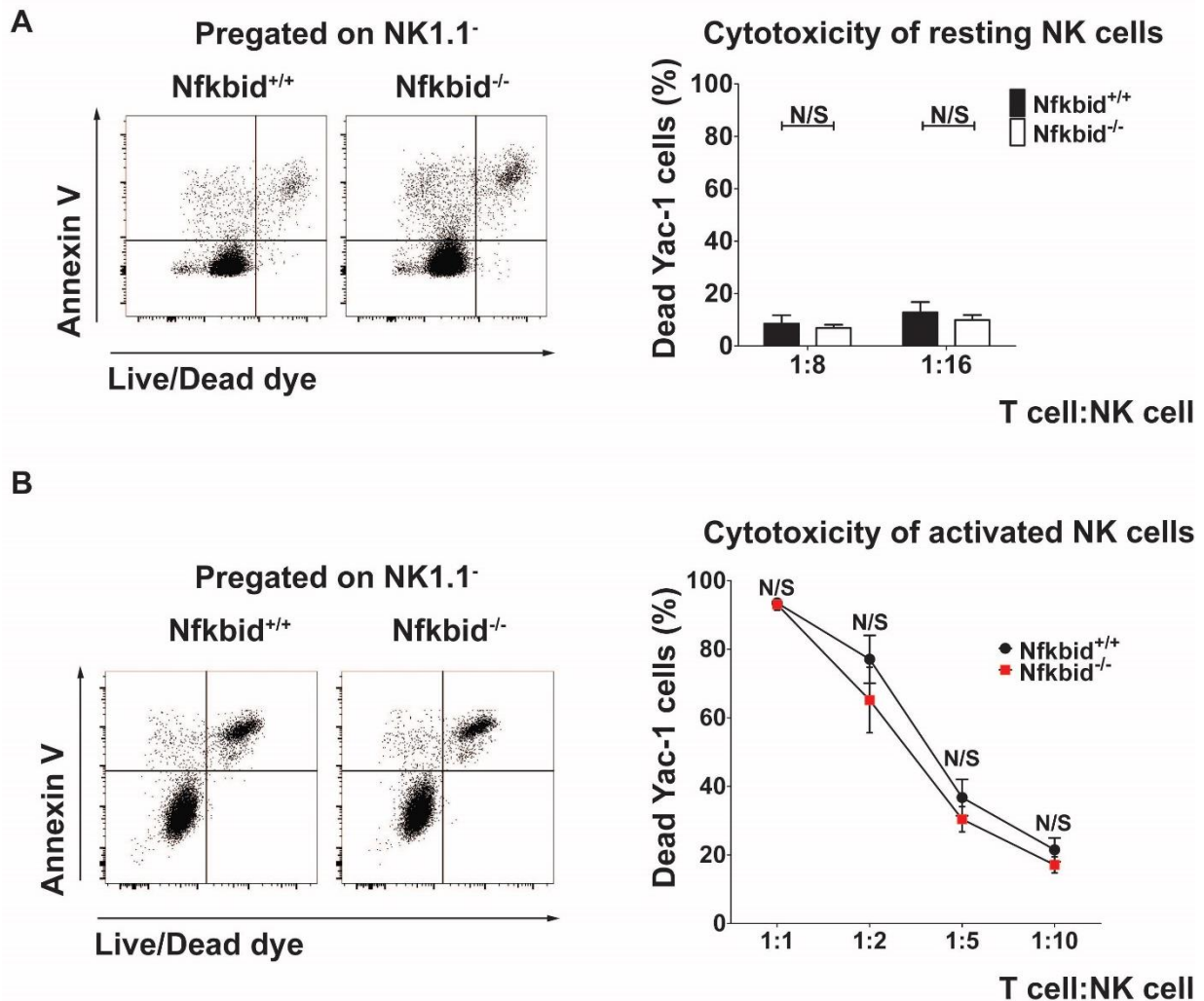


**Figure 13: *I $\kappa$ B<sub>NS</sub>*-deficient NK cells have similar to wild type cytotoxicity against Yac-1 cells.** NK cells were FACS sorted and incubated with Yac-1 cells for a period of 16 h. Then, cell death and apoptosis of Yac-1 cells was measured through flow cytometry. NK cells were either directly co-cultured with Yac-1 cells or pre-cultured with IL-2 (50 ng/ml) for 3 days. **A.** Representative graph of FACS plots (left panel) and cumulative results of Yac-1 cell death (right panel). These experiments were performed with non-activated NK cells. Results are shown as mean  $\pm$ SEM come from 3 independent experiments with n=4 *Nfkbid*<sup>-/-</sup> and n=4 *Nfkbid*<sup>+/+</sup> pooled mice per experiment. **B.** Representative graph of FACS plots (left panel) and cumulative results of Yac-1 cell death (right panel). These experiments were performed with activated NK cells. Results are shown as mean  $\pm$ SEM come from 3 independent experiments with n=4 *Nfkbid*<sup>-/-</sup> and n=4 *Nfkbid*<sup>+/+</sup> pooled mice per experiment.

#### **4.1.4: Nfkbid<sup>ΔNcr1</sup> mice show a CD4+ and CD8+ T cell inflation in the spleen at 22 weeks of age, but not high activation of those cells**

In order to investigate the role of IκB<sub>NS</sub> selectively in NK cells, an NK cell-specific knock out mouse was generated by use of the Cre-loxp system<sup>128</sup>. This was achieved by crossing Nfkbid<sup>fl/fl</sup> mice with Ncr1<sup>Cre</sup> mice. Nfkbid<sup>ΔNcr1</sup> mice were firstly characterized by FACS for irregularities in immune cells in lymphoid organs and, similarly to Nfkbid<sup>-/-</sup> mice, for NK cell maturation stages in the bone marrow. Once again, no differences were detected between Nfkbid<sup>ΔNcr1</sup> and Nfkbid<sup>fl/fl</sup> control mice (Figure 14).

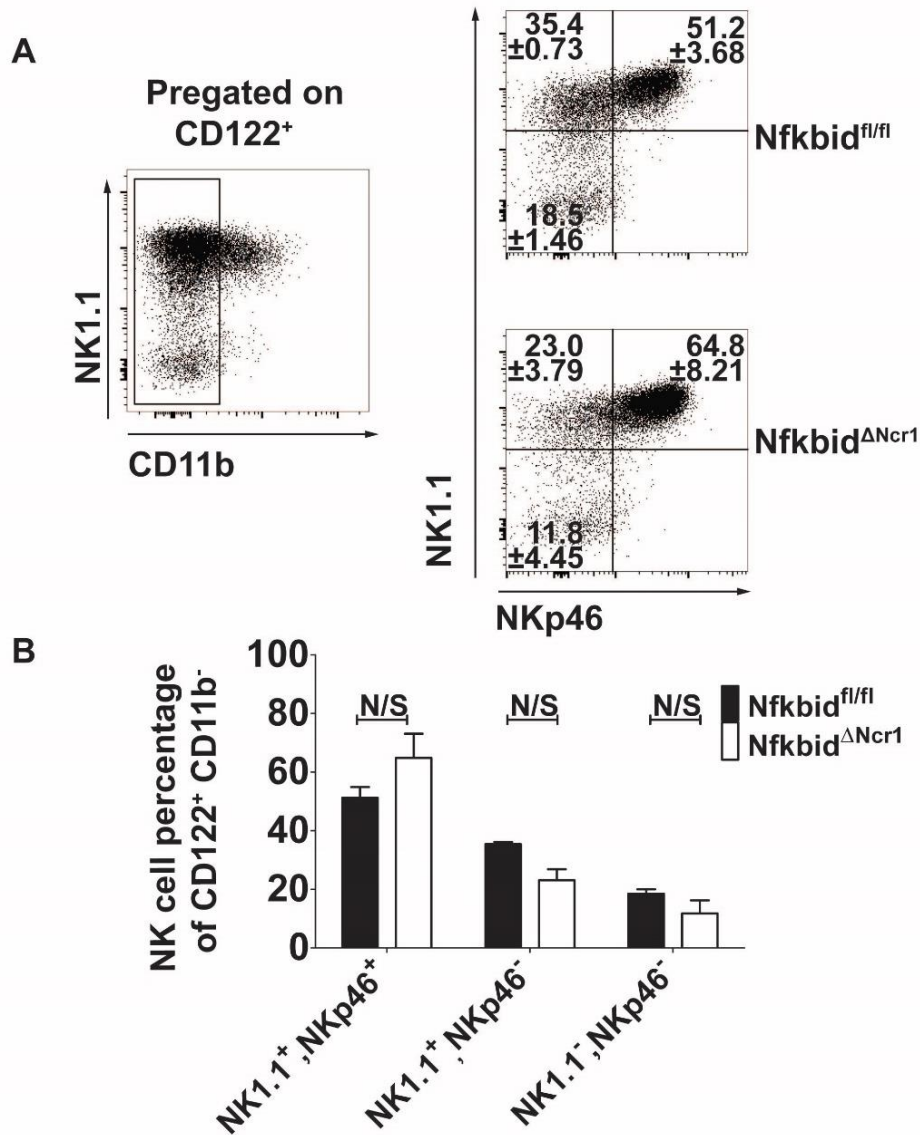


**Figure 14: Nfkbid<sup>ΔNcr1</sup> mice have similar percentages of NK cell developmental stages in the bone marrow to control mice.** **A.** Representative FACS plots of flow cytometric analysis of NK cell developmental stages in the bone marrow in Nfkbid<sup>ΔNcr1</sup> and wild type mice. The percentages are shown as mean ±SEM of graphs depicted on B. The plots are representative of 3 independent experiments with n=2 Nfkbid<sup>ΔNcr1</sup> and n=2 Nfkbid<sup>fl/fl</sup> mice per experiment. **B.** Cumulative graph of percentages of NK cell developmental stages of the same experiments depicted on A. The graphs are representative of 3 independent experiments with n=2 Nfkbid<sup>ΔNcr1</sup> and n=2 Nfkbid<sup>fl/fl</sup> mice per experiment and are shown as mean ±SEM.

Although no differences were found in the maturation stages in the bone marrow, when looking at immune populations of CD4<sup>+</sup> and CD8<sup>+</sup> T cells in the spleen, a significantly higher percentage of these populations was found in Nfkbid<sup>ΔNcr1</sup> mice at 22 weeks of age (Figure 15B). Conversely, the percentage of B cells was reduced, but although total numbers of CD4<sup>+</sup>

and CD8<sup>+</sup> T cells were also significantly reduced, this held not true for B cells (Figure 15A&B). Therefore, it was concluded that although CD4<sup>+</sup> and CD8<sup>+</sup> T cells were inflated in *Nfkbid*<sup>ΔNcr1</sup> mice, the B cell percentage was altered only because of the higher percentage of T cells. NK cell percentages and numbers showed no significant difference (Figure 15A&B).

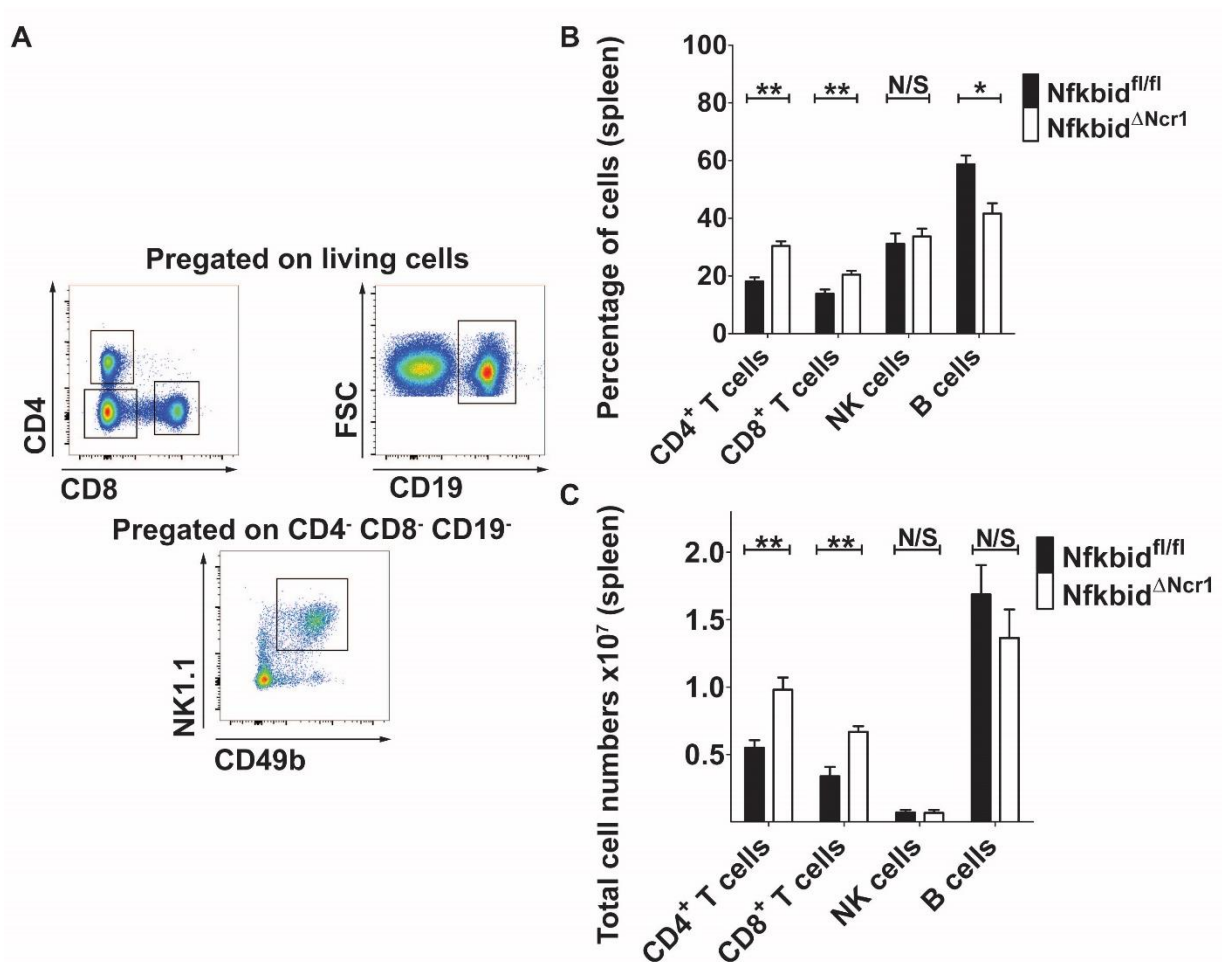


**Figure 15: 22 week old *Nfkbid*<sup>ΔNcr1</sup> have a CD4<sup>+</sup> and CD8<sup>+</sup> T cell inflation in the spleen compared to control mice. A.** Gating strategy for phenotyping of immune cell subsets through flow cytometry. **B.** Cumulative graph of percentages of immune cells in the spleen. Results are shown as mean ±SEM and are from 3 independent experiments with n=2 *Nfkbid*<sup>ΔNcr1</sup> and n=2 *Nfkbid*<sup>fl/fl</sup> mice per experiment. **C.** Cumulative graph of total numbers of immune cells in the spleen. Results are shown as mean ±SEM and are from 3 independent experiments with n=2 *Nfkbid*<sup>ΔNcr1</sup> and n=2 *Nfkbid*<sup>fl/fl</sup> mice per experiment.

Since a T cell inflation was discovered in *Nfkbid*<sup>ΔNcr1</sup> compared to control mice, the activation status of T cells was also checked in these mice, by staining for CD44 and CD62L markers. This would indicate whether the mice have developed autoimmunity, which would be one of the most common explanations for the inflation. After the experiments were performed, it was found that the percentage of CD44<sup>+</sup> CD62L<sup>-</sup> activated CD4<sup>+</sup> and CD8<sup>+</sup> T cells was not

different between  $Nfkbid^{\Delta Ncr1}$  and control mice (Figure 16A&B). Also the percentage of  $CD44^+$   $CD62L^+$  central memory  $CD8^+$  T cells<sup>145</sup> was not significantly different (Figure 16A). Therefore, the inflation of  $CD4^+$  and  $CD8^+$  T cells in the spleens of  $Nfkbid^{\Delta Ncr1}$  mice is not because of aberrant T cell activation.

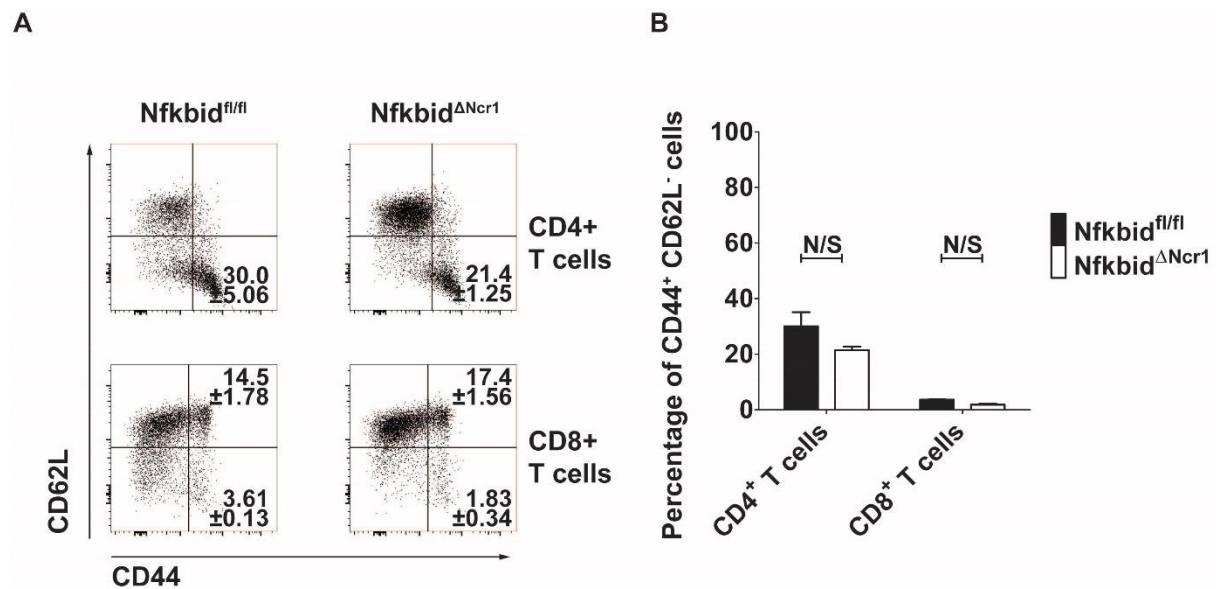


**Figure 16:  $CD4^+$  and  $CD8^+$  T cell from 22 week old  $Nfkbid^{\Delta Ncr1}$  do not have a higher activation status compared to control mice.** **A.** Representative FACS plots of flow cytometric analysis of  $CD4^+$  and  $CD8^+$  T cell activation status in the spleen  $Nfkbid^{\Delta Ncr1}$  and control mice. The percentages shown are median and standard error of all experiments. The plots are shown as mean  $\pm$ SEM and are representative of 3 independent experiments with  $n=2$   $Nfkbid^{\Delta Ncr1}$  and  $n=2$   $Nfkbid^{fl/fl}$  mice per experiment. **B.** Cumulative graph of percentages of  $CD4^+$  and  $CD8^+$  T cell activation status of the same experiments depicted on A. The graphs are shown as mean  $\pm$ SEM and are representative of 3 independent experiments with  $n=2$   $Nfkbid^{\Delta Ncr1}$  and  $n=2$   $Nfkbid^{fl/fl}$  mice per experiment.

#### 4.1.5: Differential expression analysis of NK cells from $Nfkbid^{\Delta Ncr1}$ and $Nfkbid^{fl/fl}$ mice, shows that $I\kappa B_{NS}$ suppresses B cell genes and downregulates vesicle transport genes in the steady state

To shed more light in the role of  $I\kappa B_{NS}$  in NK cells, RNA sequencing and differential expression analysis was performed in NK cells, sorted from the spleen of  $Nfkbid^{\Delta Ncr1}$  and  $Nfkbid^{fl/fl}$  mice. This showed that  $I\kappa B_{NS}$  acts more as a suppressor of genes in NK cells, since most of the differentially regulated genes were upregulated in its absence (Figure 17A). Among the genes that are normally suppressed by  $I\kappa B_{NS}$ , we surprisingly found a plethora of genes

associated with B cells, including the two main transcription factors that govern B cell development and lineage commitment, Ebf1 and Pax5 (Figure 17A)<sup>146</sup>. Also, a lot of genes that are implicated with vesicle transport, such as Rab8b<sup>147</sup> and Snx1<sup>148</sup> were found to be upregulated in I $\kappa$ B<sub>NS</sub>-deficient NK cells, something that could agree with the observed degranulation defect. Although not all of the differences were statistically significant, the mRNA of Ebf1, Pax5, Rab8b and Snx1 was found to follow the same trend as in the differential expression analysis, when results were validated through real time qPCR (Figure 17B).

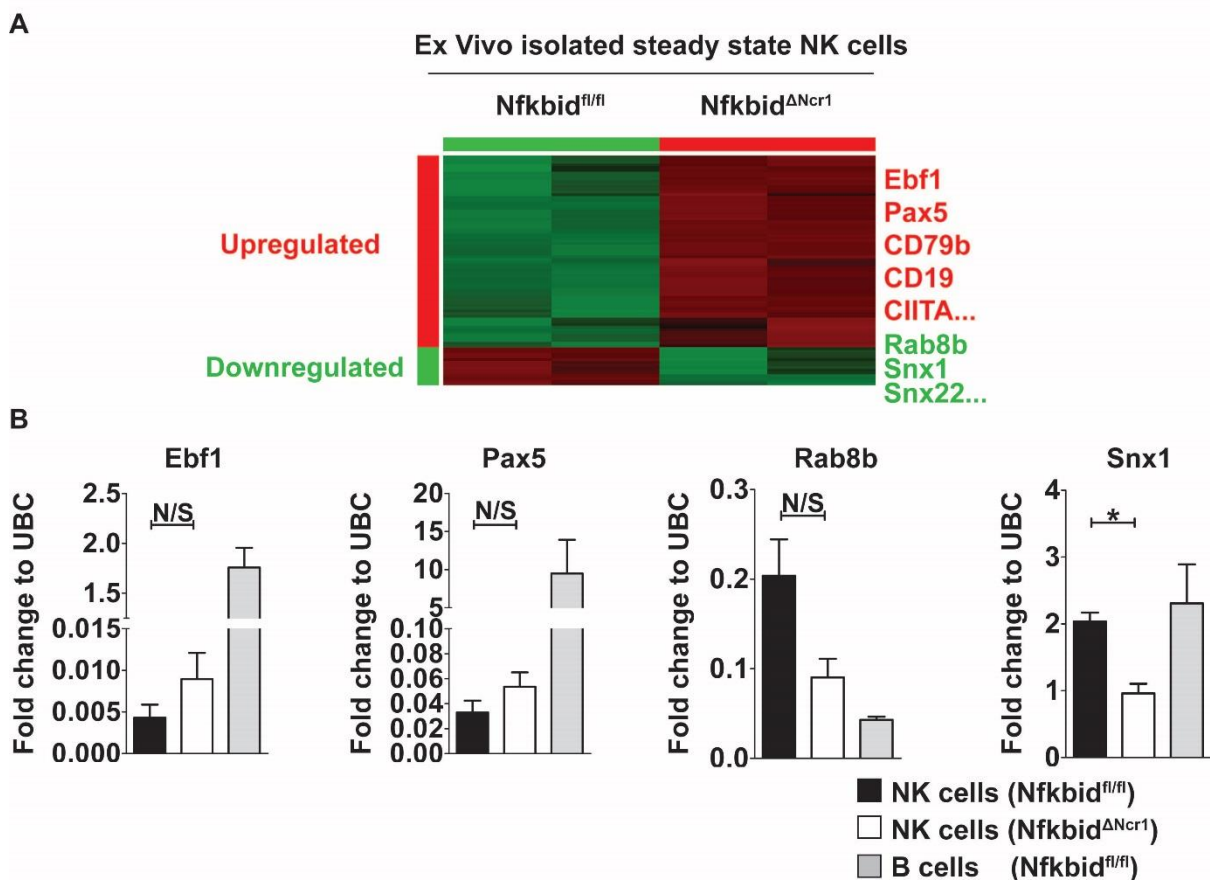


**Figure 17: Differential expression analysis of NK cells from Nfkbid<sup>ΔNcr1</sup> mice compared to control mice reveals main role for I $\kappa$ B<sub>NS</sub> as a suppressor in the steady state.** NK cells were isolated from mouse spleens of female Nfkbid<sup>ΔNcr1</sup> and Nfkbid<sup>fl/fl</sup> by sorting CD3<sup>-</sup> CD19<sup>-</sup> NK1.1<sup>+</sup> Dx5<sup>+</sup> cells. **A.** Depiction of upregulated (red) and downregulated (green) genes in I $\kappa$ B<sub>NS</sub>-deficient NK cells. The genes shown are from the ones with the with the smallest false discovery chance. **B.** Validation of differential expression analysis results through real time qPCR. The fold change to housekeeping gene UBC is shown. Graphs are depicted as mean  $\pm$ SEM and are from 3 independent experiments with n=4 Nfkbid<sup>ΔNcr1</sup> and n=4 Nfkbid<sup>fl/fl</sup> pooled mice per experiment.

## 4.2 The role of I $\kappa$ B<sub>NS</sub> in T cells

### 4.2.1: I $\kappa$ B<sub>NS</sub> is important for the early phase of T<sub>H</sub>1 differentiation

I $\kappa$ B<sub>NS</sub> has been shown to be important for T<sub>H</sub>1 differentiation, since in vitro differentiated T<sub>H</sub>1 T cells show an impairment in IFN $\gamma$  production<sup>116</sup>. However, it is unknown whether I $\kappa$ B<sub>NS</sub> is needed in the effector stage, for example by directly regulating the *Ifng* gene, or whether it is needed in the early stages of differentiation. In order to investigate this, initially the *Nfkbid*<sup>LacZ</sup> reporter mouse was used to visualize *Nfkbid* promoter activity during T<sub>H</sub>1 differentiation (Figure 18A). These experiments revealed that promoter activity during differentiation slowly rises until it peaks on day 3, at which point it drops a bit and stabilizes (Figure 18B). This suggests that I $\kappa$ B<sub>NS</sub> is more important for the early stage of differentiation.

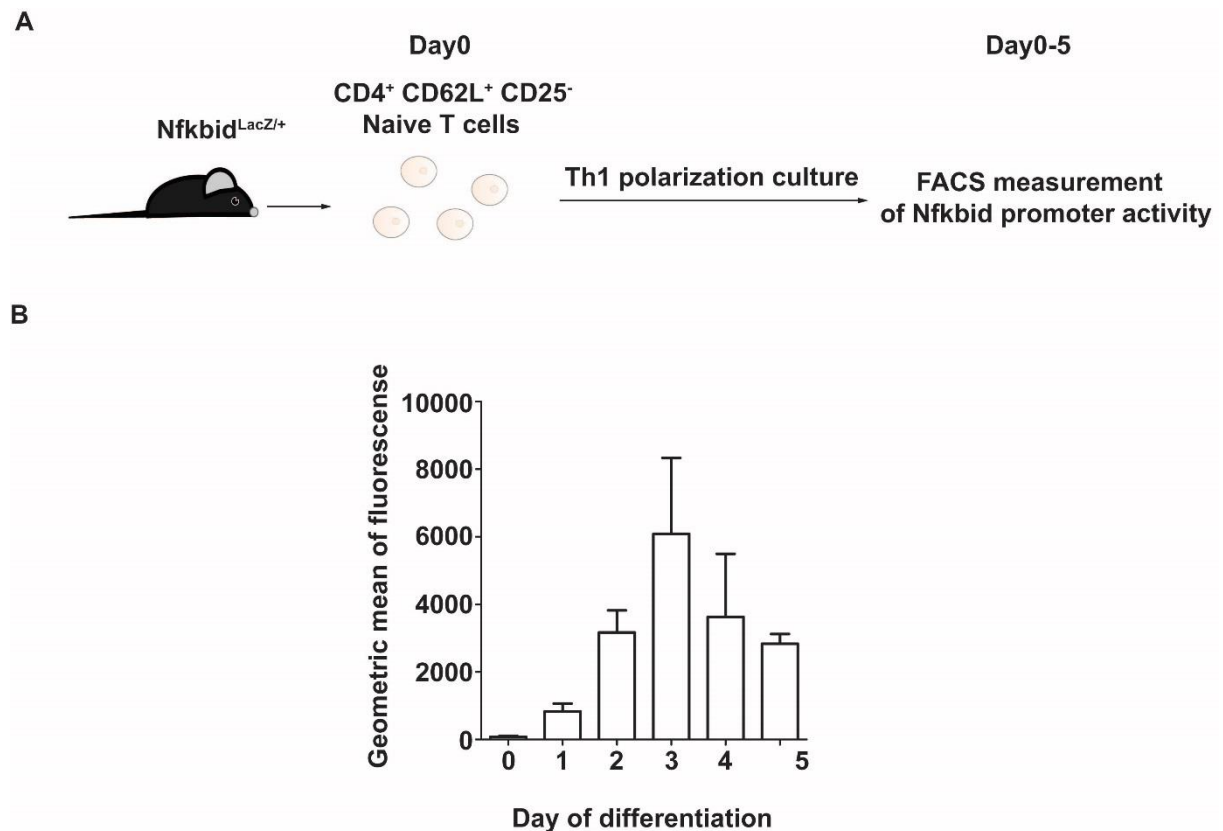


**Figure 18: *Nfkbid* promoter activity during T<sub>H</sub>1 differentiation peaks on day 3.** **A.** CD4<sup>+</sup> CD62L<sup>+</sup> CD25<sup>-</sup> naïve T cells were isolated from mouse spleen and peripheral lymph nodes of *Nfkbid*<sup>LacZ</sup> mice and T<sub>H</sub>1 differentiation was performed as described in 3.4.1. Every day of the process *Nfkbid* promoter activity was measured by flow cytometry. **B.** *Nfkbid* promoter activity during Th1 differentiation, visualized by use of the *Nfkbid*<sup>LacZ</sup> mice. Day 0 is an unstimulated sample of naïve CD4 T cells and the rest are samples where a Th1 polarization signal has been given (2  $\mu$ g/mL plate-bound anti-CD3 $\epsilon$ , 2  $\mu$ g/mL anti-CD28 in suspension, 10  $\mu$ g/mL anti-IL4 and 10 ng/mL IL12). Data are shown as mean  $\pm$ SEM (n=3) and are representative of 3 independent experiments with n=1 mouse per experiment.

To further follow up with this lead, inducible I $\kappa$ B<sub>NS</sub> knock out mice were created by crossing Nfkbid<sup>fl/fl</sup> mice with Rosa26<sup>CreERT2</sup> mice. This allowed conditional, inducible deletion of Nfkbid through the administration of 4-hydroxytamoxifen (here referred to as tamoxifen). Thus, depletion of I $\kappa$ B<sub>NS</sub> protein could be performed by treating with tamoxifen in the early or late stages of differentiation. However, before this was possible, the time between tamoxifen treatment and completed depletion of I $\kappa$ B<sub>NS</sub> had to be measured. For this reason, CD4<sup>+</sup> T cells were sorted, stimulated and treated with tamoxifen and an I $\kappa$ B<sub>NS</sub> protein kinetic assay was performed by western blot (Figure 19A). Indeed, when CD4<sup>+</sup> T cells from Nfkbid<sup>fl/fl</sup> Rosa<sup>CreERT2</sup> mice were stimulated *in vitro* and subsequently treated with tamoxifen, complete loss of I $\kappa$ B<sub>NS</sub> protein expression was observed within 48 h in the inducible I $\kappa$ B<sub>NS</sub> knock-out CD4<sup>+</sup> T cells, while I $\kappa$ B<sub>NS</sub> protein levels remained unaffected in WT control CD4<sup>+</sup> T cells (Figure 19B).

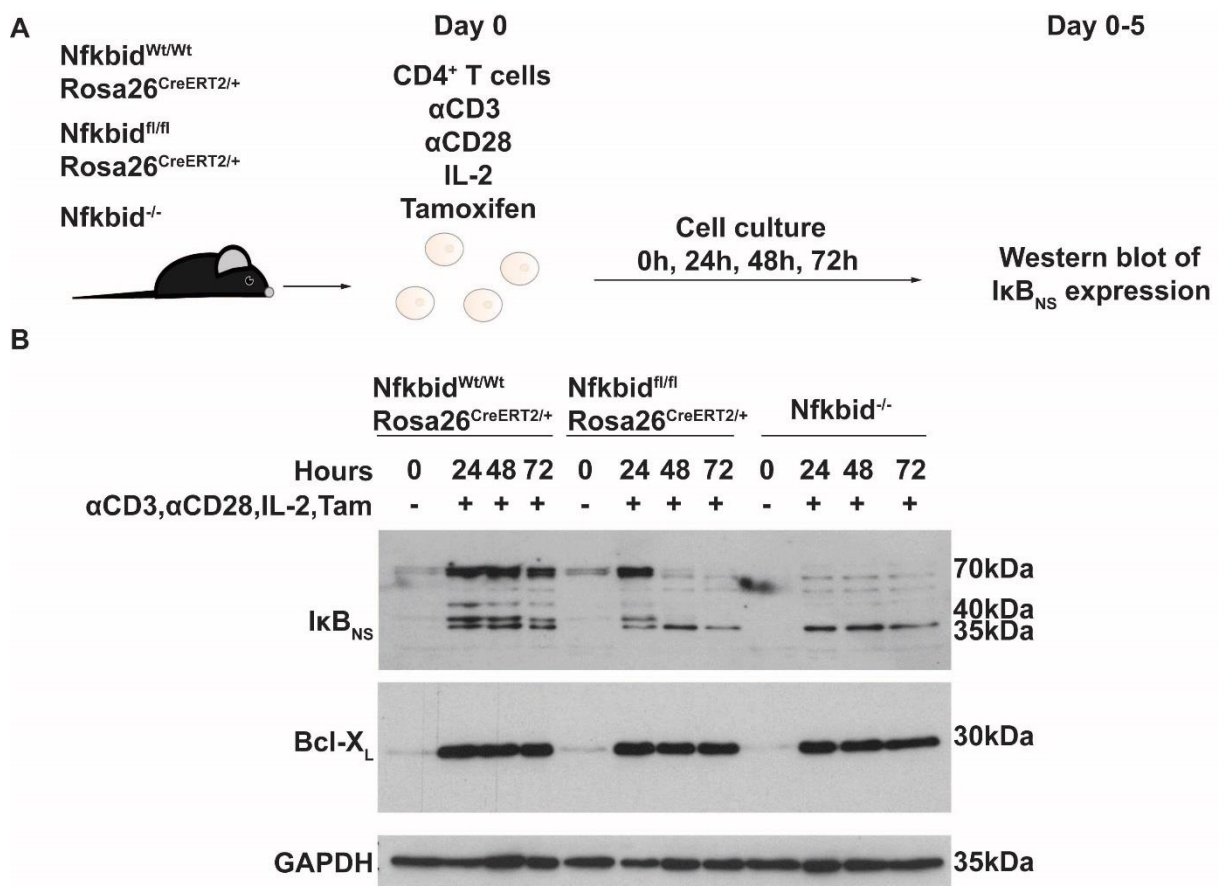


**Figure 19: I $\kappa$ B<sub>NS</sub> protein expression disappears from CD4<sup>+</sup> T cells from Nfkbid<sup>fl/fl</sup> Rosa26<sup>CreERT2/+</sup> 48h hours after tamoxifen administration.** **A.** Nfkbid<sup>WT/WT</sup> Rosa26<sup>CreERT2/+</sup> is the cre-only type control, Nfkbid<sup>Fl/Fl</sup> Rosa26<sup>CreERT2/+</sup> is where the conditional deletion will take place and Nfkbid<sup>-/-</sup> is the negative control for antibody background exclusion. CD4<sup>+</sup> T cells were FACS sorted and stimulated with anti-CD3 (2  $\mu$ g/ml plate bound), anti-CD28 (2  $\mu$ g/ml in suspension), IL-2 (50 ng/ml) and 4-hydroxytamoxifen (1  $\mu$ M) for up to 72h. **B.** Kinetic of I $\kappa$ B<sub>NS</sub> protein expression in sorted CD4<sup>+</sup> T cells

from mouse spleen and peripheral lymph nodes, after tamoxifen administration. This blot is representative of two independent experiments with n=2 mice per experiment.

After the time required for I $\kappa$ B<sub>NS</sub> depletion was determined, tamoxifen was added in T<sub>H</sub>1 differentiation culture either on day 2 or day 4, resulting in complete I $\kappa$ B<sub>NS</sub> depletion by day 4 and 6 post treatment, respectively (Figure 20A). It was observed that both IFN $\gamma$  production and CD44 expression were significantly reduced in I $\kappa$ B<sub>NS</sub>-deficient CD4<sup>+</sup> T cells, compared to the control samples, when I $\kappa$ B<sub>NS</sub> deficiency was induced early on (day 2) during *in vitro* Th1 differentiation (Figure 20B). In contrast, IFN $\gamma$  production and CD44 expression in Th1 cells were not affected when tamoxifen was added on day 4, resulting in complete I $\kappa$ B<sub>NS</sub> deficiency on day 6 of differentiation, which is a time-point of terminally differentiated cells (Figure 20B). Although T-bet expression was not affected in either setting, these results suggest that I $\kappa$ B<sub>NS</sub> expression in CD4<sup>+</sup> T cells is important during the early stages of Th1 cell differentiation, while its function in terminally differentiated cells appears to be inferior.

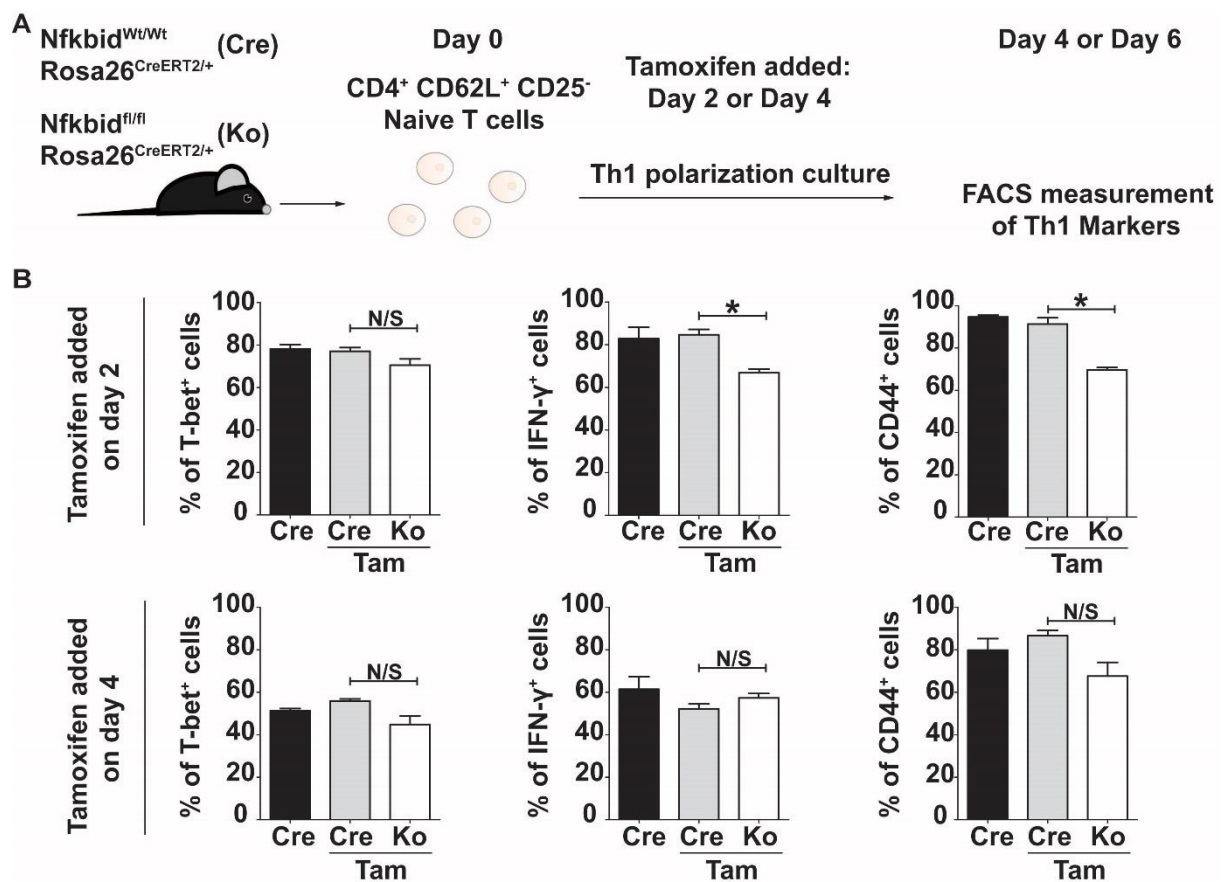


**Figure 20: Conditional deletion of  $I\kappa B_{NS}$  reveals a role at the early stages of  $T_H1$  differentiation. A.**  $CD4^+ CD62L^+ CD25^-$  naïve T cells were isolated from mouse spleen and peripheral lymph nodes of  $Nfkbid^{WT/WT} Rosa26^{CreERT2/+}$  (here referred as Cre) and  $Nfkbid^{fl/fl} Rosa26^{CreERT2/+}$  (here referred as Ko) mice and  $T_H1$  differentiation was performed as described in 3.4.1. Day 4 and 6 deletion means that tamoxifen was added 2 days prior, leading to complete protein depletion on that day. **B.** Conditional deletions of  $Nfkbid$  during Th1 differentiation. Cre is a  $Nfkbid^{WT/WT} Rosa26^{CreERT2/+}$  sample without addition of tamoxifen and Cre Tam is the same sample with addition of tamoxifen used as a control. Ko indicates a tamoxifen treated  $Nfkbid^{fl/fl} Rosa26^{CreERT2/+}$  sample, where the conditional deletion will take place. Day 4 and 6 deletion means that tamoxifen was added 2 days prior, leading to complete protein depletion on that day. Data are shown as mean  $\pm$  SEM ( $n=3$  for T-bet and CD44,  $n=6$  for IFN $\gamma$ ) and are pooled from 6 (IFN $\gamma$ ) or 3 (T-bet, CD44) independent experiments with  $n=1$  mouse per condition (Cre, Ko) per experiment.

#### 4.2.2: $Nfkbid^{\Delta CD4}$ mice have a reduced regulatory T cell compartment and show impaired $T_H1$ differentiation and iTreg generation *in vitro*

In order to investigate the role of  $I\kappa B_{NS}$  in T cells, when it is still expressed in other immune cells, a T cell-specific knock out mouse line was created.  $Nfkbid^{\Delta CD4}$  mice were generated by crossing  $Nfkbid^{fl/fl}$  mice with mice expressing Cre recombinase under the CD4 promoter. This

led to I $\kappa$ B<sub>NS</sub> being a knockout in all T cells. Sorting of CD4<sup>+</sup> T cells from the spleen and peripheral lymph nodes and checking I $\kappa$ B<sub>NS</sub> protein expression, after stimulation with PMA and ionomycin, proved that the generated mouse line is truly a knockout (Figure 21A). Similarly to Nfkbid<sup>-/-</sup> mice, the Nfkbid<sup>ΔCD4</sup> mouse line did not have aberrant T cell percentages and numbers in peripheral lymphoid organs (Figure 21B) and also no difference in activated CD4<sup>+</sup> T cells was detected, compared to control mice (Figure 21C). Similarly to CD4<sup>+</sup> T cells, CD8<sup>+</sup> T cells were also not altered in percentages and number, and did not show an aberrant activation status (Data not shown).

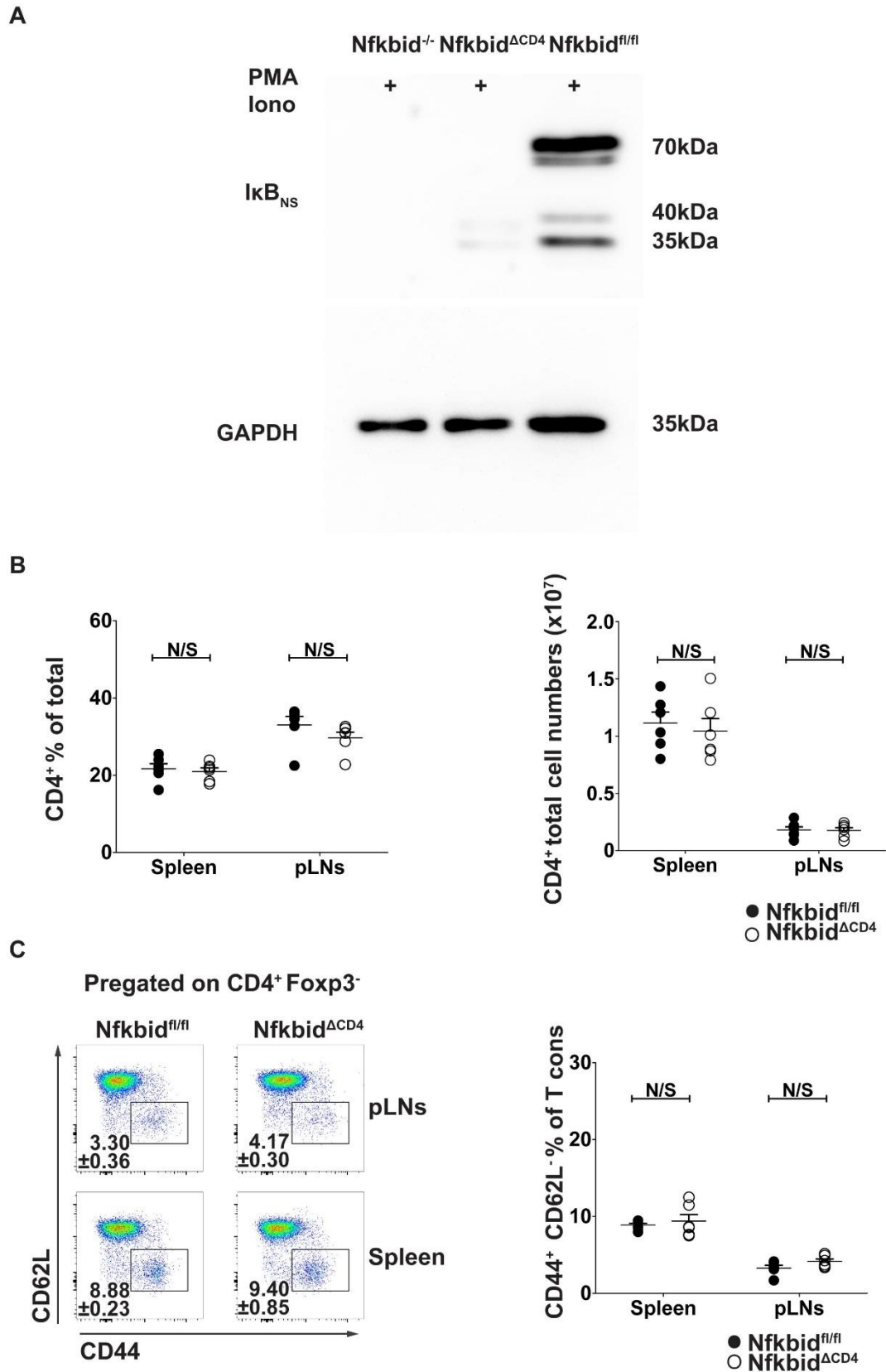


**Figure 21: Nfkbid<sup>ΔCD4</sup> mice have a normal CD4<sup>+</sup> T cell compartment.** **A.** CD4<sup>+</sup> T cells were sorted from spleen and peripheral lymph nodes and stimulated with PMA (10 μg/ml) and Ionomycin (1 μM) for 3h. Then expression of IkB<sub>NS</sub> was measured through western blotting. This blot is representative of two independent experimental repeats with n=1 mouse per experiment. **B.** CD4<sup>+</sup> T cell percentages (left panel) and total numbers (right panel) in spleen and peripheral lymph nodes of Nfkbid<sup>ΔCD4</sup> and

control mice. The data is shown as mean  $\pm$ SEM and are representative of 3 independent experiments with  $n=2$   $Nfkbid^{\Delta CD4}$  and  $n=2$   $Nfkbid^{fl/fl}$  mice per experiment. **C.** (left panel) Representative FACS plots of flow cytometric analysis of  $CD4^+$  T cell activation status in  $Nfkbid^{\Delta CD4}$  and control mice. The plots are shown as mean  $\pm$ SEM and are representative of 3 independent experiments with  $n=2$   $Nfkbid^{\Delta CD4}$  and  $n=2$   $Nfkbid^{fl/fl}$  mice per experiment (right panel). Cumulative graph of percentages of  $CD4^+$  T cell activation status of the same experiments depicted on A. The graphs are shown as mean  $\pm$ SEM and are representative of 3 independent experiments with  $n=2$   $Nfkbid^{\Delta CD4}$  and  $n=2$   $Nfkbid^{fl/fl}$  mice per experiment.

Since a T cell-specific was created, it made sense to check whether previous findings, about  $I\kappa B_{NS}$ -deficient naïve T cells showing impaired  $T_H1$  differentiation<sup>116</sup>, could be confirmed. For this reason naïve  $CD4^+$   $CD62L^+$   $CD44^-$   $CD25^-$  were sorted from  $Nfkbid^{\Delta CD4}$  and control mice and  $T_H1$  differentiation was performed *in vitro* as described in 3.4.1. As expected, IFN $\gamma$  production from  $I\kappa B_{NS}$ -deficient T cells was significantly reduced after *in vitro* differentiation, compared to control mice, while there was no significant difference in T-bet (Figure 22).

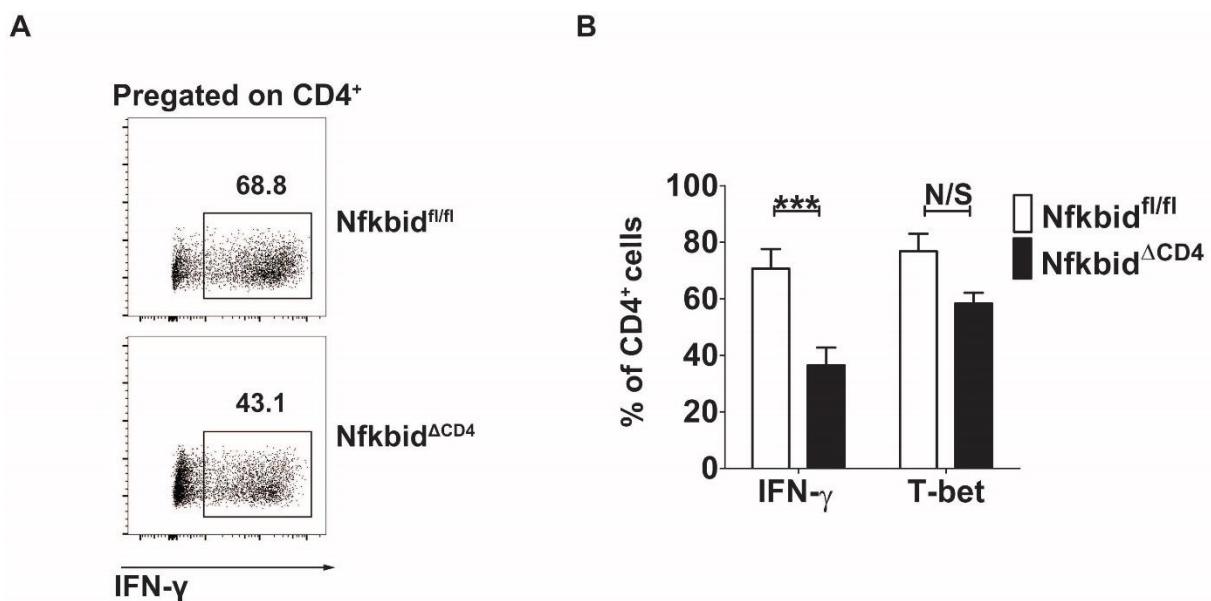


**Figure 22: Naive T cells from  $Nfkbid^{\Delta CD4}$  mice show a defect during *in vitro*  $T_H1$  differentiation. A.** Representative FACS plot of IFN $\gamma$  expression after  $T_H1$  differentiation, performed as described in 3.4.1. The data are representative of 4 independent experiments with  $n=1$   $Nfkbid^{\Delta CD4}$  and  $n=1$   $Nfkbid^{fl/fl}$  mice per experiment. **B.** Cumulative graphs of IFN $\gamma$  and T-bet expression of the experiment shown in A. The graphs are shown as mean  $\pm$ SEM and are representative of 4 independent experiments with  $n=1$   $Nfkbid^{\Delta CD4}$  and  $n=1$   $Nfkbid^{fl/fl}$  mice per experiment.

To further test whether existing literature could be confirmed with the  $Nfkbid^{\Delta CD4}$  mice, the Treg compartment was measured by flow cytometry.  $Nfkbid^{-/-}$  mice have been shown to possess 50% reduced  $Foxp3^+$  Tregs in the thymus and peripheral lymphoid organs, compared to wild type mice<sup>112</sup>.  $Nfkbid^{\Delta CD4}$  were similarly found to have significantly reduced percentages and total cell numbers of Tregs in the thymus, spleen and peripheral lymph nodes (Figure 23).

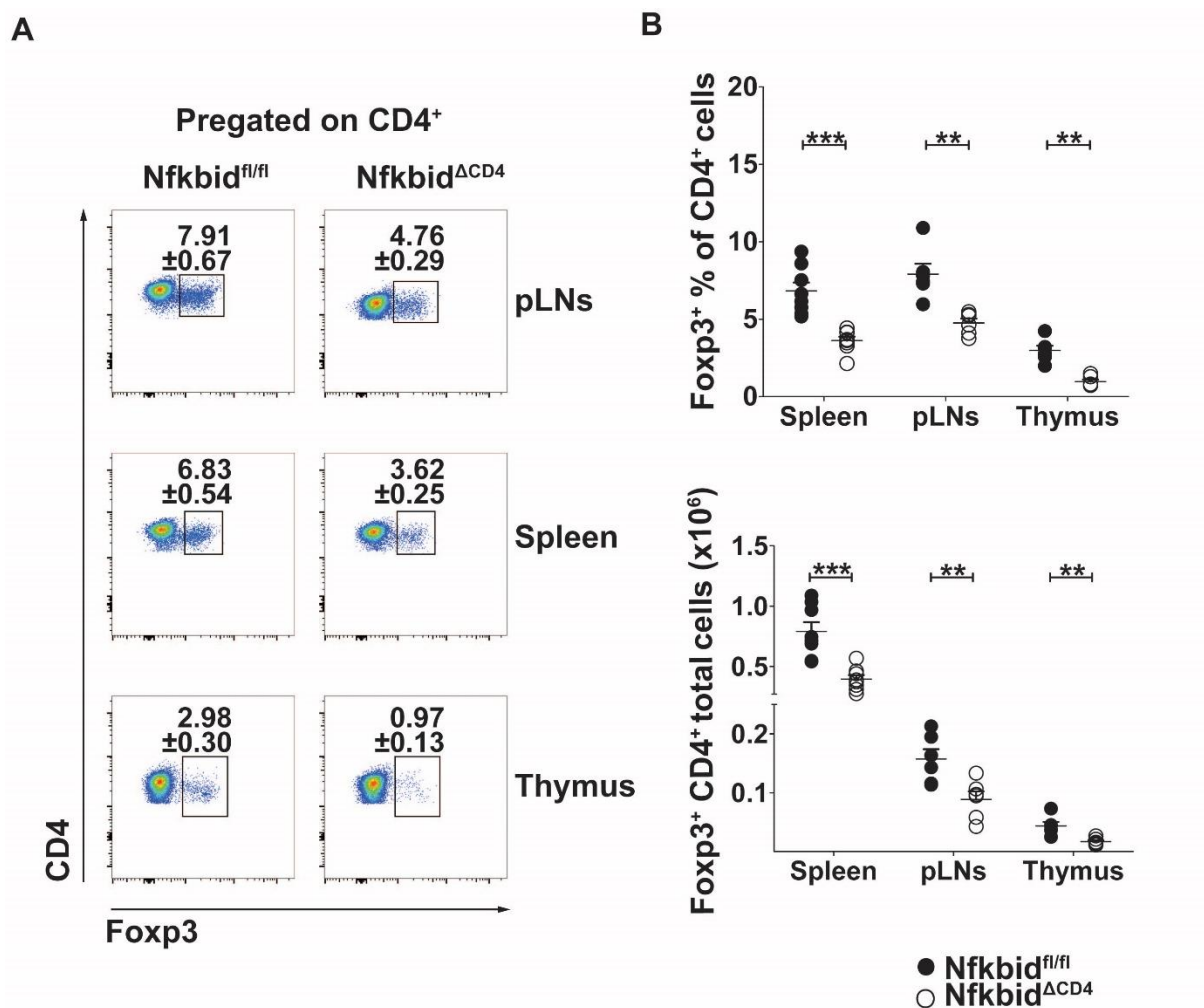


**Figure 23:  $Nfkbid^{\Delta CD4}$  mice have reduced numbers of Tregs in the periphery compared to control mice.** **A.** Representative FACS plots of flow cytometric analysis of Treg percentages in spleen, thymus and pLNs of  $Nfkbid^{\Delta CD4}$  and control mice. The plots are shown as mean  $\pm$ SEM and are representative of 3 independent experiments with n=2  $Nfkbid^{\Delta CD4}$  and n=2  $Nfkbid^{fl/fl}$  mice per experiment. **B.** Cumulative graph of Treg percentages (upper panel) and total numbers (lower panel) of the same experiments depicted on A. The graphs are shown as mean  $\pm$ SEM and are representative of 3 independent experiments with n=2  $Nfkbid^{\Delta CD4}$  and n=2  $Nfkbid^{fl/fl}$  mice per experiment.

$I\kappa B_{NS}$ -deficient naïve T cells were also reported to have impaired iTreg generation<sup>112</sup>. To investigate whether this holds true for the T cell-specific knockout, naïve CD4<sup>+</sup> CD62L<sup>+</sup> CD44<sup>-</sup>

CD25<sup>-</sup> were sorted from Nfkbid<sup>ΔCD4</sup> and control mice and iTreg induction was performed *in vitro*, as described in 3.4.2. Then, the percentages of Foxp3<sup>+</sup> cells were visualized with flow cytometry. As expected, Foxp3<sup>+</sup> generation from IκB<sub>NS</sub>-deficient T cells was significantly reduced, compared to control mice, when low amounts (0.5 ng/ml) of TGF-β were used as the induction stimulus (Figure 24). At higher concentrations of TGF-β, the defect is compensated by the strong induction stimulus<sup>112</sup>.

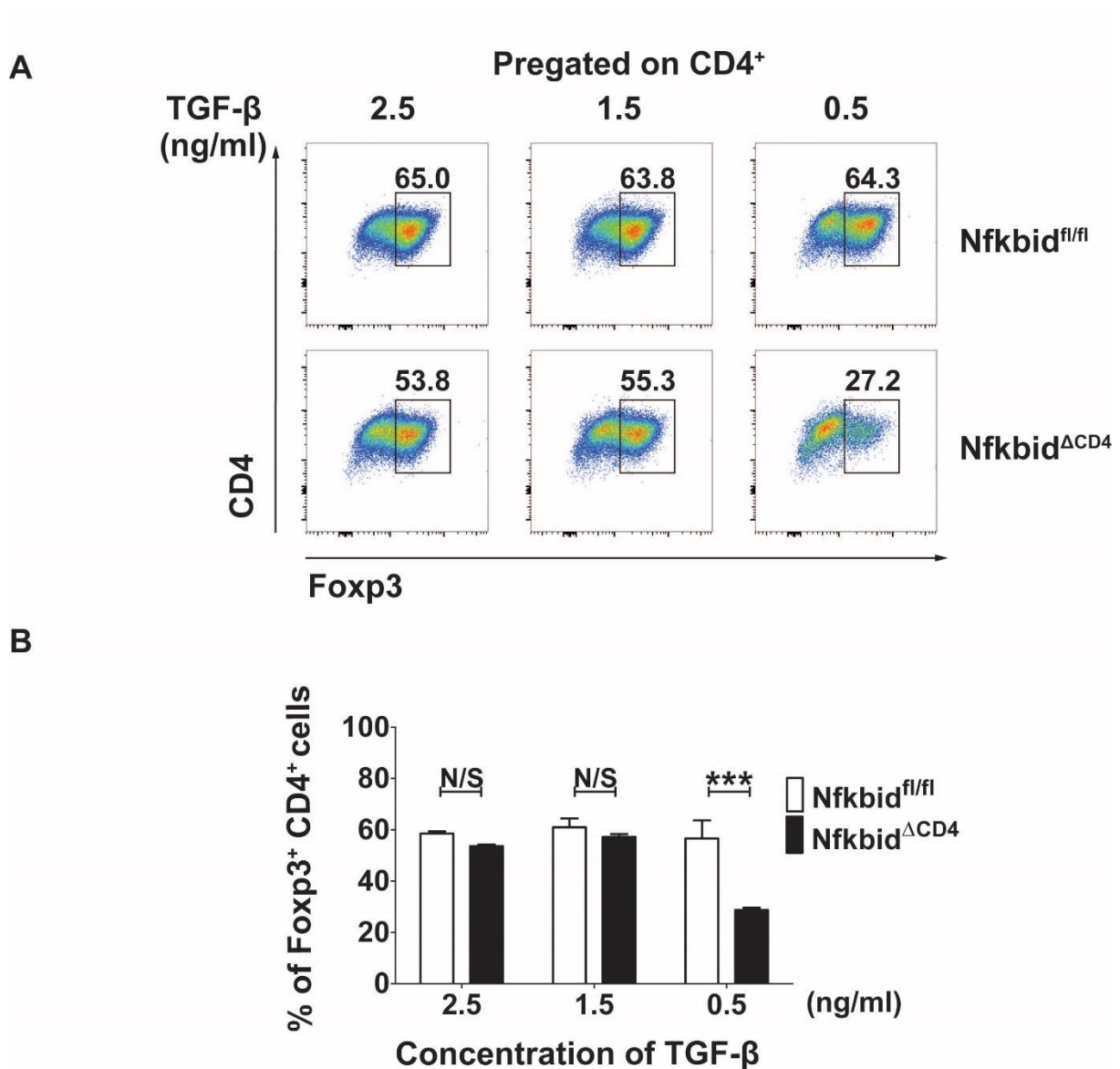


**Figure 24: Naive T cells from Nfkbid<sup>ΔCD4</sup> mice show a defect during *in vitro* iTreg differentiation. A.** Representative FACS plot of Foxp3 expression after iTreg differentiation, performed as described in 3.4.2. The data are representative of 3 independent experiments with n=1 Nfkbid<sup>ΔCD4</sup> and n=1 Nfkbid<sup>fl/fl</sup> mice per experiment. **B.** Cumulative graphs of Foxp3 expression of the experiment shown in A. The graphs are shown as mean ±SEM and are representative of 4 independent experiments with n=1 Nfkbid<sup>ΔCD4</sup> and n=1 Nfkbid<sup>fl/fl</sup> mice per experiment.

#### 4.2.3: $Nfkbid^{\Delta CD4}$ mice cope better with *Leishmania major* infection and have lower parasite numbers, compared to control mice

The  $T_H1$  immune response is very important for clearance of the *Leishmania major* infection, and Tregs were implicated with perpetuating the infection, allowing it to become chronic<sup>123</sup>. Therefore, *Leishmania major* looks like a relevant infection model to investigate the importance of results described in 4.2.2. *in vivo*. For this,  $Nfkbid^{\Delta CD4}$  and  $Nfkbid^{fl/fl}$  mice were infected with 2 million promastigotes of *L. major*, by subcutaneous injection, in the ear pinna and the infection was monitored for up to 18 weeks (Figure 25A). When ear thickness was measured as a marker of disease progression, it was found that although there are not significant differences until 4 weeks post infection, from the 5<sup>th</sup> week  $Nfkbid^{\Delta CD4}$  mice show significantly smaller ear thickness (Figure 25B), suggesting that  $I\kappa B_{NS}$  deficiency in T cells is beneficial for fighting a *L. major* infection.

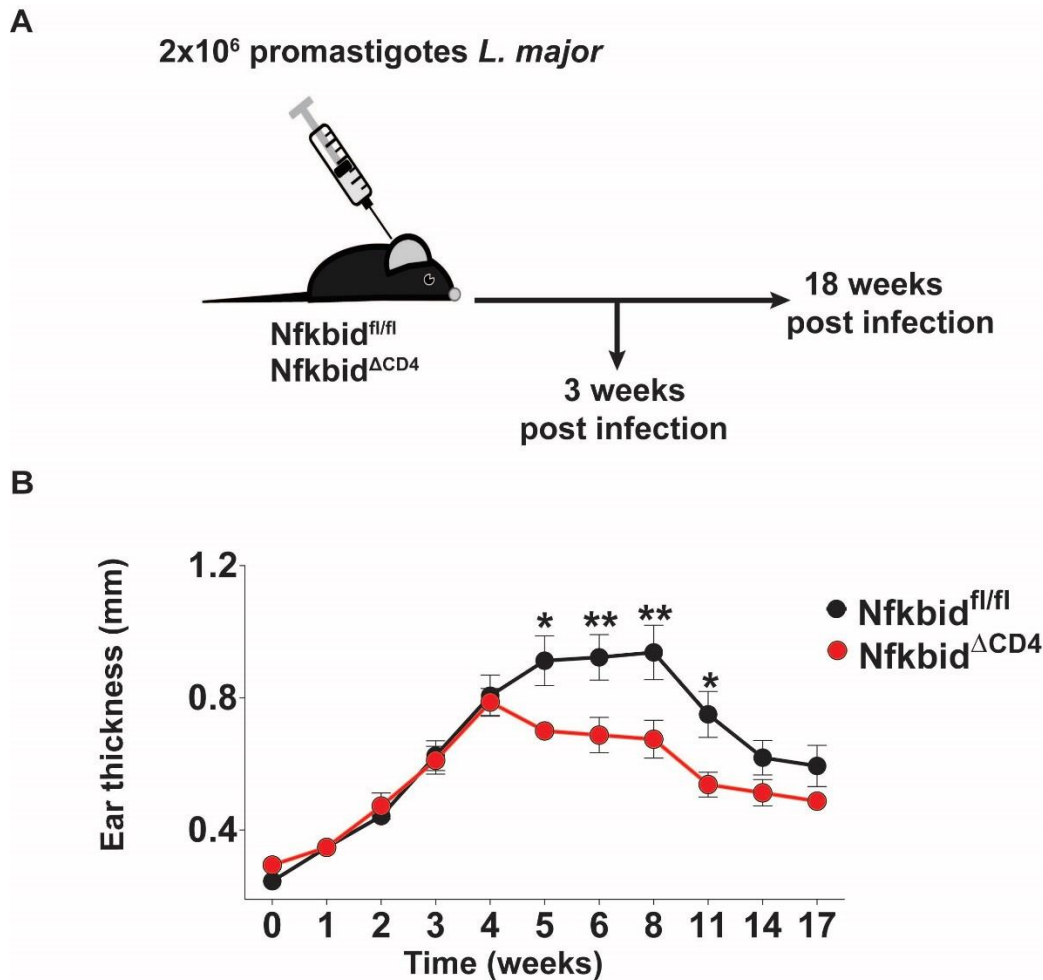


**Figure 25: Nfkbid<sup>ΔCD4</sup> mice show better disease progression after *Leishmania major* infection. A.** 8-14 week old Nfkbid<sup>ΔCD4</sup> and Nfkbid<sup>fl/fl</sup> mice were infected with 2 million promastigotes of *Leishmania major* and disease progression was followed up to a period of 18 weeks. To visualize infected cells *L.m.* DSRED was used. **B.** Ear thickness of infected Nfkbid<sup>ΔCD4</sup> and Nfkbid<sup>fl/fl</sup> mice over a period of 17 weeks. The graphs are shown as mean ±SEM and are representative of 2 independent experiments with n=4 Nfkbid<sup>ΔCD4</sup> and n=4 Nfkbid<sup>fl/fl</sup> mice per experiment.

iNos produced from innate immune cells, induced by T<sub>H</sub>1 cytokines such as IFN $\gamma$  is important for clearance of *L. major* parasites<sup>123</sup>. When looking at iNos expression in infected and non-infected dendritic cells and macrophages at 3 weeks post infection, no significant differences were detected between Nfkbid<sup>ΔCD4</sup> and control mice at the site of infection. However, there was a trend of a higher percentage of iNos producing infected macrophages in Nfkbid<sup>ΔCD4</sup> mice (Figure 26A). Moreover, percentages of CD4<sup>+</sup> T cells, dendritic cells, macrophages and neutrophils did not show a difference (Figure 26B). However, both the percentages of infected innate immune cells, visualized in FACS by the use of *L. major* DSRED, (Figure 26C)

and total parasite counts in the ear (Figure 26D) were significantly reduced in  $Nfkbid^{\Delta CD4}$  mice.

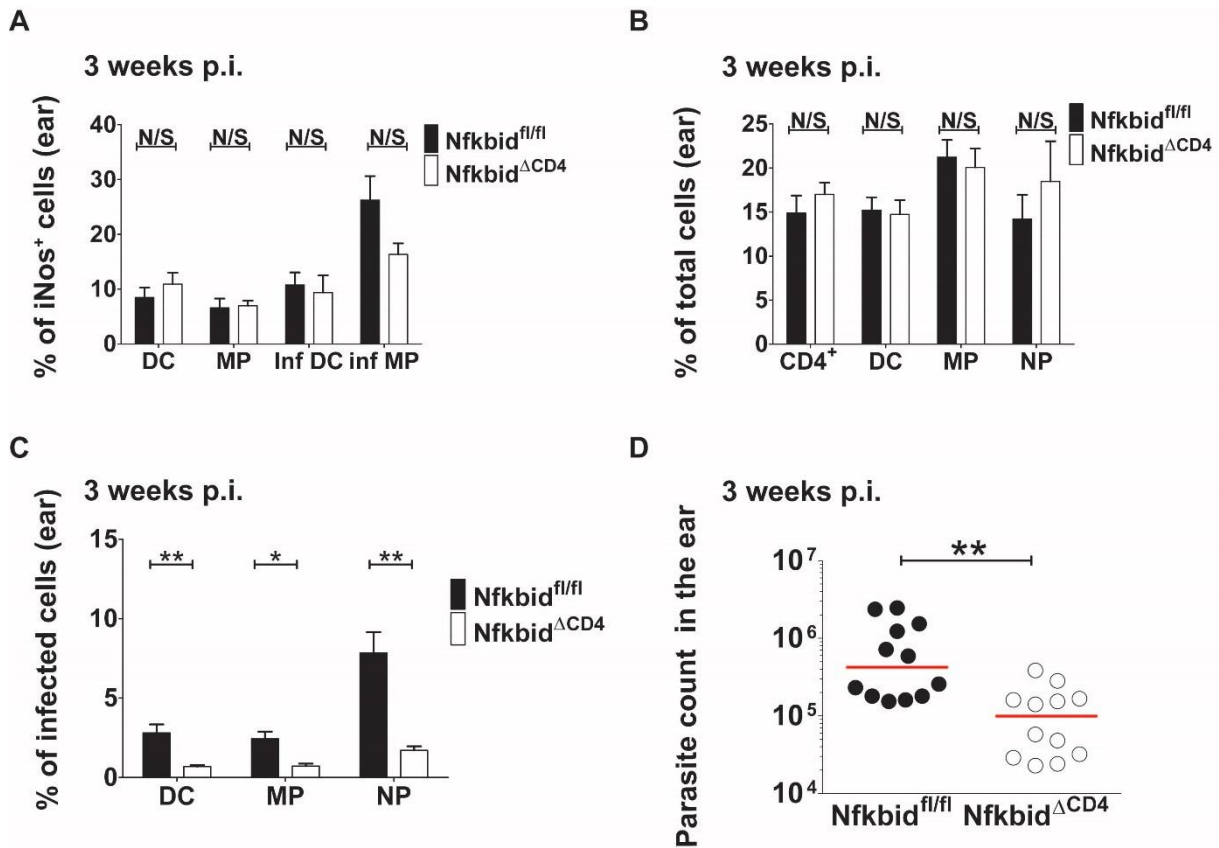


**Figure 26:  $Nfkbid^{\Delta CD4}$  mice show smaller *L.m.* parasite counts and infected innate immune cells in the ear pinna 3 weeks post infection, compared to control mice. A.** Percentages of iNos expressing dendritic cells and macrophages in the ear pinna, infected or not infected with *L.m.* at 3 weeks post infection, as shown by flow cytometry. The graphs are shown as mean  $\pm$ SEM and are representative of 2 independent experiments with  $n=4$   $Nfkbid^{\Delta CD4}$  and  $n=4$   $Nfkbid^{fl/fl}$  mice per experiment. **B.** Percentages CD4<sup>+</sup> T cells, dendritic cells, macrophages and neutrophils in the ear pinna at 3 weeks post infection, as shown by flow cytometry. The graphs are shown as mean  $\pm$ SEM and are representative of 2 independent experiments with  $n=4$   $Nfkbid^{\Delta CD4}$  and  $n=4$   $Nfkbid^{fl/fl}$  mice per experiment. **C.** Percentages infected dendritic cells, macrophages and neutrophils in the ear pinna at 3 weeks post infection, as shown by flow cytometry. The graphs are shown as mean  $\pm$ SEM and are representative of 2 independent experiments with  $n=4$   $Nfkbid^{\Delta CD4}$  and  $n=4$   $Nfkbid^{fl/fl}$  mice per experiment. **D.** Total parasite counts in the ear pinna at 3 weeks post infection, as shown by limiting dilution assay. The graphs are shown as mean  $\pm$ SEM and are representative of 2 independent experiments with  $n=4$   $Nfkbid^{\Delta CD4}$  and  $n=4$   $Nfkbid^{fl/fl}$  mice per experiment.

To further illuminate the immune response against *L. major* at 3 weeks post infection, the draining lymph nodes (cervical) were investigated. Total draining lymph node cellularity was not significantly different between  $Nfkbid^{\Delta CD4}$  and control mice (Figure 27A). Also, the percentages of CD44<sup>+</sup> CD62L<sup>-</sup> activated CD4<sup>+</sup> T cells in spleen and draining lymph nodes were

not different between  $Nfkbid^{\Delta CD4}$  and control mice (Figure 27B). These results show that, although parasite numbers are reduced in  $Nfkbid^{\Delta CD4}$  mice at 3 weeks post infection, the important immune response is not different compared to control mice.

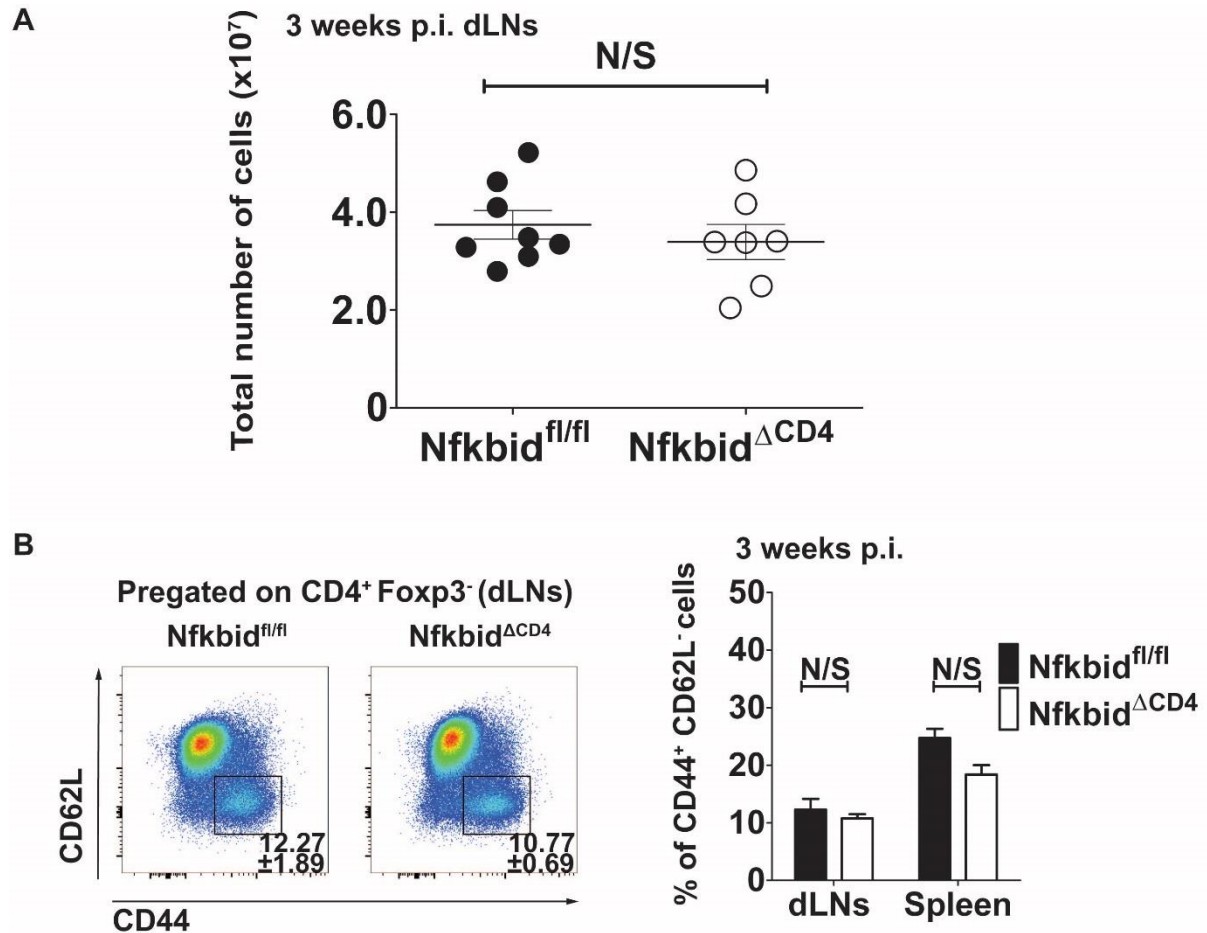


**Figure 27:  $Nfkbid^{\Delta CD4}$  mice have similar draining lymph node cellularity and  $CD4^+$  activation status to control mice 3 weeks post infection.** **A.** Total cellularity of draining lymph nodes 3 weeks post infection. The graphs are shown as mean  $\pm$ SEM and are representative of 2 independent experiments with  $n=4$   $Nfkbid^{\Delta CD4}$  and  $n=4$   $Nfkbid^{fl/fl}$  mice per experiment. **B.** (left panel) Representative FACS plots of flow cytometric analysis of  $CD4^+$  T cell activation status in  $Nfkbid^{\Delta CD4}$  and control mice, at 3 weeks post infection. The plots are shown as mean  $\pm$ SEM and are representative of 2 independent experiments with  $n=4$   $Nfkbid^{\Delta CD4}$  and  $n=4$   $Nfkbid^{fl/fl}$  mice per experiment. (right panel) Cumulative graph of percentages of  $CD4^+$  T cell activation status of the same experiments depicted on the left panel. The graphs are shown as mean  $\pm$ SEM and are representative of 2 independent experiments with  $n=4$   $Nfkbid^{\Delta CD4}$  and  $n=4$   $Nfkbid^{fl/fl}$  mice per experiment.

#### **4.2.3: Nfkbid<sup>ΔCD4</sup> mice have reduced inflammation 18 weeks post *L. major* infection, compared to control mice**

*Leishmania major* infected C57BL/6 mice have lesions that heal, leaving behind a small persistent population of parasites, that has been reported to persist due to IL-10 signalling and regulatory T cells<sup>123,124,149</sup>. Therefore, it made sense to investigate the phenotype of the infection model at a very late time-point of 18 weeks post infection. At that time, draining lymph nodes from Nfkbid<sup>ΔCD4</sup> mice were found to be much smaller compared to control mice (Figure 28A). Indeed total draining lymph node cellularity was significantly decreased in Nfkbid<sup>ΔCD4</sup> mice (Figure 28B). Moreover, total parasite counts in the ear of Nfkbid<sup>ΔCD4</sup> mice were significantly lower compared to control mice, and in a lot of mice lower than the detection limit (Figure 28C).

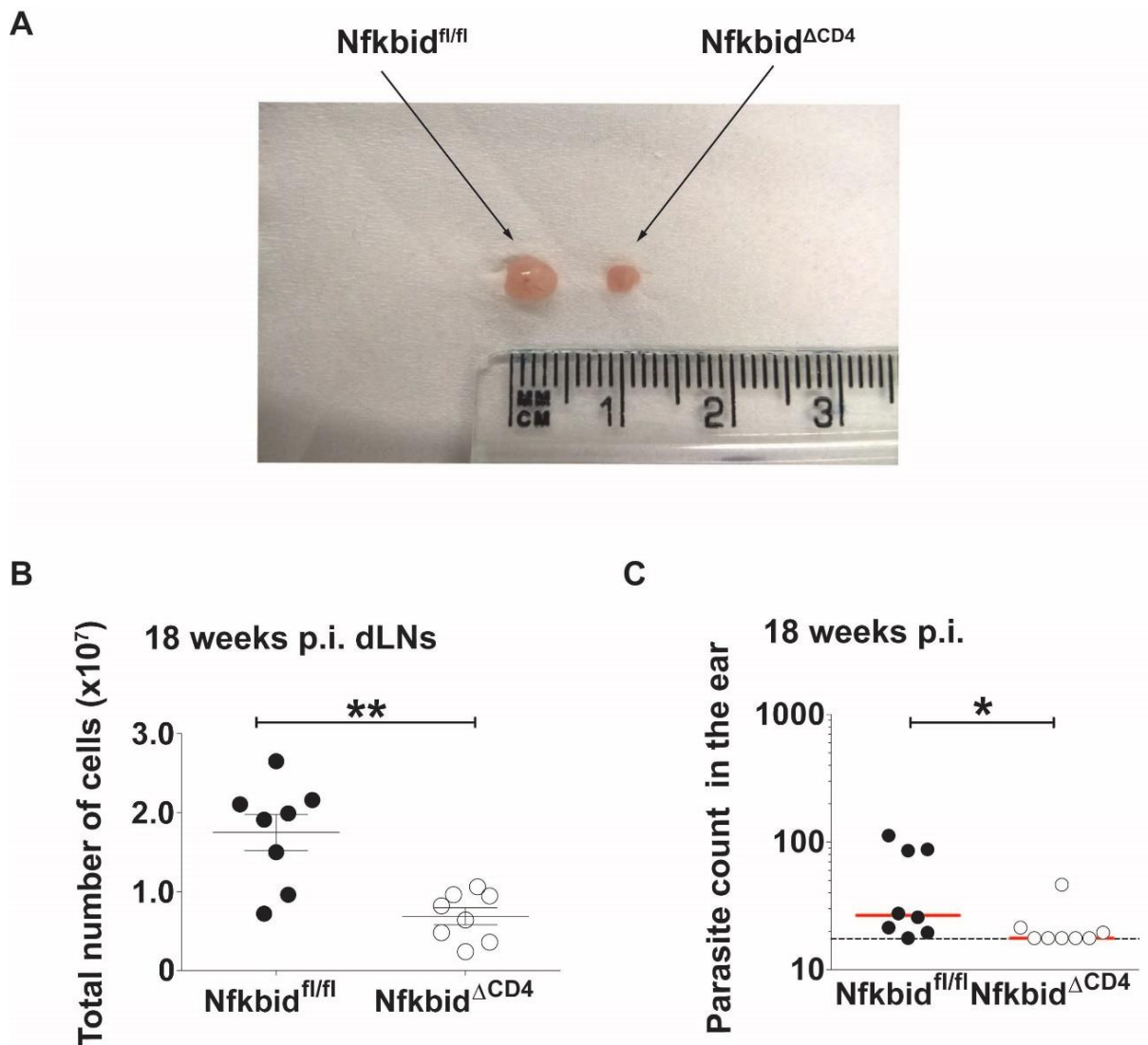


**Figure 28: Nfkbid<sup>ΔCD4</sup> mice have lower draining lymph node cellularity and L.m. parasite numbers than control mice 18 weeks post infection.** **A.** Draining lymph nodes of Nfkbid<sup>ΔCD4</sup> and Nfkbid<sup>fl/fl</sup> at 18 weeks post infection. **B.** Total cellularity of draining lymph nodes 18 weeks post infection. The graphs are shown as mean ±SEM and are representative of 2 independent experiments with n=4 Nfkbid<sup>ΔCD4</sup> and n=4 Nfkbid<sup>fl/fl</sup> mice per experiment. **C.** Total parasite counts in the ear pinna at 18 weeks post infection, as shown by limiting dilution assay. The graphs are shown as mean ±SEM and are representative of 2 independent experiments with n=4 Nfkbid<sup>ΔCD4</sup> and n=4 Nfkbid<sup>fl/fl</sup> mice per experiment.

Furthermore, when the activation status of CD4<sup>+</sup> T cells in the draining lymph nodes was investigated at 18 weeks post infection, Nfkbid<sup>ΔCD4</sup> mice were found to possess significantly lower percentages of CD44<sup>+</sup> CD62L<sup>-</sup> activated T cells, compared to control mice (Figure 29 A&B). Activated T cell percentages in the spleen did not show the same difference (Figure 29B), which could be explained by the localized nature of the infection. The close to normal

activated CD4<sup>+</sup> T cell percentages could be suggesting that Nfkbid<sup>ΔCD4</sup> mice have cleared the infection.

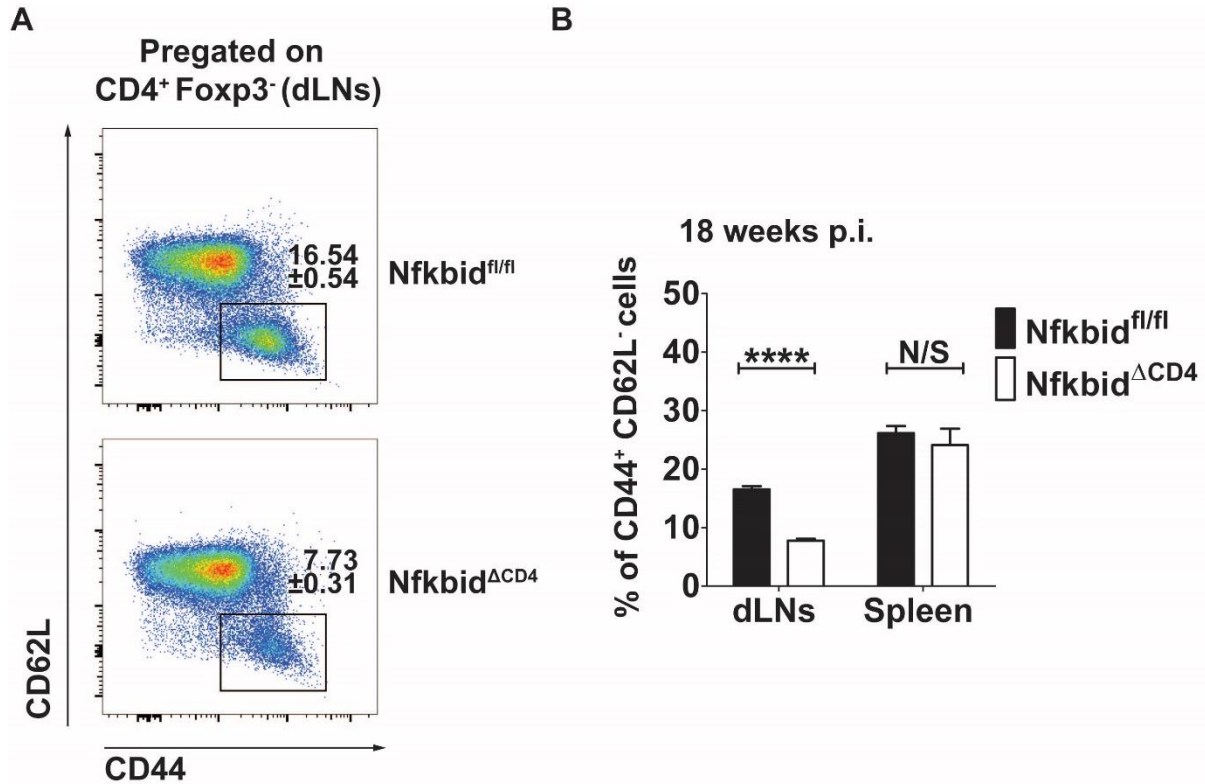
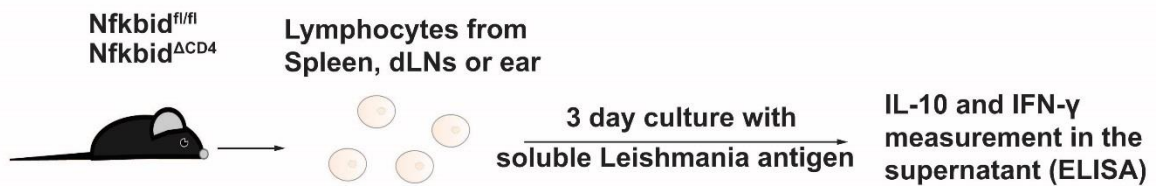


**Figure 29: Nfkbid<sup>ΔCD4</sup> mice have lower percentages of activated CD4<sup>+</sup> T cells than control mice 18 weeks post infection.** **A.** Representative FACS plots of flow cytometric analysis of CD4<sup>+</sup> T cell activation status in Nfkbid<sup>ΔCD4</sup> and control mice, at 18 weeks post infection. The plots are shown as mean ± SEM and are representative of 2 independent experiments with n=4 Nfkbid<sup>ΔCD4</sup> and n=4 Nfkbid<sup>fl/fl</sup> mice per experiment. **B.** Cumulative graph of percentages of CD4<sup>+</sup> T cell activation status of the same experiments depicted on A. The graphs are shown as mean ± SEM and are representative of 2 independent experiments with n=4 Nfkbid<sup>ΔCD4</sup> and n=4 Nfkbid<sup>fl/fl</sup> mice per experiment.

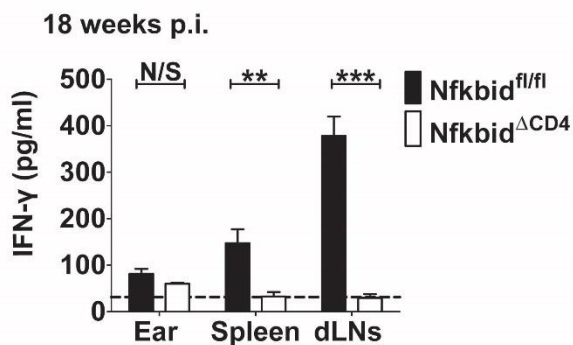
To further investigate whether Nfkbid<sup>ΔCD4</sup> have cleared the *L. major* infection the response to re-stimulation was measured. This is because it has been reported that IL-10-deficient mice, or mice where Tregs are depleted, completely clear the parasites and lose the ability to form a memory response<sup>123,149</sup>. To achieve this, lymphocytes from ear, draining lymph nodes and spleen of infected Nfkbid<sup>ΔCD4</sup> and Nfkbid<sup>fl/fl</sup> mice at 18 weeks post infection, were re-stimulated *in vitro* with soluble Leishmania antigen. After a period of 3 days, IL-10 and IFN $\gamma$  expression was measured by ELISA (Figure 30A). Supernatants from the Nfkbid<sup>ΔCD4</sup> lymphocyte culture, did not contain IL-10 and IFN $\gamma$  much higher than the detection limit of 32 pg/ml (Figure 30B&C). In contrast, supernatants from control mice contained high

amounts of IFN $\gamma$  in lymphocyte cultures from spleen and draining lymph nodes and high amounts of IL-10 in lymphocyte cultures from ear and draining lymph nodes (Figure 30B&C). This seems to support the hypothesis that Nfkbid $\Delta$ CD4 have cleared the infection at the 18 week time point.

A



B



C

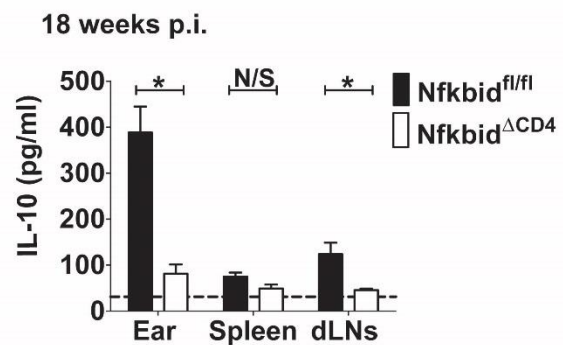


**Figure 30: Lymphocytes from Nfkbid $\Delta$ CD4 mice 18 weeks post infection do not respond to *Leishmania major* soluble leishmania antigen stimulation.** A. Lymphocytes from Nfkbid $\Delta$ CD4 and Nfkbid<sup>fl/fl</sup> spleens, draining lymph nodes and ear were incubated with SLA (50  $\mu$ g/ml) for a period of three days. Then, supernatants were collected and IFN $\gamma$  and IL-10 was measured by ELISA assay. B. Cumulative graph of IFN $\gamma$  concentration of the experiments described in A. The graphs are shown as mean  $\pm$ SEM and are representative of 2 independent experiments with n=4 Nfkbid $\Delta$ CD4 and n=4 Nfkbid<sup>fl/fl</sup> mice per experiment. C. Cumulative graph of IL-10 concentration of the experiments described in A. The graphs are shown as mean  $\pm$ SEM and are representative of 1 independent experiment with n=4 Nfkbid $\Delta$ CD4 and n=4 Nfkbid<sup>fl/fl</sup> mice per experiment.

#### **4.2.4: $Nfkbid^{\Delta CD4}$ mice have reduced Treg percentages in the spleen and draining lymph node during *L. major* infection, but higher Treg percentages at the site of infection, compared to control mice**

Since a phenotype that has been associated with regulatory T cells was found in 4.2.3. it was logical to monitor Treg percentages during infection. It was found that similarly to the steady state, the percentages of  $CD4^+$   $Foxp3^+$  T cells were significantly reduced in the spleen and draining lymph nodes of  $Nfkbid^{\Delta CD4}$  mice, compared to control mice, both at 3 weeks and 18 weeks post *L. major* infection (Figure 31A&B). However, the percentages of  $CD4^+$   $Foxp3^+$  T cells in the infected ear were significantly higher in  $Nfkbid^{\Delta CD4}$  mice, compared to control mice, at 3 weeks post infection (Figure 31C). Tregs in the ear 18 weeks post infection were not possible to be measured, due to the lesion having healed.

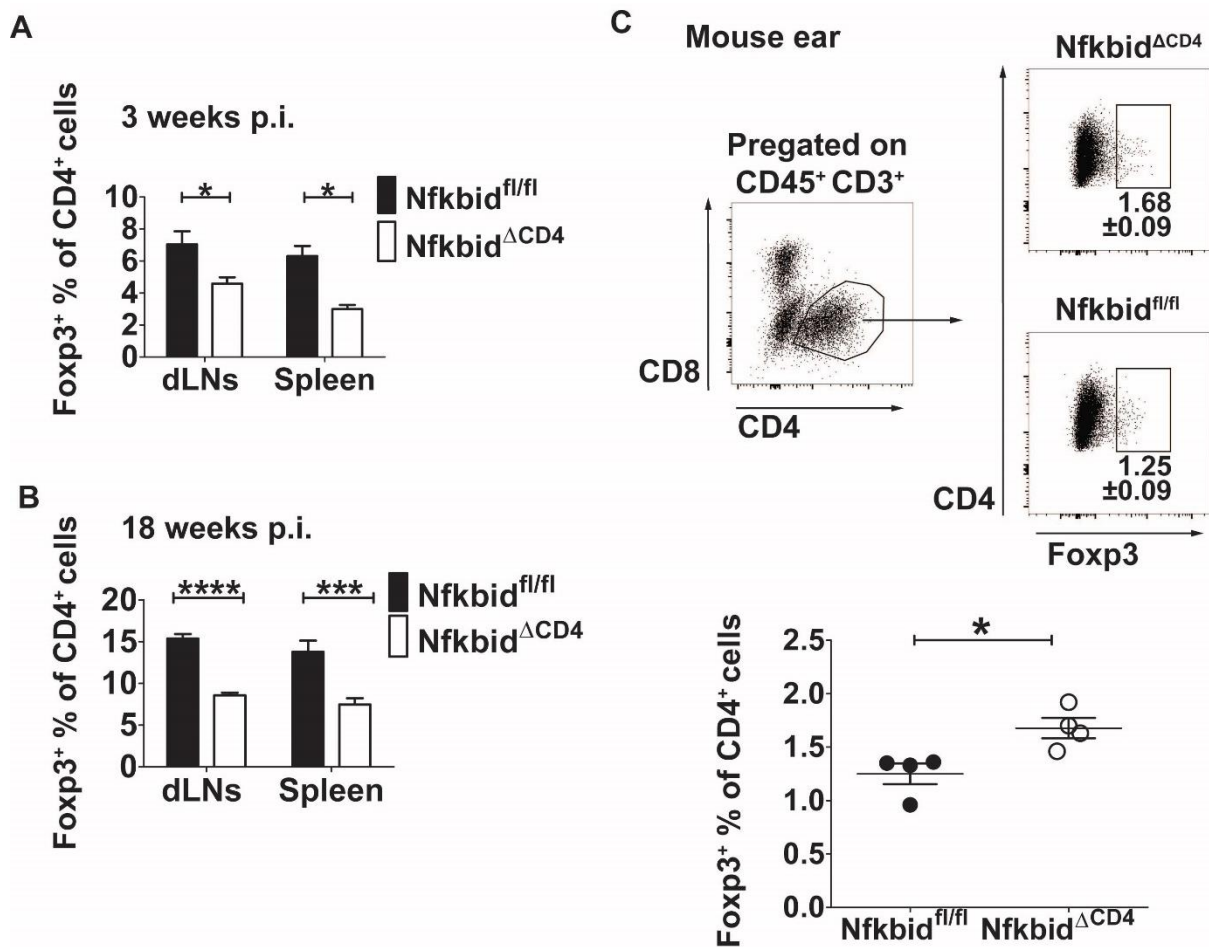


**Figure 31: Nfkbid<sup>ΔCD4</sup> mice have lower percentages of Tregs in dLNs and spleen, but higher in the ear than control mice during infection.** **A.** Cumulative graph of percentages of Tregs in dLNs and spleen of Nfkbid<sup>ΔCD4</sup> and Nfkbid<sup>fl/fl</sup> 3 weeks post infection. The graphs are shown as mean ±SEM and are representative of 2 independent experiments with n=4 Nfkbid<sup>ΔCD4</sup> and n=4 Nfkbid<sup>fl/fl</sup> mice per experiment. **B.** Cumulative graph of percentages of Tregs in dLNs and spleen of Nfkbid<sup>ΔCD4</sup> and Nfkbid<sup>fl/fl</sup> 18 weeks post infection. The graphs are shown as mean ±SEM and are representative of 2 independent experiments with n=4 Nfkbid<sup>ΔCD4</sup> and n=4 Nfkbid<sup>fl/fl</sup> mice per experiment. **C.** (upper panel) Representative FACS plots of flow cytometric analysis of Tregs in the ear of Nfkbid<sup>ΔCD4</sup> and control mice, at 3 weeks post infection. The plots are shown as mean ±SEM and are representative of 1 independent experiment with n=4 Nfkbid<sup>ΔCD4</sup> and n=4 Nfkbid<sup>fl/fl</sup> mice. (lower panel) Cumulative graph of percentages of Tregs of the same experiment depicted on the upper panel. The graphs are shown as mean ±SEM and are representative of 1 independent experiment with n=4 Nfkbid<sup>ΔCD4</sup> and n=4 Nfkbid<sup>fl/fl</sup> mice.

To further confirm whether Tregs are truly elevated in the ear of Nfkbid<sup>ΔCD4</sup> mice at 3 weeks post infection, immunohistochemical staining was performed. Sections of the ear lesion and the draining lymph node were made and Foxp3<sup>+</sup> cells (brown) were stained (Figure32A). Then 10 40x reading frames were selected randomly per mouse and the average number of

Foxp3<sup>+</sup> cells was counted (Figure 32B). It is clear that although there is a significantly smaller number of Foxp3<sup>+</sup> cells in the draining lymph node of Nfkbid<sup>ΔCD4</sup> mice, compared to control mice, there is a significantly higher number of Foxp3<sup>+</sup> cells in the ear lesion (Figure 32A&B). This confirms the result shown in Figure 31.

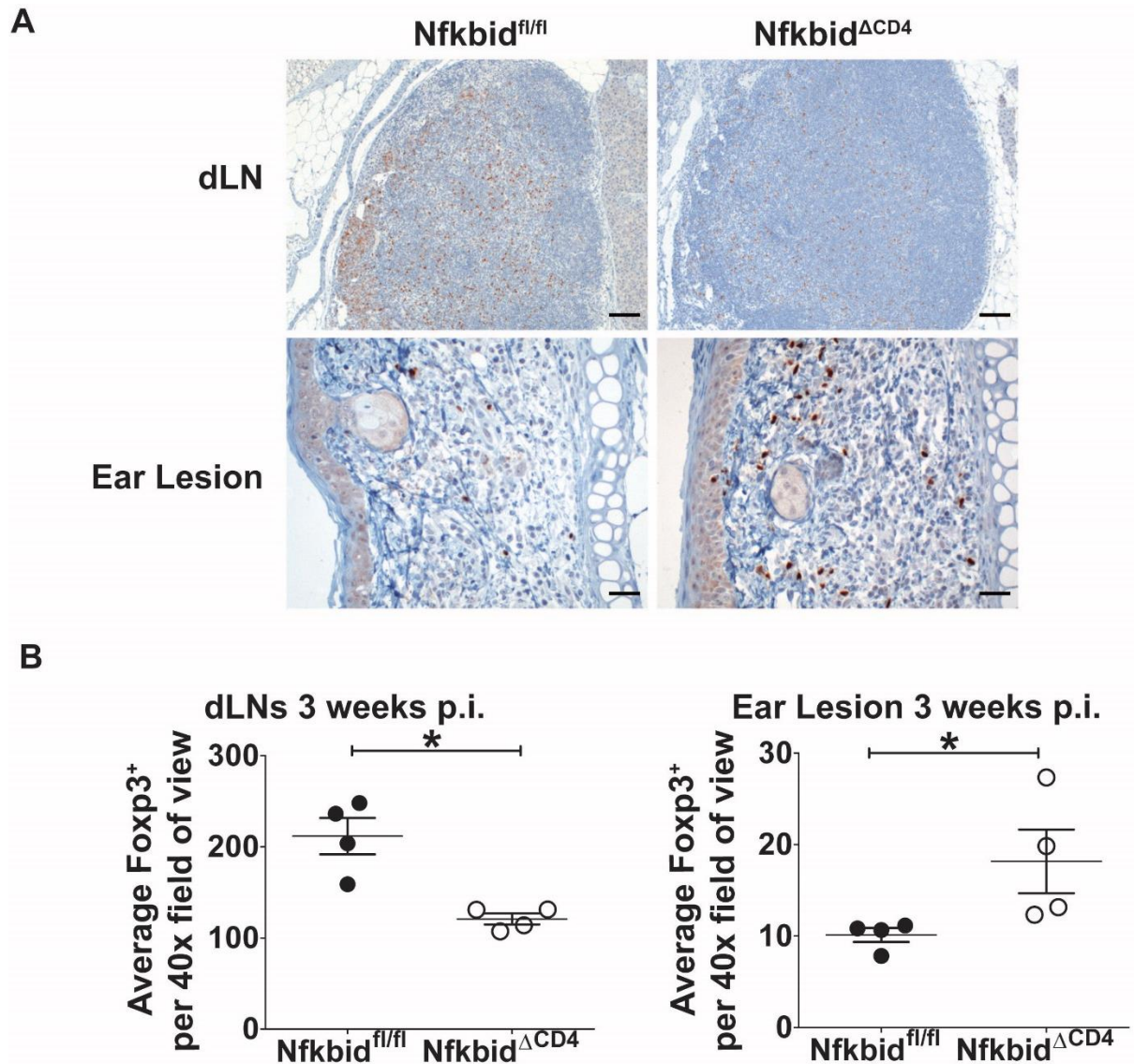


**Figure 32: Nfkbid<sup>ΔCD4</sup> mice have lower percentages of Tregs in dLNs, but higher in the ear than control mice during infection.** **A.** Immuno-histological staining of Foxp3 (brown dots) of the draining lymph node and ear lesion of Nfkbid<sup>ΔCD4</sup> and Nfkbid<sup>fl/fl</sup> 3 weeks post infection. The results are representative of 1 independent experiment with n=4 Nfkbid<sup>ΔCD4</sup> and n=4 Nfkbid<sup>fl/fl</sup> mice. **B.** Cumulative graph of Tregs numbers of the same experiment depicted on A. 10 40x open reading frames were selected blindly and average Foxp3<sup>+</sup> cells were counted blindly per mouse, then each dot depicts the average for each mouse. The graphs are shown as mean ± SEM and are representative of 1 independent experiment with n=4 Nfkbid<sup>ΔCD4</sup> and n=4 Nfkbid<sup>fl/fl</sup> mice.

#### 4.2.5: $Nfkbid^{\Delta CD4}$ mice show signs of an earlier starting immune response to *L. major*, compared to control mice

Since a smaller number of *L. major* parasites was found in  $Nfkbid^{\Delta CD4}$  mice at 3 weeks post infection, but no differences were found in immune cell numbers, iNos expression at the site of infection or percentages of activated T cells in the draining lymph nodes, looking at an earlier point of the infection seemed sensible. Thus, the 1.5 week post infection time point was investigated. During this, the total draining lymph node cellularity of  $Nfkbid^{\Delta CD4}$  mice was found to be significantly higher than control mice, but the percentages of  $CD44^+ CD62L^-$  activated T cells showed no significant difference (Figure 33A). Total parasite counts and percentages of infected innate immune cells in the ear, also showed no difference between  $Nfkbid^{\Delta CD4}$  and  $Nfkbid^{fl/fl}$  mice (Figure 33B). When looking at percentages of  $CD4^+$  T cells, dendritic cells, macrophages and neutrophils, a significantly higher percentage of dendritic cells was found in  $Nfkbid^{\Delta CD4}$  mice (Figure 33C left panel). But a smaller percentage of iNos expressing infected DCs was observed in  $Nfkbid^{\Delta CD4}$  mice, compared to control mice (Figure 33C right panel). Moreover, when  $CD4^+ CD44^+ CD62L^-$  activated T cells were sorted from spleen, and IFN $\gamma$  and IL-10 mRNA ratios to the housekeeping gene UBC were measured through RT-qPCR,  $Nfkbid^{\Delta CD4}$  had a significantly higher ratio of IFN $\gamma$  and lower ratio of IL-10, compared to control mice (Figure 33D). Although the phenotype is not very strong, the higher draining lymph node cellularity, the DC inflation and the IFN $\gamma$  and IL-10 mRNA transcription in activated T cells, might suggest that the immune response in  $Nfkbid^{\Delta CD4}$  mice is begins faster compared to control mice.

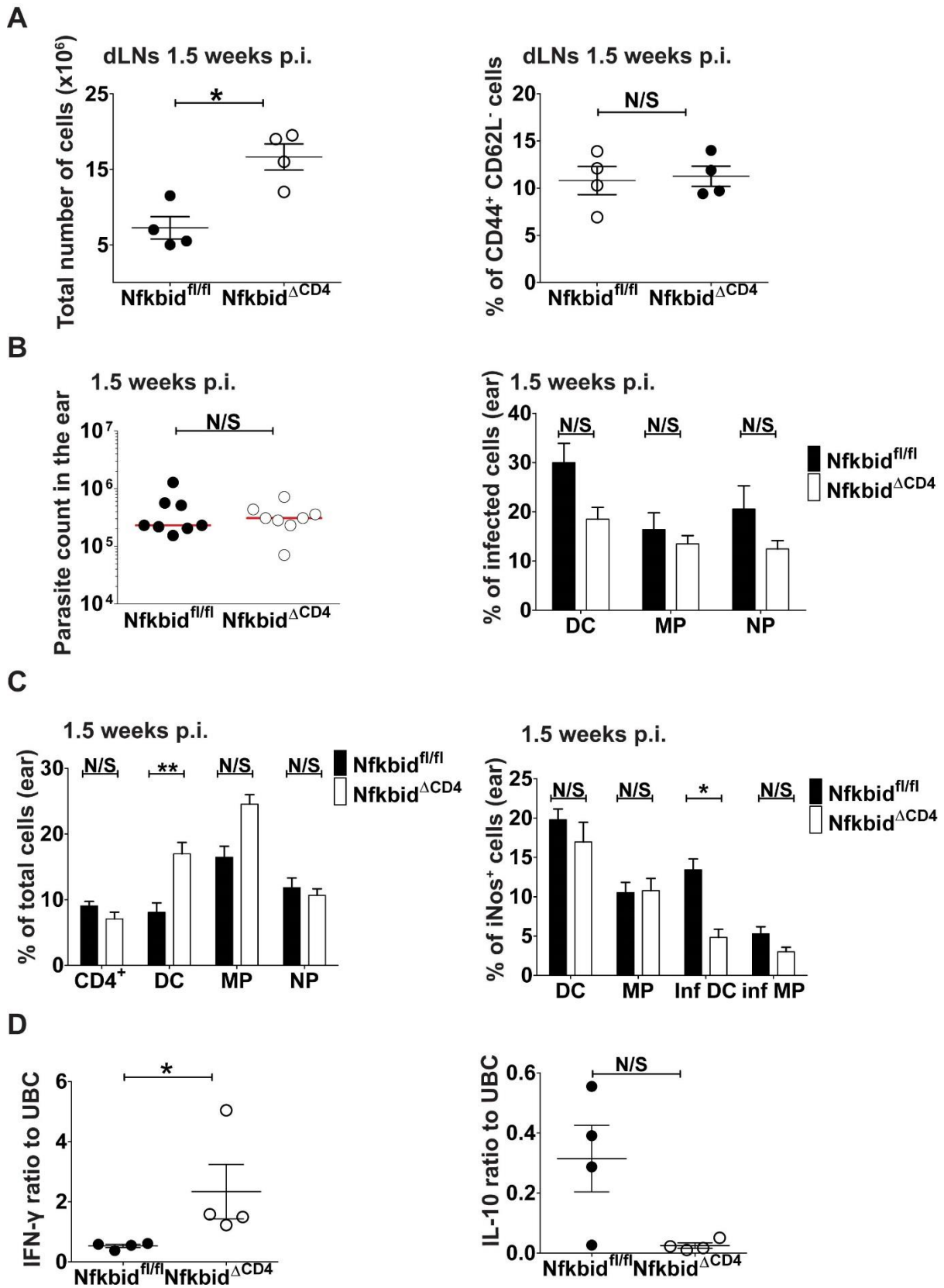


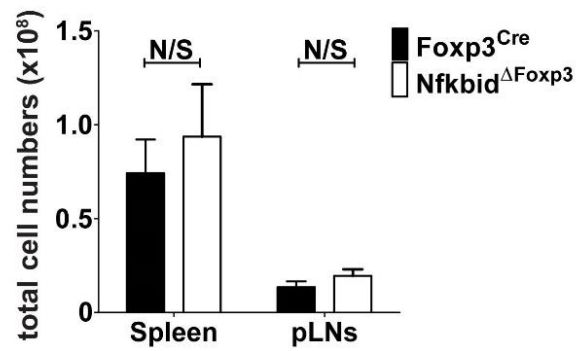
**Figure 33: *Nfkbid* <sup>$\Delta$ CD4</sup> mice show mild signs of an accelerated immune response at 1.5 weeks post infection, compared to control mice. A. (left panel) Total cellularity of draining lymph nodes 1.5 weeks post infection. The graphs are shown as mean  $\pm$  SEM and are representative of 1 independent experiment with n=4 *Nfkbid* <sup>$\Delta$ CD4</sup> and n=4 *Nfkbid*<sup>fl/fl</sup> mice per experiment. (right panel) Cumulative**

graph of percentages of CD4<sup>+</sup> T cell activation status of the same experiment depicted on the left panel. The graphs are shown as mean  $\pm$ SEM and are representative of 1 independent experiment with n=4 Nfkbid <sup>$\Delta$ CD4</sup> and n=4 Nfkbid<sup>fl/fl</sup> mice. **B.** (left panel) Total parasite counts in the ear pinna at 1.5 weeks post infection, as shown by limiting dilution assay. The graphs are shown as mean  $\pm$ SEM and are representative of 2 independent experiments with n=4 Nfkbid <sup>$\Delta$ CD4</sup> and n=4 Nfkbid<sup>fl/fl</sup> mice per experiment. (right panel) Percentages infected dendritic cells, macrophages and neutrophils in the ear pinna at 1.5 weeks post infection, as shown by flow cytometry. The graphs are shown as mean  $\pm$ SEM and are representative of 1 independent experiment with n=4 Nfkbid <sup>$\Delta$ CD4</sup> and n=4 Nfkbid<sup>fl/fl</sup> mice. **C.** (left panel) Percentages CD4<sup>+</sup> T cells, dendritic cells, macrophages and neutrophils in the ear pinna at 1.5 weeks post infection, as shown by flow cytometry. The graphs are shown as mean  $\pm$ SEM and are representative of 1 independent experiment with n=4 Nfkbid <sup>$\Delta$ CD4</sup> and n=4 Nfkbid<sup>fl/fl</sup> mice. (right panel) Percentages of iNos expressing dendritic cells and macrophages in the ear pinna, infected or not infected with L.m. at 1.5 weeks post infection, as shown by flow cytometry. The graphs are shown as mean  $\pm$ SEM and are representative of 1 independent experiment with n=4 Nfkbid <sup>$\Delta$ CD4</sup> and n=4 Nfkbid<sup>fl/fl</sup> mice per experiment. **D.** Cumulative graphs of IFN $\gamma$  (right panel) and IL-10 (left panel) mRNA copies, compared to UBC, of sorted CD4<sup>+</sup> CD44<sup>+</sup> CD62L<sup>-</sup> cells from spleen at 1.5 weeks post infection. The graphs are shown as mean  $\pm$ SEM and are representative of 1 independent experiment with n=4 Nfkbid <sup>$\Delta$ CD4</sup> and n=4 Nfkbid<sup>fl/fl</sup> mice per experiment.

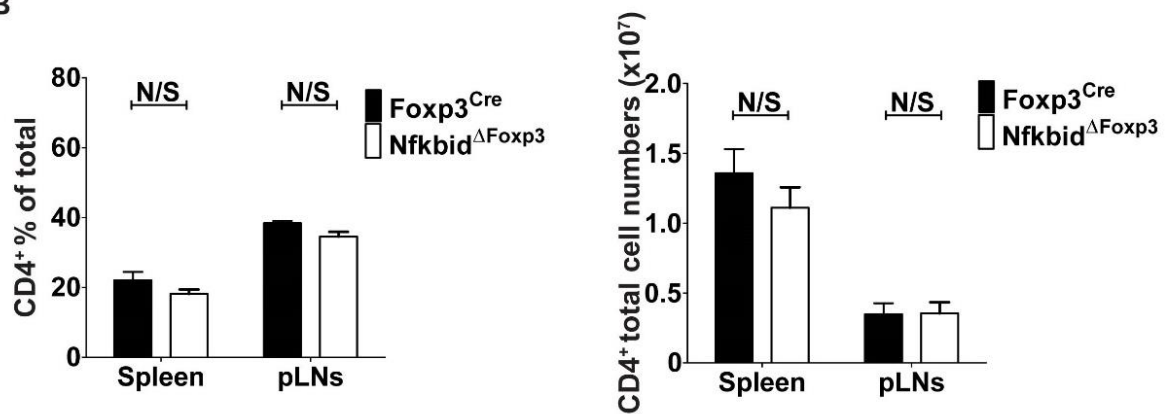
#### **4.2.6: Nfkbid <sup>$\Delta$ Foxp3</sup> mice have a normal regulatory T cell compartment and do not develop spontaneous autoimmunity by 8-11 weeks of age**

Nfkbid<sup>-/-</sup> mice have reduced numbers of regulatory T cells in the thymus and periphery, due to I $\kappa$ B<sub>NS</sub>-deficient T regs remaining in the CD4<sup>+</sup> Foxp3<sup>-</sup> CD25<sup>+</sup> GITR<sup>+</sup> precursor stage, since they are defective in Foxp3 induction during thymic selection<sup>112</sup>. In this thesis it was shown that when *Nfkbid* is deleted under the CD4 promoter, which leads to deletion before the precursor stage, the mice still have a reduced Treg compartment (Figure 23). Also, during *L. major* infection of Nfkbid <sup>$\Delta$ CD4</sup> mice a Treg-associated phenotype was observed. Therefore, a Foxp3-specific I $\kappa$ B<sub>NS</sub> knockout mouse line was generated. When characterizing the Nfkbid <sup>$\Delta$ Foxp3</sup> mice, no differences were observed in total cellularity of spleen and peripheral lymph nodes compared to control (cre only) mice (Figure 34A). Moreover, the percentages and total numbers of CD4<sup>+</sup> T cells in the spleen and peripheral lymph nodes of Nfkbid <sup>$\Delta$ Foxp3</sup> mice were not different, compared to control mice (Figure 34B). This held also true for CD8<sup>+</sup> T cells (Data not shown) Lastly, when looking at activated T cells, Nfkbid <sup>$\Delta$ Foxp3</sup> mice also show no difference to control mice (Figure 34C).

A



B



C

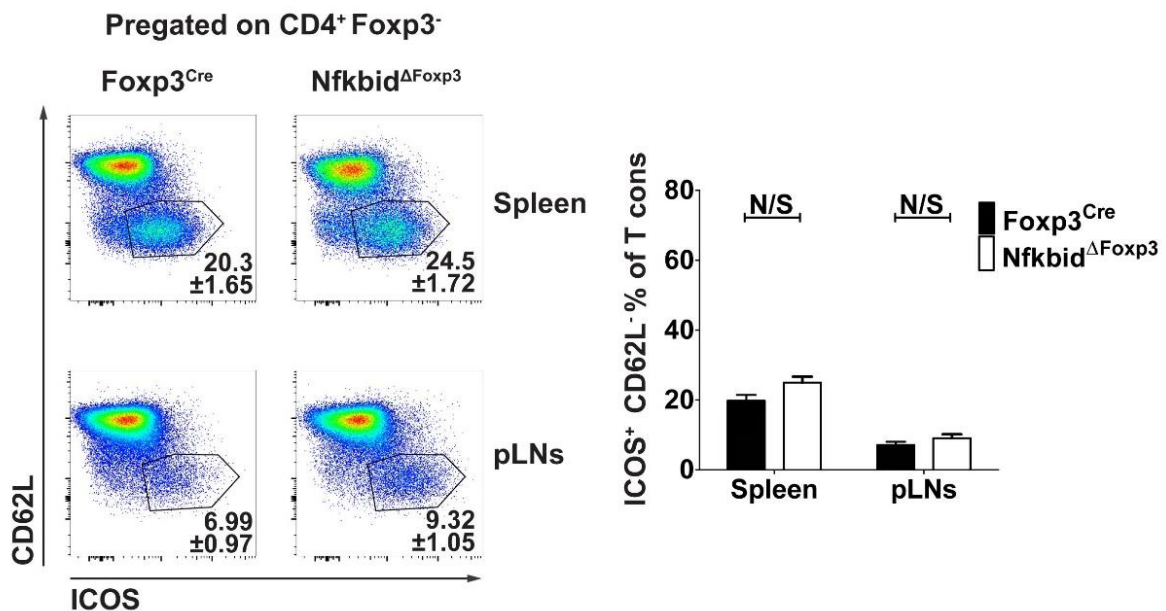


**Figure 34: Nfkbid<sup>ΔFoxp3</sup> mice have a normal CD4<sup>+</sup> T cell compartment, compared to control mice.** Total cellularity of spleen and peripheral lymph nodes of 8-11 week old Nfkbid<sup>ΔFoxp3</sup> and control mice. The graphs are shown as mean ± SEM and are representative of 3 independent experiment with n=4 Nfkbid<sup>ΔFoxp3</sup> and n=4 Nfkbid<sup>Wt/Wt</sup> Foxp3<sup>Cre</sup> mice per experiment. **B.** CD4<sup>+</sup> T cell percentages (left panel)

and total numbers (right panel) in spleen and peripheral lymph nodes of  $Nfkbid^{\Delta Foxp3}$  and control mice. The data is shown as mean  $\pm$ SEM and are representative of 3 independent experiments with  $n=2$   $Nfkbid^{\Delta Foxp3}$  and  $n=2$   $Nfkbid^{Wt/Wt} Foxp3^{Cre}$  mice per experiment. **C.** (left panel) Representative FACS plots of flow cytometric analysis of CD4<sup>+</sup> T cell activation status in  $Nfkbid^{\Delta Foxp3}$  and control mice. The plots are shown as mean  $\pm$ SEM and are representative of 3 independent experiments with  $n=2$   $Nfkbid^{\Delta Foxp3}$  and  $n=2$   $Nfkbid^{Wt/Wt} Foxp3^{Cre}$  mice per experiment. (right panel) Cumulative graph of percentages of CD4<sup>+</sup> T cell activation status of the same experiments depicted on A. The graphs are shown as mean  $\pm$ SEM and are representative of 2 independent experiments with  $n=2$   $Nfkbid^{\Delta Foxp3}$  and  $n=2$   $Nfkbid^{Wt/Wt} Foxp3^{Cre}$  mice per experiment.

When looking at the Treg compartment,  $Nfkbid^{\Delta Foxp3}$  mice show no difference in Foxp3<sup>+</sup> T cell percentages and numbers in the spleen, pLNs or Thymus (Figure 35). This further supports existing literature, since in the  $Nfkbid^{\Delta Foxp3}$  mice I $\kappa$ B<sub>NS</sub> is deleted after Foxp3 is expressed, which happens after the CD4<sup>+</sup> Foxp3<sup>-</sup> CD25<sup>+</sup> GITR<sup>+</sup> precursor stage<sup>112</sup>.

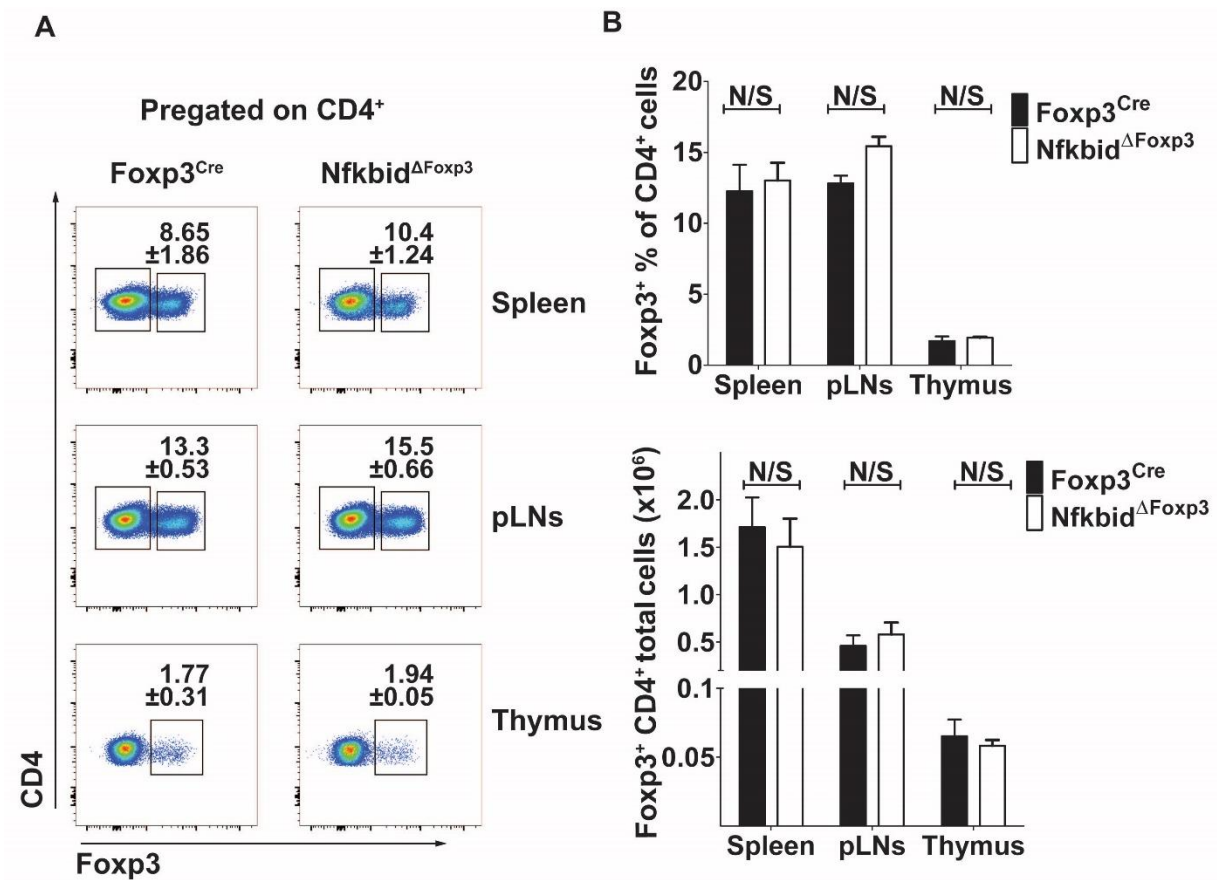


**Figure 35: Nfkbid<sup>ΔFoxp3</sup> mice have similar numbers of Tregs in the periphery, compared to control mice. A.** Representative FACS plots of flow cytometric analysis of Treg percentages in spleen, thymus and pLNs of Nfkbid<sup>ΔFoxp3</sup> and control mice. The plots are shown as mean ±SEM and are representative of 3 independent experiments with n=2 Nfkbid<sup>ΔFoxp3</sup> and n=2 Nfkbid<sup>wt/wt</sup> Foxp3<sup>Cre</sup> mice per experiment. **B.** Cumulative graph of Treg percentages (upper panel) and total numbers (lower panel) status of the same experiments depicted on A. The graphs are shown as mean ±SEM and are representative of 3 independent experiments with n=2 Nfkbid<sup>ΔFoxp3</sup> and n=2 Nfkbid<sup>wt/wt</sup> Foxp3<sup>Cre</sup> mice per experiment.

To further investigate the role of IκB<sub>NS</sub> in Tregs, effector and naïve Tregs were sorted (Figure 36A) from Nfkbid<sup>ΔFoxp3</sup> and control mice and differential expression analysis was performed. For sorting of Foxp3<sup>+</sup> cells YFP was expressed under the *Foxp3* promoter. As effector, CD4<sup>+</sup> CD25<sup>+</sup> Foxp3<sup>+</sup> CD44<sup>+</sup> CD62L<sup>-</sup> cells were defined and as naïve CD4<sup>+</sup> CD25<sup>+</sup> Foxp3<sup>+</sup> CD44<sup>-</sup> CD62L<sup>+</sup>. Similar to the total percentages of Tregs (Figure 35) effector and naïve Treg percentages were not different between Nfkbid<sup>ΔFoxp3</sup> and control mice (Figure 36B).

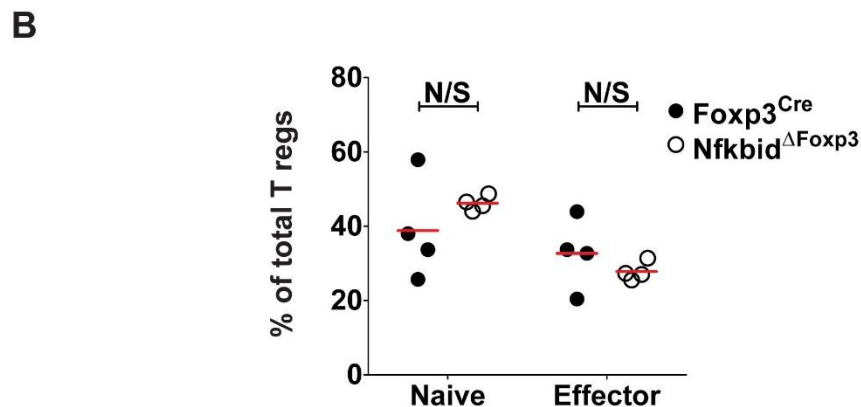
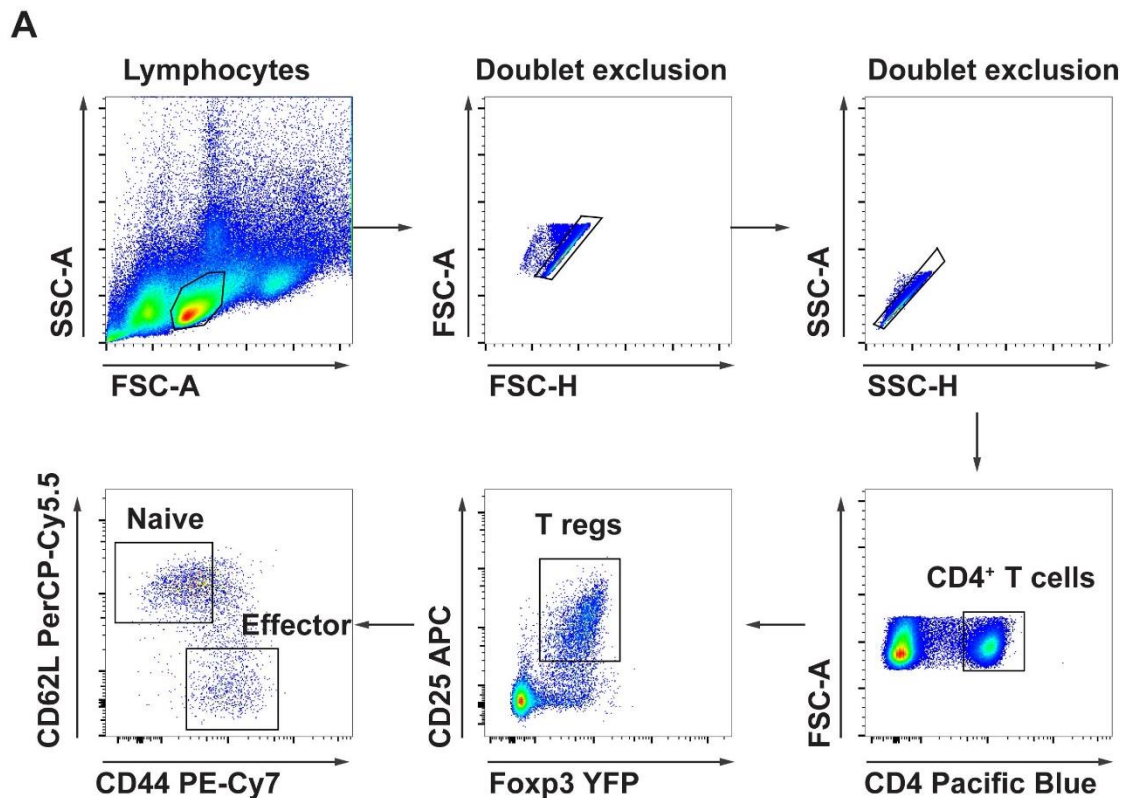


**Figure 36: Nfkbid<sup>ΔFxp3</sup> mice have similar percentages of effector and naïve Tregs in the periphery, compared to control mice.** Effector and naïve Tregs were sorted from pooled spleens and pLNs of Nfkbid<sup>ΔFxp3</sup> and Nfkbid<sup>Wt/Wt</sup> Fxp3<sup>Cre</sup> mice. For each sample 3 male and 3 female mice were pooled together. **A.** Sorting strategy for collection of effector and naïve Tregs for RNA sequencing. **B.** Percentages of naïve and effector Tregs from the sorting depicted in A. The graphs are shown as mean and are representative of 4 independent experiments with n=6 Nfkbid<sup>ΔFxp3</sup> and n=6 Nfkbid<sup>Wt/Wt</sup> Fxp3<sup>Cre</sup> mice per experiment.

Principal component analysis shows visible differences in differential expression between Nfkbid<sup>ΔFxp3</sup> and control mice. As we can see the four groups of samples are nicely separated in the four corners of the plot and the replicate samples (1,2,3) are clustering together. Effector Treg samples are as expected closer to each other than to the naïve Treg samples.

59.8% of the differences, in the selected differentially expressed genes, can be explained by the difference between naïve and effector and 10.8% between  $I\kappa B_{NS}$  knock out and control (Figure 37).

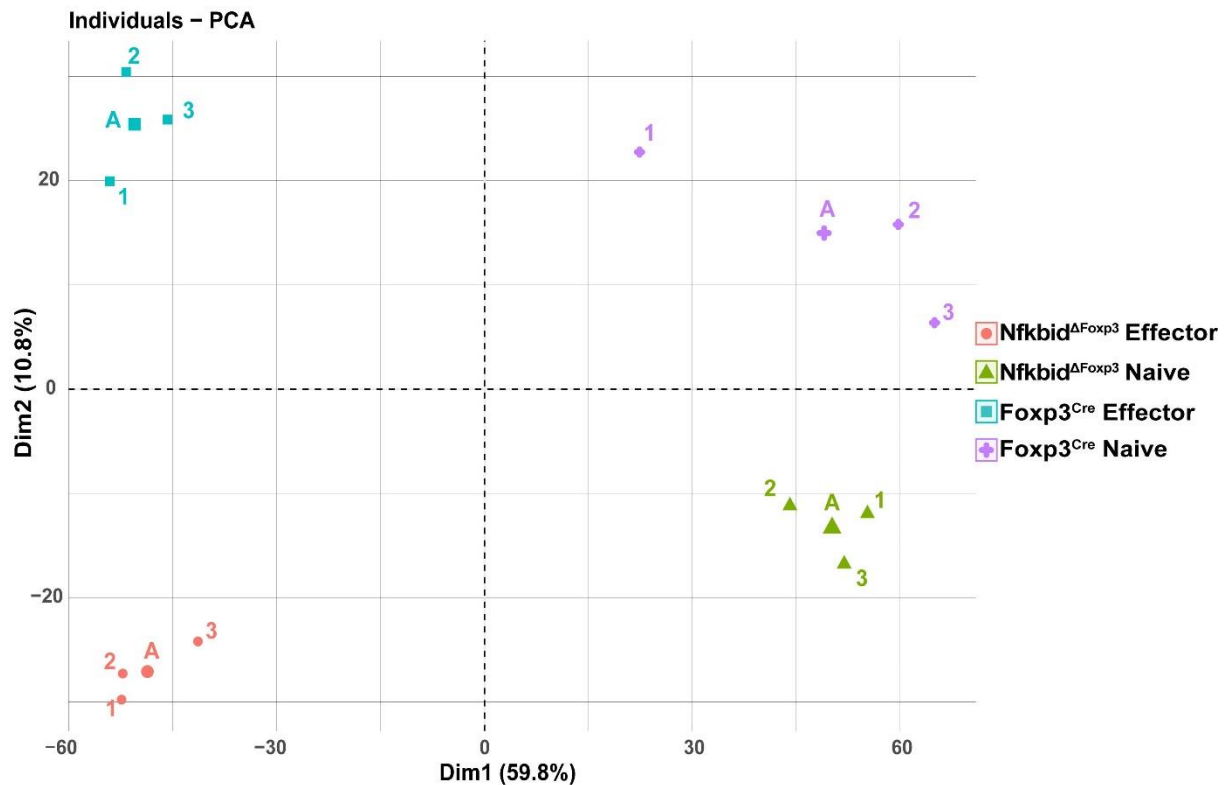


**Figure 37:  $I\kappa B_{NS}$ -deficient effector and naïve Tregs have strong differences in gene expression compared to control.** Principal component analysis of differentially expressed genes from effector and naïve Tregs from  $Nfkbid^{\Delta Foxp3}$  and  $Nfkbid^{Wt/Wt}$   $Foxp3^{Cre}$  mice. The 500 genes with the smallest false positive discovery rates were used. The 1,2,3 samples were collected as shown in figure 36 and the A point is the average of the 3. Each sample is representative of 3 male and 3 female pooled mice.

After gene clustering was performed, in the 500 differentially regulated genes with false positive discovery rate smaller than 0.05, four distinct gene clusters were found (Figure 38).

Cluster 1 is highly expressed in naïve control Tregs and is heavily downregulated in the  $I\kappa B_{NS}$ -deficient effector Tregs. When looking at the differences between the same cell type, it is observed that this cluster contains a lot of signalling genes containing Src homology domains (SH). For example *Tns1* codes for the protein tensin 1, which has been reported to enhance RhoA activity by binding DLC-1 through its SH2 homology domain<sup>150</sup>. In turn, RhoA has been shown to be required for TCR signalling<sup>151</sup>. *Tns1* is 3.6 fold downregulated in  $I\kappa B_{NS}$ -deficient effector Tregs and 1.4 fold in naïve, compared to the control. Another interesting molecule,

found downregulated in I $\kappa$ B<sub>NS</sub>-deficient Tregs, was *Nod1*. This gene codes for a pattern recognition receptor that can sense bacterial fragments and has been reported to cooperate with TLR2 to enhance TCR mediated activation of CD8<sup>+</sup> T cells<sup>152</sup>. Interestingly, *Lamp1* and *Snx20* were also found to be downregulated in I $\kappa$ B<sub>NS</sub>-deficient Tregs, which would match with the NK cell findings. *Foxp1* was similarly downregulated in effector Tregs. This is a transcription factor that regulates induced Treg generation<sup>153</sup>.

Cluster 2 contains genes that are upregulated in I $\kappa$ B<sub>NS</sub>-deficient effector and naïve Tregs, compared to the effector and naïve control, respectively. An interesting group of these genes are those that are implicated in WNT signaling. We see *Wnt3* and *Tcf7l1*, which is not surprising since WNT proteins regulate Tcf transcription factors<sup>154</sup>. *Pak4* has been associated with the WNT pathway by modulating intracellular translocation of  $\beta$ -catenin<sup>155</sup>. Notably, canonical Wnt3 signaling has been reported to negatively modulate Treg function and suppression capacity, while suppression of the pathway elevated it<sup>156</sup>.

Cluster 3 is composed of genes that are highly expressed in control effector Tregs, and downregulated in I $\kappa$ B<sub>NS</sub>-deficient effector and naïve Tregs. This cluster contains genes that are involved in Ca<sup>2+</sup> signaling. Both *Dmd* and *Ryr2* were heavily downregulated (4 fold and 4.9 fold respectively) in I $\kappa$ B<sub>NS</sub>-deficient effector Tregs, compared to the control. *Dmd* codes for the protein Dynein, which has been associated with aberrant calcium, through regulation of ion channels, although it's mechanism of action is not yet completely known<sup>157</sup>. The ryanodine receptor (RYR) is a Ca<sup>2+</sup> channel that facilitates release of calcium from intracellular stores<sup>158</sup>. This receptor is required for anti-CD3 induced T cell proliferation and IL-2 synthesis<sup>159</sup>. *Itpr2* codes for the 1,4,5-triphosphate receptor, type 2, which was reported to mediate the release of intracellular calcium deposits from the endoplasmic reticulum<sup>160</sup>. Interestingly, in this cluster *Ctla4*, *Cx3cl1* and *Ccr6* were also found to be downregulated in I $\kappa$ B<sub>NS</sub> knockout effector Tregs. *Ctla4* is one of the proteins Tregs use to suppress T cells, by blocking the CD28 co-activation signal<sup>161</sup>. The chemokine receptor CCR6 is expressed in effector Tregs and regulates their migration to inflammatory tissues<sup>162</sup>. Lastly, *Cx3cl1* codes for the unique cytokine fractalkine, that acts as chemoattractant of CX3CR1 expressing cells (NK cells, DCs, T helper and cytotoxic cells, macrophages) in its soluble form, and as an adhesion molecule, implicated in T-cell activation, in its membrane bound form<sup>163,164</sup>. *Cx3cl1* was 6.5 fold downregulated in I $\kappa$ B<sub>NS</sub>-deficient effector Tregs.

Cluster 4 contains genes that are upregulated in I $\kappa$ B<sub>NS</sub>-deficient Tregs, compared to their control counterparts. A plethora of cell cycle and proliferation genes are located in this cluster, some notable mentions would be the serine/threonine kinases *Cdk5r1* and *Cdk1* that control cell cycle checkpoints, as well as the aurora kinase B (*Aurkb*) that controls chromosome segregation during mitosis<sup>165–167</sup>. *Hapln1* was also found in this cluster and expression of this protein was associated with upregulated WNT signalling<sup>168</sup>. Interestingly, a few genes implicated with T-cell activation and Treg suppressive capacity, such as *Runx2*, *Runx3* and *Icam1*, were found in this cluster as well<sup>169–171</sup>.

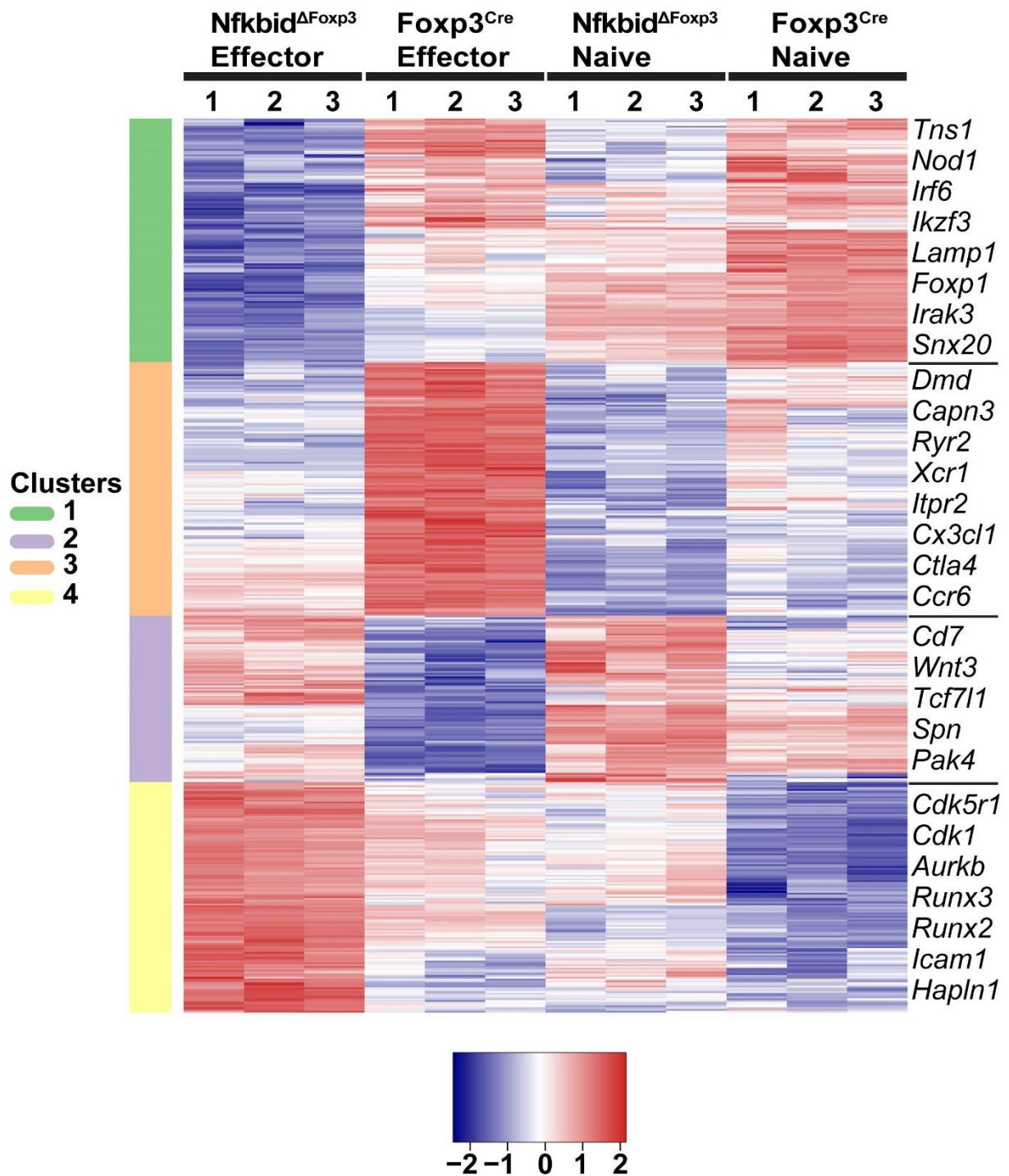


**Figure 38: Gene clustering reveals diverse gene expression in *I $\kappa$ B<sub>NS</sub>*-deficient effector and naïve Tregs compared to the control, forming 4 distinct gene clusters.** Gene clustering of the 500 differentially regulated genes with smallest false positive discovery rates (adjusted p value < 0.05). Blue colour means that the gene is downregulated and red that is upregulated. The clusters are colour as seen on the left and each sample (1,2,3) is shown in a row as depicted. On the right, a few representative genes of each cluster are shown.

## 5. Discussion

In the past years, a lot of important roles have been illuminated for I $\kappa$ B<sub>NS</sub> in T cells, B cells and macrophages (see 2.8), but little is known about its function in other immune cell types. Also, all studies to date have taken place in mouse models in which I $\kappa$ B<sub>NS</sub> is deleted in all cells, making it unclear whether observed effects are direct or a result of cross-play between cell types. The purpose of this thesis was to investigate the importance of I $\kappa$ B<sub>NS</sub> in effector cells of the immune system, and more specifically in NK cells, T cells and Tregs. For this, classical immunological techniques, such as FACS, were used in conjunction with novel conditional knock-out and reporter mouse models and cutting edge molecular techniques, such as RNA sequencing and differential expression analysis. Also, the importance of I $\kappa$ B<sub>NS</sub> in T cells was investigated *in vivo*, using the *Leishmania major* infection model, which is relevant for investigating T<sub>H</sub>1 and Treg immune responses. This is because T<sub>H</sub>1 cells are necessary for infection clearance and Tregs were associated with suppressing the immune response, leading to a slower early recovery and establishment of chronic cutaneous *Leishmania m.* infection<sup>123</sup>.

### 5.1 I $\kappa$ B<sub>NS</sub> in NK cells is responsible for maintaining T cell homeostasis

Natural killer cells have been shown to regulate the T cell immune response both in autoimmune and infection contexts<sup>172</sup>. For example, natural killer cells can regulate T cells indirectly by modulating dendritic cell function. In vitro experiments using human cells have shown that DCs promote NK cell activity via the production of type I interferon, IL-12 and TNF $\alpha$ , and subsequently NK cells secrete IFN $\gamma$  and TNF $\alpha$ , through engagement of NKp30, which further promotes DC maturation<sup>173-175</sup>.

Moreover, at the early stages of infection, NK cells migrate into the lymph node in a CXCR3 dependent but CCR7 independent manner and activate T cells directly by providing IFN $\gamma$ <sup>176</sup>. Also, NK cells have the ability to selectively lyse activated CD8<sup>+</sup> and CD4<sup>+</sup> T cells<sup>177</sup>. In the context of LCMV infection in mice, a lack of NK cells lead to prevention of the chronic form of the disease. The studies showed that, during the infection, NK cells lyse CD8<sup>+</sup> and CD4<sup>+</sup> T cells, which lead to reduced CD8<sup>+</sup> T cell numbers and function<sup>178-180</sup>. Furthermore, activated T cells have developed mechanisms to evade NK cell mediated killing. Studies have shown

that sensing of type I interferons is one of them, since *Ifnar*-deficient activated T cells were not able to protect themselves from NCR1-induced NK cell lysis, in contrast to wild type cells<sup>181,182</sup>.

In this study it was found that  $\text{I}\kappa\text{B}_{\text{NS}}$ -deficient NK cells show reduced CD107a expression after co-incubation with Yac-1 cells (Figure 11). This shows that NK cells lacking  $\text{I}\kappa\text{B}_{\text{NS}}$  have a degranulation defect, since CD107a (LAMP-1) is rapidly transferred to the membrane during degranulation and protects the cytotoxic cell from self lysis<sup>142,183</sup>. Since LAMP-1 comprises a large percentage of cytolytic granules and has a role in lysosome biogenesis and autophagy<sup>143</sup>, the number of acidic granules in wild type and  $\text{I}\kappa\text{B}_{\text{NS}}$  was investigated, but no differences were found (Figure 12). Also, no difference in NK cell cytotoxicity towards Yac-1 cells was observed (Figure 13). But, results from RNA sequencing and differential expression analysis, indicated that  $\text{I}\kappa\text{B}_{\text{NS}}$ -deficient NK cells have genes such as *Rab8b* and *Snx1* downregulated, in comparison to the control (Figure 17). Both of these genes have been implicated in vesicle trafficking inside the cell<sup>147,148</sup>, which could explain why transportation of CD107a to the membrane is impaired in  $\text{I}\kappa\text{B}_{\text{NS}}$ -deficient NK cells. Moreover, *Nfkbid* <sup>$\Delta\text{Ncr1}$</sup>  mice show an inflation of CD8<sup>+</sup> and CD4<sup>+</sup> T cells in the spleen at 22 weeks of age (Figure 15). However, the T cells do not exhibit an aberrant activation phenotype (Figure 16). This suggests that NK cells are controlling T cell numbers in the steady state. It has been shown that NK cells distinguish between activated and resting T cells based on NKG2D signalling, and selectively lyse activated ones<sup>177,179,180</sup>. Also, Yac-1 killing by NK cells, where a degranulation defect was observed (Figure 11), is NKG2D mediated<sup>141,184</sup>. So it is possible that the T cell inflation is observed because  $\text{I}\kappa\text{B}_{\text{NS}}$ -deficient NK cells fail to control T cell numbers due to impaired NKG2D signalling. Another possibility is that the observed T cell inflation is a direct result of NK cells modulating thymic development. However, although an NK cell population exists in the thymus, they follow a different maturation phenotype compared to conventional NK cells, and during their development do not express *Ncr1*<sup>185–187</sup>. This would lead to them not being  $\text{I}\kappa\text{B}_{\text{NS}}$ -deficient in *Nfkbid* <sup>$\Delta\text{Ncr1}$</sup>  mice.

The degranulation effect and vesicle trafficking in  $\text{I}\kappa\text{B}_{\text{NS}}$ -deficient NK cells should be further investigated. This can be done by looking at co-localization of CD107a with perforin and granzyme B, as well as real time movement of vesicles by using confocal microscopy. Also, *Rab8b* and *Snx1* knockout NK cell lines can be generated, or the genes can be deleted in

primary NK cells, with the CRISPR/Cas9 method<sup>188</sup>. Then the effect on degranulation can be compared to I $\kappa$ B<sub>NS</sub>-deficient NK cells. Moreover, to further investigate the T cell inflation, an *in vitro* NK cell cytotoxicity assay could be performed with activated T cells as targets. Lastly, immunophenotyping of thymic NK cells and T cell populations could be performed in Nfkbid<sup>ΔNcr1</sup> mice, to exclude the possibility that thymic NK cells are affected.

## 5.2 I $\kappa$ B<sub>NS</sub> may be suppressing B cell developmental pathways in NK cells

NK cells are mainly generated in the bone marrow and originate from a common lymphoid progenitor like many other cells of the immune system<sup>189</sup>. It has been reported that, in terms of development, NK cells have more similarities with T cells<sup>190</sup>. Which is also supported by the fact that a T cell subset exists that has characteristics of both T cells and NK cells, named NK T cells<sup>191</sup>. In this study it was found that I $\kappa$ B<sub>NS</sub> is expressed in NK cells both on the mRNA and protein level (Figure 3). This is also supported by a recent study, where RNA sequencing was used to identify and characterize NK cell subsets in the mouse and human. There, *Nfkbid* was frequently appearing as one of the characteristic genes<sup>192</sup>.

Surprisingly, when RNA sequencing and differential expression analysis was performed in I $\kappa$ B<sub>NS</sub>-deficient and control NK cells, a plethora of genes that are associated with B cells were found to be upregulated in the knock out (Figure 17). Among those were classical B cell markers such as CD19, CD79b and CIITA, but also the master transcription factors of B cell development Ebf1 and Pax5<sup>146,193</sup>. Both of these transcription factors are necessary for B cell lineage commitment, by suppressing genes that lead to generation of other immune cells from the CLP, but also for the production and maintenance of many mature B cell types<sup>194,195</sup>. Moreover, Ebf1-deficient mice lack marginal zone and B1 B cells and have reduced follicular and germinal center B cells<sup>196</sup>. If we take into account that I $\kappa$ B<sub>NS</sub>-deficient mice also lack marginal zone and B1 B cells, and also that Ebf1 is structurally similar to Rel proteins<sup>115,197</sup>, it is not improbable that I $\kappa$ B<sub>NS</sub> is regulating Ebf1, either in the protein or RNA level. Also, it appears that I $\kappa$ B<sub>NS</sub> is normally suppressing a B cell developmental pathway in NK cells.

Of course these results need to be further investigated. An immune phenotyping of I $\kappa$ B<sub>NS</sub>-deficient NK cells could show whether genes like CD19 are expressed on the protein level.

Also, co-immunoprecipitation could be performed to see whether I $\kappa$ B<sub>NS</sub> interacts directly with the Ebf1 protein. Additionally, chromatin immunoprecipitation could answer whether I $\kappa$ B<sub>NS</sub> is regulating the *Ebf1* gene.

### 5.3 I $\kappa$ B<sub>NS</sub> is necessary for the early stages of T<sub>H</sub>1 differentiation

It has been shown that the NF- $\kappa$ B family of transcription factors is important for T<sub>H</sub>1 differentiation<sup>95</sup>. For example, it is known that RelA/p65 is recruited to highly conserved, non-coding sequences on the enhancer region of the *Ifng* gene. This leads to impaired IFN $\gamma$  production in Th1 cells when p65 is missing<sup>99</sup>. Moreover, it has been speculated that RelA in conjunction with c-Rel work to drive *Ifng* transcription<sup>95</sup>. However, both p50 and c-Rel single deficiency has been shown to be dispensable for T<sub>H</sub>1 responses, since single deficient mice have normal IFN $\gamma$  production and T-bet expression<sup>97,198</sup>. Thus, different combinations of NF- $\kappa$ B proteins may be implicated in different T helper differentiation outcomes.

As an extra layer of regulation of the NF- $\kappa$ B pathway, the atypical I $\kappa$ B proteins are also involved in T<sub>H</sub>1 responses<sup>108</sup>. For example, I $\kappa$ B $\zeta$  counteracts RelA/p65 activity at the *Ifng* locus, which leads to reduced gene activity because of deacetylation of histones at the locus<sup>199</sup>. This happens because I $\kappa$ B $\zeta$  can interact with histone modifying enzymes<sup>200,201</sup>. Moreover Bcl-3 can act as a bridge to nuclear co-regulators<sup>202,203</sup>. Furthermore, although mice lacking Bcl-3 show an impaired T<sub>H</sub>1 response to intracellular pathogens, such as *Listeria monocytogenes* and *Toxoplasma gondii*<sup>204,205</sup>, T cell-specific deletion of I $\kappa$ B $\zeta$  results in increased IFN $\gamma$  expression<sup>199</sup>. Thus, different I $\kappa$ B proteins can have different effects on T<sub>H</sub>1 responses.

In the case of I $\kappa$ B<sub>NS</sub> it has been previously reported that deficiency leads to impaired *in vitro* T<sub>H</sub>1 differentiation, with reduced proliferation and IFN $\gamma$  production<sup>114,116</sup>. But during two different induced colitis models in mice, IFN $\gamma$  production was found to be increased instead<sup>112,113</sup>. Therefore it remained unknown whether I $\kappa$ B<sub>NS</sub> is important for the differentiation process or for terminally differentiated T<sub>H</sub>1 cells. In this study, the results from the Nfkbid<sup>LacZ</sup> mice clearly indicate that I $\kappa$ B<sub>NS</sub> is important at early stages of the Th1 development (Figure 18). It was obvious that when I $\kappa$ B<sub>NS</sub> was deleted at an early point of the

differentiation process, expression of CD44 and IFN $\gamma$  was significantly reduced, compared to the control. This effect could not be seen when I $\kappa$ B<sub>NS</sub> was deleted when T<sub>H</sub>1 cells were fully differentiated (Figure 20). However, the expression of the T<sub>H</sub>1-defining transcription factor T-bet<sup>206</sup> was not affected (Figure 20). This is suggesting that I $\kappa$ B<sub>NS</sub> is acting on different targets, leading to defective T<sub>H</sub>1 responses.

The induction of the transcription factor STAT1 by IFN $\gamma$  is important for successful amplification of T<sub>H</sub>1 differentiation<sup>89,90</sup>. Moreover, it has been shown that IL2<sup>-/-</sup> cells have impaired IFN- $\gamma$  production when cultured under Th1-polarizing conditions. This was attributed to the ability of IL-2 to upregulate the IL12RB2 and IL12RB1 receptors, which are necessary for T<sub>H</sub>1 differentiation but are not highly expressed in naïve T cells<sup>207</sup>. When growing under T<sub>H</sub>1 conditions, naïve T cells express large amounts of IL-2 after the initial TCR stimulation<sup>208</sup>. I $\kappa$ B<sub>NS</sub> has been shown to bind to the promoter of IL-2 and was implicated in the upregulation of the cytokine after anti-CD3 and anti-CD28 stimulation. Also I $\kappa$ B<sub>NS</sub>-deficient T cells have an *in vitro* proliferation defect that is rescued by the addition of IL-2 in the culture<sup>114</sup>. Thus, it can be speculated that the reduced IFN $\gamma$  and IL-2 expression in the absence of I $\kappa$ B<sub>NS</sub> is responsible for impaired T<sub>H</sub>1 responses. The exact mechanism should be further investigated.

#### **5.4 I $\kappa$ B<sub>NS</sub> deficiency in T cells leads to better disease outcome of *Leishmania major* infection in a Treg-related manner**

The common understanding about *Leishmania major* infection is that a T<sub>H</sub>1 response is responsible for clearance, because nitric oxide produced by IFN $\gamma$ -stimulated macrophages is responsible for parasite killing<sup>209</sup>. Conversely, a T<sub>H</sub>2 response is associated with a bad outcome for the disease<sup>210</sup>. Following infection, CD4<sup>+</sup> T cells are recruited to the site of the infection and although they don't directly interact with all macrophages, IFN $\gamma$  can act at long range<sup>211</sup>. After the infection has been resolved, immunity to re-infection is established in a CD4<sup>+</sup> T cell-mediated way<sup>212</sup>. This immunity to re-infection is maintained due to a small number of persisting parasites at the site of infection. These parasites survive due to an IL-10-mediated downregulation of the immune response, and their existence leads to the maintenance of a short-lived, *Leishmania major*-specific, population of CD4<sup>+</sup> that can

respond immediately upon re-infection<sup>124,213</sup>. IL-10-deficient mice, both the highly susceptible Balb/c and resistant C57BL/6 strains, completely clear the infection and in the process of losing this persisting parasite population, relinquish their immunity to re-infection<sup>124,214</sup>. During *Leishmania major* infection, IL-10 can be produced by myeloid cells, Tregs, and conventional T cells<sup>124,215,216</sup>. Regulatory T cells have been found in *Leishmania major* lesions, both in humans and mice, and after isolation they have been shown to possess a suppressive phenotype<sup>124,217,218</sup>. Natural Tregs from C57BL/6 mice home to the site of infection in a CCR5 dependent manner and suppress CD4<sup>+</sup> T cell responses, which promotes parasite persistence. This leads to CCR5-deficient mice having smaller parasite loads and a stronger immune response, which results to infection clearance similarly to mice lacking natural Tregs<sup>219,220</sup>.

Nfkbid<sup>ΔCD4</sup> mice have a reduced regulatory T cell compartment (Figure 23) and show impaired iTreg generation (Figure 24) and IFN $\gamma$  production after T<sub>H</sub>1 differentiation *in vitro* (Figure 22). Moreover, it was shown in chapter 5.3 that I $\kappa$ B<sub>NS</sub> is important for the early stages of T<sub>H</sub>1 differentiation. Therefore, it was logical to investigate the effect of I $\kappa$ B<sub>NS</sub> deficiency during *Leishmania major* infection. When Nfkbid<sup>ΔCD4</sup> mice were infected subcutaneously, a more favourable disease progression was observed compared to the control. This consisted of smaller ear thickness over a period of 18 weeks (Figure 25), as well as smaller parasite numbers at both 3 (Figure 26D) and 18 weeks (Figure 28C) post infection. Moreover, a significantly smaller percentage of infected dendritic cells, macrophages and neutrophils was observed at 3 weeks post infection (Figure 26C). This improved response against the infection suggests that the observed result is because of the regulatory T cell defect, since a T<sub>H</sub>1 problem would be expected to result in worse disease progression. Furthermore, at the very late timepoint of 18 weeks post infection, it was observed that Nfkbid<sup>ΔCD4</sup> mice were mostly parasite free (Figure 28C). Also, the inflammation had largely subsided in infected Nfkbid<sup>ΔCD4</sup> mice, manifesting as smaller draining lymph node cellularity (Figure 28A&B) and reduced percentages of activated CD4<sup>+</sup> CD44<sup>+</sup> CD62L<sup>-</sup> T cells (Figure 29). Moreover, lymphocytes from infected Nfkbid<sup>ΔCD4</sup> mice at 18 weeks post infection, failed to produce IFN $\gamma$  and IL-10 *in vitro* after soluble *Leishmania* antigen stimulation, in contrast to the control (Figure 30). Because the observed phenotype has been associated with the lack of Tregs and also with problems in their migration and function<sup>124,149,219</sup>, it is logical to conclude that this is a Treg influenced phenotype.

Interestingly, when looking at Treg percentages during the infection, they were found to be reduced in *Nfkbid*<sup>ΔCD4</sup> mice in dLNs and spleen at all examined time-points, but they were increased in the ear pinna at 3 weeks post infection (Figures 31&32). This could perhaps be explained by either a functional defect, since increased numbers of Tregs are normally associated with worse disease outcome<sup>124,219</sup>, so although they are increased their suppressive activity is reduced. Or it is possible that because a faster and stronger immune response takes place in *Nfkbid*<sup>ΔCD4</sup> mice, the infection is at a different stage, where the parasite numbers have been lowered (Figure 26D) and the increased Tregs are needed for limiting inflammation-induced damage and tissue repair<sup>221</sup>. There are indications that the early immune response is faster in *Nfkbid*<sup>ΔCD4</sup> mice. When investigating the very early time-point of 1.5 weeks post infection, the draining lymph node cellularity was increased in *Nfkbid*<sup>ΔCD4</sup> mice, showing a stronger immune response (Figure 33A). In addition, a significantly increased percentage of dendritic cells was observed at the site of infection. Dendritic cells are the main source of early IL-12 and therefore the initiators of the T<sub>H</sub>1 response<sup>222</sup>. Most dendritic cells during *Leishmania major* infection are derived from inflammatory monocytes that are recruited in the lesion, differentiate into DCs and migrate to the lymph node<sup>223</sup>. Thus, it can be speculated that the increased inflammatory environment due to the Treg defect in the steady state, could have led to the increased DC percentages. Moreover, CD4<sup>+</sup> CD44<sup>+</sup> CD62L<sup>-</sup> T cells in the spleen were found to be harbouring more mRNA of the *Ifng* and less of the *Il10* genes in *Nfkbid*<sup>ΔCD4</sup> mice at the same time point (Figure 33D), supporting the conclusion that there is increased inflammation early.

Due to extremely low numbers of Tregs in the ear lesion qRT-PCR is very difficult, so a very good experiment for dissecting their phenotype would be single cell RNA sequencing. Also, perhaps histological or FACS staining for Treg tissue repair molecules, such as amphiregulin<sup>224</sup>, in the ear at 3 weeks post infection could shed more light to the data. Finally, a re-infection with *Leishmania major*, could be used in order to completely confirm that *Nfkbid*<sup>ΔCD4</sup> mice completely clear the infection at 18 weeks post infection.

## 5.5 Differential expression analysis of naïve and effector Tregs from *Nfkbid*<sup>ΔFoxp3</sup> mice reveals a more active cell cycle profile, but also functional deficiency

After a Treg related phenotype was observed during *Leishmania major* infection (see chapter 5.4), it was logical to investigate the role of IκB<sub>NS</sub> in more depth. For this purpose *Nfkbid*<sup>ΔFoxp3</sup> mice were generated. Expectedly, the mice did not have a reduced regulatory T cell compartment (Figure 35) like *Nfkbid*<sup>ΔCD4</sup> (Figure 23) and *Nfkbid*<sup>-/-</sup> mice. This agrees with existing literature, stating that IκB<sub>NS</sub>-deficiency leads to Tregs being stuck in the Foxp3<sup>-</sup> CD4<sup>+</sup> CD25<sup>+</sup> GITR<sup>+</sup> precursor stage<sup>112</sup>. Because the deletion in *Nfkbid*<sup>ΔFoxp3</sup> mice happens after that stage, reduced numbers of Tregs in the periphery are not observed. Moreover *Nfkbid*<sup>ΔFoxp3</sup> mice did not develop autoimmunity until the age of 8 weeks and no differences in percentages of effector and naïve Tregs were observed between them and control mice (Figures 34&36).

However, when RNA sequencing and differential expression analysis was performed in effector and naïve Tregs from *Nfkbid*<sup>ΔFoxp3</sup> and control mice, apparent differences were observed (Figures 37&38). IκB<sub>NS</sub>-deficient Tregs, both effector and naïve, had upregulated a plethora of genes, such as *Cdk5r1*, *Cdk1* and *Aurkb*, that control cell cycle checkpoints and proliferation<sup>165-167</sup>. Interestingly, the heat map signature in cluster 4, where these genes are located, of IκB<sub>NS</sub>-deficient naïve Tregs is similar to control effector Tregs.

But, although IκB<sub>NS</sub>-deficient Tregs had a more active cell cycle profile, a lot of genes associated with release of intracellular calcium, such as *Dmd*, *Ryr2* and *Itpr2* were heavily downregulated<sup>157,158,160</sup>. This would suggest that IκB<sub>NS</sub>-deficient Tregs are impaired in their ability to raise intracellular Ca<sup>2+</sup>. The release of intracellular calcium ions is crucial for T cell receptor signal transduction, which is required for proper Treg differentiation and function<sup>225</sup>. Moreover, elevation of intracellular calcium is a critical early event in the activation of several signalling pathways, such as NFAT, NF-κB and JNK and thus determines the final response of an immune cell<sup>226</sup>.

Furthermore, WNT signalling was found to be upregulated in IκB<sub>NS</sub>-deficient Tregs. Not only the *Wnt3*, gene that forms the basis of the pathway, but also *Tcf7l1* and *Pak4*<sup>154,155</sup>. Elevated WNT signaling has been linked with reduced Treg suppressive ability<sup>156</sup>. In conjunction with

the downregulation of the suppressive molecule *Ctla4* and the chemokine receptor *Ccr6*, which is responsible for T cell homing to inflamed tissues<sup>74,161,162</sup>, it is obvious that I $\kappa$ B<sub>NS</sub>-deficient Tregs, both effector and naïve, seem to be functionally impaired. This could explain the phenotype that is observed during the *Leishmania major* infection experiments (Chapter 5.4), since calcium signalling impairment and WNT signalling are major pathways that are unlikely to be altered due to the inflammatory context.

Lastly, the transcription factor gene *Foxp1* was downregulated in I $\kappa$ B<sub>NS</sub>-deficient Tregs. This could also be revealing a functional deficiency, because Foxp1 has been shown to coordinate Foxp3 binding to chromatin, thus regulating Treg function and also to be essential for preserving an active Foxp3 locus in iTregs<sup>153,227</sup>. Foxp1-deficiency lead to Tregs having reduced IL-2 responsiveness and CTLA-4 expression<sup>227</sup>.

Of course, the RNA sequencing results would need to be validated. This could be done by performing qRT-PCR of important genes. In addition, in the case of calcium signalling, elevation of intracellular calcium after TCR stimulation can be measured by flow cytometry. Finally, the *Nfkb1d*<sup>ΔFoxp3</sup> mice could be infected with *Leishmania major* in order to better dissect the role of I $\kappa$ B<sub>NS</sub>-deficient Tregs in the infection model.

## 5.5 Conclusion

I $\kappa$ B<sub>NS</sub> plays a crucial role in T cell proliferation and function by regulating NF- $\kappa$ B signalling. In addition, its ability to act either as an enhancer or suppressor of NF- $\kappa$ B, depending on the cell type, allows it to fine tune the immune response and thus raises its potential as a future drug target<sup>107,108</sup>. Therefore, investigation of the role of I $\kappa$ B<sub>NS</sub> in the immune system is important. During this thesis, the expression of I $\kappa$ B<sub>NS</sub> in several types of immune cells was measured and its role in NK, T<sub>H</sub>1 and Treg cells was investigated by the use of novel conditional deletion mouse models.

In NK cells, I $\kappa$ B<sub>NS</sub> appears to be responsible for regulating T cell homeostasis in the steady state, perhaps by modulating vesicle transport and NKG2D signalling. It may also be suppressing a B cell developmental gene pathway. This is an interesting phenotype that should be further investigated.

In T cells, it was shown that I $\kappa$ B<sub>NS</sub> is necessary for the early stages of T<sub>H</sub>1 differentiation. Moreover, mice where I $\kappa$ B<sub>NS</sub> is missing in T cells, cope better with *Leishmania major* infection. This appears to be due to a faster early immune response, but also to the ability to clear the persisting infection at a very late stage. This phenotype has been associated with IL-10 deficiency or Treg impairment<sup>149,217,228</sup>. It was shown here, that calcium signalling impairment and WNT upregulation, could be responsible for impaired function of I $\kappa$ B<sub>NS</sub>-deficient effector and naïve Tregs. Also, I $\kappa$ B<sub>NS</sub> was found to regulate IL-10 in T<sub>H</sub>17 cells<sup>116</sup>.

The fact that I $\kappa$ B<sub>NS</sub>-deficiency in T cells does not cause autoimmunity but helps with clearance of *Leishmania major* raises the potential of I $\kappa$ B<sub>NS</sub> as a pharmacological target.

## 7. Table of abbreviations

ADAP	Adhesion and degranulation-promoting adapter protein
AhR	Aryl-hydrocarbon receptor
ANK	Ankyrin repeat
ARD	Ankyrin repeat domain
Aurkb	Aurora kinase B
cAMP	Cyclic adenosine monophosphate
Capn3	Calpain 3
Ccr6	Chemokine receptor 6
CD	Cluster of differentiation
Cdk	Cyclin dependent kinase
Ciita	Class II Major histocompatibility complex transactivator
CLP	Common lymphoid progenitor
CNS	Conserved non-coding sequence
CTLA-4	Cytotoxic T-lymphocyte associated protein 4
Cx3cl1	C-X3-C motif chemokine ligand 1
CXCR5	C-X-C motif chemokine receptor 5
DCs	Dendritic cells
dLNs	Draining lymph nodes
Dmd	Dystrophin
DNA	Deoxyribonucleic acid
Ebf1	Early B cell factor 1
FACS	Fluorescence-activated cell sorting
FCS	Fetal calf serum
Foxp1	Forkhead box protein 1
Foxp3	Forkhead box protein 3
GATA3	GATA binding protein 3
GM-CSF	Granulocyte macrophage colony stimulating factor
Hapln1	Haploitin 1
HO-1	Heme oxygenase 1
Icam1	Intercellular adhesion molecule 1
IFN $\gamma$	Interferon gamma
IgA	Immunoglobulin A
IgE	Immunoglobulin E
IKK	I kappa B kinase
Ikzf3	IKAROS family zinc finger 3
IL-10	Interleukin 10
IL-12	Interleukin 12
IL-13	Interleukin 13

IL-1 $\beta$	Interleukin 1 beta
IL-21	Interleukin 21
IL-22	Interleukin 22
IL-23	Interleukin 23
IL-27	Interleukin 27
IL-4	Interleukin 4
IL-5	Interleukin 5
IL-6	Interleukin 6
IL-7R $\alpha$	Interleukin 7 receptor alpha
IL-9	Interleukin 9
ILCs	Innate lymphoid cells
iNK	Immature natural killer cells
Irak3	Interleukin 1 receptor associated kinase 3
ITAM	Immunoreceptor tyrosine-based motif
Itpr2	Inositol 1,4,5-Triphosphate receptor type 2
iTreg	Induced Treg
LacZ	Lac operon Z
Lamp1	Lysosomal associated membrane protein 1
LCMV	Lymphocytic choriomeningitis mammarenavirus
LFA-1	Lymphocyte function associated antigen 1
LPS	Lipopolysaccharides
MHC	Major histocompatibility
MPs	Macrophages
mRNA	Messenger RNA
MTOC	Microtubule organizing centre
NF- $\kappa$ B	Nuclear factor binding to the $\kappa$ light-chain in B cells
Nfkbid	Nuclear factor $\kappa$ B inhibitor delta
NIK	NF- $\kappa$ B inducing kinase
NK	Natural killer cells
NK1.1	Natural killer 1.1
NKG2D	Natural killer group 2D
NKP	Natural killer precursor
NLS	Nuclear localization signal
Nod1	Nucleotide binding oligomerization domain containing 1
NPs	Neutrophils
Pak4	P21 activated kinase 4
PAMPs	Pathogen associated molecular patterns
Pax5	Paired box 5
PCR	polymerase chain reaction
pLNs	Peripheral lymph nodes
PMA	Phorbol 1-12-myristate-13-acetate
Rab8b	Ras related protein 8B
RHD	Rel homology domain
RLRs	Retinoic acid-inducible gene I-like receptors

RNA	Ribonucleic Acid
ROR $\gamma$ T	Retinoid-related orphan receptor gamma
Runx3	Runt-related transcription factor 1
Ryr2	Ryanodine receptor 2
SLA	Soluble leishmania antigen
SLAM	Signalling lymphocytic activating molecule
Snx1	Sortin nexin 1
Snx20	Sortin nexin 20
SPF	Specific pathogen free
Spn	Sialophorin
STAT	Signal transducer and activator of transcription
T-bet	T box expressed in T cells
TAD	Transcriptional activation domain
Tcf7l1	Transcription factor 7 like 1
TCR	T cell receptor
Tfh	Follicular helper T cells
TGF- $\beta$	Transforming growth factor beta
TH	Helper T cells
TLRs	Toll like receptors
TNF- $\alpha$	Tumor necrosis factor alpha
TNFRSF	Tumor necrosis factor superfamily receptor
Tns1	Tensin 1
Treg	Regulatory T cells
tTregs	Thymic derived regulatory T cells
Ubc	Ubiquitin C
Wnt3	Wingless type family member 3
Xcr1	X-C Motif chemokine receptor 1

## 8. Bibliography

1. Marshall, J. S., Warrington, R., Watson, W. & Kim, H. L. An introduction to immunology and immunopathology. *Allergy Asthma. Clin. Immunol.* **14**, 49 (2018).
2. Rioux, J. D. & Abbas, A. K. Paths to understanding the genetic basis of autoimmune disease. *Nature* **435**, 584–589 (2005).
3. Turvey, S. E. & Broide, D. H. Innate immunity. *J. Allergy Clin. Immunol.* **125**, S24–32 (2010).
4. Bonilla, F. A. & Oettgen, H. C. Adaptive immunity. *J. Allergy Clin. Immunol.* **125**, S33–S40 (2010).
5. Newton, K. & Dixit, V. M. Signaling in innate immunity and inflammation. *Cold Spring Harb. Perspect. Biol.* **4**, (2012).
6. Franz, K. M. & Kagan, J. C. Innate Immune Receptors as Competitive Determinants of Cell Fate. *Mol. Cell* **66**, 750–760 (2017).
7. Iwasaki, A. & Medzhitov, R. Regulation of adaptive immunity by the innate immune system. *Science* **327**, 291–5 (2010).
8. Seleme, M. C., Kosmac, K., Jonjic, S. & Britt, W. J. Tumor Necrosis Factor Alpha-Induced Recruitment of Inflammatory Mononuclear Cells Leads to Inflammation and Altered Brain Development in Murine Cytomegalovirus-Infected Newborn Mice. *J. Virol.* **91**, e01983-16 (2017).
9. Lacy, P. & Stow, J. L. Cytokine release from innate immune cells: association with diverse membrane trafficking pathways. *Blood* **118**, 9–18 (2011).
10. Cooper, M. D. & Alder, M. N. The Evolution of Adaptive Immune Systems. *Cell* **124**, 815–822 (2006).
11. Tonegawa, S. Somatic generation of antibody diversity. *Nature* **302**, 575–581 (1983).
12. Hesslein, D. G. T. & Schatz, D. G. Factors and Forces Controlling V(D)J Recombination. *Adv. Immunol.* **78**, 169–232 (2001).
13. Bassing, C. H., Swat, W. & Alt, F. W. The Mechanism and Regulation of Chromosomal V(D)J Recombination. *Cell* **109**, S45–S55 (2002).
14. Crotty, S. & Ahmed, R. Immunological memory in humans. *Semin. Immunol.* **16**, 197–203 (2004).
15. Farber, D. L., Netea, M. G., Radbruch, A., Rajewsky, K. & Zinkernagel, R. M. Immunological memory: lessons from the past and a look to the future. *Nat. Rev. Immunol.* **16**, 124–128 (2016).
16. Paul, W. E. Bridging innate and adaptive immunity. *Cell* **147**, 1212–5 (2011).
17. Blander, J. M. & Medzhitov, R. Toll-dependent selection of microbial antigens for presentation by dendritic cells. *Nature* **440**, 808–812 (2006).
18. Esensten, J. H., Helou, Y. A., Chopra, G., Weiss, A. & Bluestone, J. A. CD28 Costimulation: From Mechanism to Therapy. *Immunity* **44**, 973–988 (2016).
19. Acuto, O. & Michel, F. CD28-mediated co-stimulation: a quantitative support for TCR

- signalling. *Nat. Rev. Immunol.* **3**, 939–951 (2003).
20. O’Sullivan, T. E., Sun, J. C. & Lanier, L. L. Natural Killer Cell Memory. *Immunity* **43**, 634–645 (2015).
  21. Martinez-Gonzalez, I., Mathä, L., Steer, C. A. & Takei, F. Immunological Memory of Group 2 Innate Lymphoid Cells. *Trends Immunol.* **38**, 423–431 (2017).
  22. Cerwenka, A. & Lanier, L. L. Natural killer cell memory in infection, inflammation and cancer. *Nat. Rev. Immunol.* **16**, 112–123 (2016).
  23. Bezman, N. A. *et al.* Molecular definition of the identity and activation of natural killer cells. *Nat. Immunol.* **13**, 1000–1009 (2012).
  24. Lucas, M., Schachterle, W., Oberle, K., Aichele, P. & Diefenbach, A. Dendritic Cells Prime Natural Killer Cells by trans-Presenting Interleukin 15. *Immunity* **26**, 503–517 (2007).
  25. Lanier, L. L. NK CELL RECOGNITION. *Annu. Rev. Immunol.* **23**, 225–274 (2005).
  26. Lanier, L. L. Up on the tightrope: natural killer cell activation and inhibition. *Nat. Immunol.* **9**, 495–502 (2008).
  27. Dustin, M. L. & Groves, J. T. Receptor Signaling Clusters in the Immune Synapse. *Annu. Rev. Biophys.* **41**, 543–556 (2012).
  28. Pagoon, S. V *et al.* Superresolution microscopy reveals nanometer-scale reorganization of inhibitory natural killer cell receptors upon activation of NKG2D. *Sci. Signal.* **6**, ra62 (2013).
  29. Bryceson, Y. T., Ljunggren, H.-G. & Long, E. O. Minimal requirement for induction of natural cytotoxicity and intersection of activation signals by inhibitory receptors. *Blood* **114**, 2657–66 (2009).
  30. Clément, M.-V. *et al.* Involvement of granzyme B and perforin gene expression in the lytic potential of human natural killer cells. *Res. Immunol.* **141**, 477–489 (1990).
  31. Mace, E. M. *et al.* Cell biological steps and checkpoints in accessing NK cell cytotoxicity. *Immunol. Cell Biol.* **92**, 245–255 (2014).
  32. Kumar, S. Natural killer cell cytotoxicity and its regulation by inhibitory receptors. *Immunology* **154**, 383–393 (2018).
  33. Fauriat, C., Long, E. O., Ljunggren, H.-G. & Bryceson, Y. T. Regulation of human NK-cell cytokine and chemokine production by target cell recognition. *Blood* **115**, 2167–76 (2010).
  34. Paolini, R., Bernardini, G., Molfetta, R. & Santoni, A. NK cells and interferons. *Cytokine Growth Factor Rev.* **26**, 113–120 (2015).
  35. Reefman, E. *et al.* Cytokine secretion is distinct from secretion of cytotoxic granules in NK cells. *J. Immunol.* **184**, 4852–62 (2010).
  36. Vivier, E., Ugolini, S. & Nunès, J. A. ADAPted secretion of cytokines in NK cells. *Nat. Immunol.* **14**, 1108–1110 (2013).
  37. Rosmaraki, E. E. *et al.* Identification of committed NK cell progenitors in adult murine bone marrow. *Eur. J. Immunol.* **31**, 1900–1909 (2001).
  38. Geiger, T. L. & Sun, J. C. Development and maturation of natural killer cells. *Curr. Opin. Immunol.* **39**, 82–89 (2016).
  39. Kim, S. *et al.* In vivo developmental stages in murine natural killer cell maturation. *Nat.*

- Immunol.* **3**, 523–528 (2002).
40. Plank, M. W. *et al.* Th22 Cells Form a Distinct Th Lineage from Th17 Cells In Vitro with Unique Transcriptional Properties and Tbet-Dependent Th1 Plasticity. *J. Immunol.* **198**, 2182–2190 (2017).
  41. Kara, E. E. *et al.* Tailored Immune Responses: Novel Effector Helper T Cell Subsets in Protective Immunity. *PLoS Pathog.* **10**, e1003905 (2014).
  42. Zhu, J. & Paul, W. E. Peripheral CD4<sup>+</sup> T-cell differentiation regulated by networks of cytokines and transcription factors. *Immunol. Rev.* **238**, 247–262 (2010).
  43. Joffre, O., Nolte, M. A., Spörri, R. & Sousa, C. R. e. Inflammatory signals in dendritic cell activation and the induction of adaptive immunity. *Immunol. Rev.* **227**, 234–247 (2009).
  44. Golubovskaya, V. & Wu, L. Different Subsets of T Cells, Memory, Effector Functions, and CAR-T Immunotherapy. *Cancers (Basel)*. **8**, (2016).
  45. Korzus, E. *et al.* Transcription Factor-Specific Requirements for Coactivators and Their Acetyltransferase Functions. *Science (80-. )*. **279**, 703–707 (1998).
  46. Szabo, S. J. *et al.* A Novel Transcription Factor, T-bet, Directs Th1 Lineage Commitment. *Cell* **100**, 655–669 (2000).
  47. Pennock, N. D. *et al.* T cell responses: naive to memory and everything in between. *Adv. Physiol. Educ.* **37**, 273–83 (2013).
  48. Taylor-Robinson, A. W., Phillips, R. S., Severn, A., Moncada, S. & Liew, F. Y. The role of TH1 and TH2 cells in a rodent malaria infection. *Science* **260**, 1931–4 (1993).
  49. Taylor-Robinson, A. W. & Phillips, R. S. Functional characterization of protective CD4<sup>+</sup> T-cell clones reactive to the murine malaria parasite *Plasmodium chabaudi*. *Immunology* **77**, 99–105 (1992).
  50. Zheng, W. & Flavell, R. A. The transcription factor GATA-3 is necessary and sufficient for Th2 cytokine gene expression in CD4 T cells. *Cell* **89**, 587–96 (1997).
  51. Veldhoen, M. *et al.* Transforming growth factor- $\beta$  ‘reprograms’ the differentiation of T helper 2 cells and promotes an interleukin 9–producing subset. *Nat. Immunol.* **9**, 1341–1346 (2008).
  52. Dardalhon, V. *et al.* IL-4 inhibits TGF- $\beta$ -induced Foxp3<sup>+</sup> T cells and, together with TGF- $\beta$ , generates IL-9<sup>+</sup> IL-10<sup>+</sup> Foxp3<sup>-</sup> effector T cells. *Nat. Immunol.* **9**, 1347–1355 (2008).
  53. Goswami, R. & Kaplan, M. H. A brief history of IL-9. *J. Immunol.* **186**, 3283–8 (2011).
  54. Schmitt, E., Klein, M. & Bopp, T. Th9 cells, new players in adaptive immunity. *Trends Immunol.* **35**, 61–68 (2014).
  55. Perumal, N. B. & Kaplan, M. H. Regulating IL9 transcription in T helper cells. *Trends Immunol.* **32**, 146–150 (2011).
  56. Aarvak, T., Chabaud, M., Miossec, P. & Natvig, J. B. IL-17 is produced by some proinflammatory Th1/Th0 cells but not by Th2 cells. *J. Immunol.* **162**, 1246–51 (1999).
  57. Mangan, P. R. *et al.* Transforming growth factor- $\beta$  induces development of the TH17 lineage. *Nature* **441**, 231–234 (2006).
  58. Huang, W., Na, L., Fidel, P. L. & Schwarzenberger, P. Requirement of Interleukin-17A for Systemic Anti-*Candida albicans* Host Defense in Mice. *J. Infect. Dis.* **190**, 624–631 (2004).

59. Yang, X. O. *et al.* T Helper 17 Lineage Differentiation Is Programmed by Orphan Nuclear Receptors ROR $\alpha$  and ROR $\gamma$ . *Immunity* **28**, 29–39 (2008).
60. Puel, A. *et al.* Autoantibodies against IL-17A, IL-17F, and IL-22 in patients with chronic mucocutaneous candidiasis and autoimmune polyendocrine syndrome type I. *J. Exp. Med.* **207**, 291–7 (2010).
61. Liu, X. *et al.* Bcl6 expression specifies the T follicular helper cell program in vivo. *J. Exp. Med.* **209**, 1841–1852 (2012).
62. Breitfeld, D. *et al.* Follicular B helper T cells express CXC chemokine receptor 5, localize to B cell follicles, and support immunoglobulin production. *J. Exp. Med.* **192**, 1545–52 (2000).
63. Liang, S. C. *et al.* Interleukin (IL)-22 and IL-17 are coexpressed by Th17 cells and cooperatively enhance expression of antimicrobial peptides. *J. Exp. Med.* **203**, 2271–2279 (2006).
64. Trifari, S., Kaplan, C. D., Tran, E. H., Crellin, N. K. & Spits, H. Identification of a human helper T cell population that has abundant production of interleukin 22 and is distinct from TH-17, TH1 and TH2 cells. *Nat. Immunol.* **10**, 864–871 (2009).
65. Duhon, T., Geiger, R., Jarrossay, D., Lanzavecchia, A. & Sallusto, F. Production of interleukin 22 but not interleukin 17 by a subset of human skin-homing memory T cells. *Nat. Immunol.* **10**, 857–863 (2009).
66. Tang, Q. & Bluestone, J. A. The Foxp3<sup>+</sup> regulatory T cell: a jack of all trades, master of regulation. *Nat. Immunol.* **9**, 239–244 (2008).
67. Sakaguchi, S., Sakaguchi, N., Asano, M., Itoh, M. & Toda, M. Immunologic self-tolerance maintained by activated T cells expressing IL-2 receptor  $\alpha$ -chains (CD25). Breakdown of a single mechanism of self-tolerance causes various autoimmune diseases. *J. Immunol.* **155**, 1151–64 (1995).
68. Van Parijs, L., Abbas, A. K. & Sakaguchi, S. Homeostasis and self-tolerance in the immune system: turning lymphocytes off. *Science* **280**, 243–8 (1998).
69. Gavin, M. A. *et al.* Foxp3-dependent programme of regulatory T-cell differentiation. *Nature* **445**, 771–775 (2007).
70. Zheng, Y. & Rudensky, A. Y. Foxp3 in control of the regulatory T cell lineage. *Nat. Immunol.* **8**, 457–462 (2007).
71. Lee, W. & Lee, G. R. Transcriptional regulation and development of regulatory T cells. *Exp. Mol. Med.* **50**, e456 (2018).
72. Kim, J. M., Rasmussen, J. P. & Rudensky, A. Y. Regulatory T cells prevent catastrophic autoimmunity throughout the lifespan of mice. *Nat. Immunol.* **8**, 191–197 (2007).
73. Eleonora Gambineri, T. R. T. H. D. O. Immune dysregulation, polyendocrinopathy, enteropathy, and X-linked inheritance (ipex), a syndrome of systemic autoimmunity caused by mutations of &lt; *Curr. Opin. Rheumatol.* **15**, 430–435 (2003).
74. Rowshanravan, B., Halliday, N. & Sansom, D. M. CTLA-4: a moving target in immunotherapy. *Blood* **131**, 58–67 (2018).
75. Qin, H.-Y. *et al.* A novel mechanism of regulatory T cell-mediated down-regulation of autoimmunity. *Int. Immunol.* **18**, 1001–1015 (2006).
76. Sen, R. & Baltimore, D. Multiple nuclear factors interact with the immunoglobulin enhancer sequences. *Cell* **46**, 705–716 (1986).

77. Zhang, Q., Lenardo, M. J. & Baltimore, D. 30 Years of NF- $\kappa$ B: A Blossoming of Relevance to Human Pathobiology. *Cell* **168**, 37–57 (2017).
78. Hayden, M. S. & Ghosh, S. NF- $\kappa$ B, the first quarter-century: remarkable progress and outstanding questions. *Genes Dev.* **26**, 203–34 (2012).
79. Hayden, M. S. & Ghosh, S. NF- $\kappa$ B in immunobiology. *Cell Res.* **21**, 223–244 (2011).
80. Liu, T., Zhang, L., Joo, D. & Sun, S.-C. NF- $\kappa$ B signaling in inflammation. *Signal Transduct. Target. Ther.* **2**, 17023 (2017).
81. Hayden, M. S. & Ghosh, S. Shared Principles in NF- $\kappa$ B Signaling. *Cell* **132**, 344–362 (2008).
82. Smale, S. T. Dimer-specific regulatory mechanisms within the NF- $\kappa$ B family of transcription factors. *Immunol. Rev.* **246**, 193–204 (2012).
83. Ghosh, S., May, M. J. & Kopp, E. B. NF- $\kappa$ B AND REL PROTEINS: Evolutionarily Conserved Mediators of Immune Responses. *Annu. Rev. Immunol.* **16**, 225–260 (1998).
84. Pannicke, U. *et al.* Deficiency of Innate and Acquired Immunity Caused by an IKK $\beta$  Mutation. *N. Engl. J. Med.* **369**, 2504–2514 (2013).
85. Orange, J. S. *et al.* Deficient natural killer cell cytotoxicity in patients with IKK-gamma/NEMO mutations. *J. Clin. Invest.* **109**, 1501–9 (2002).
86. Hoshino, K. *et al.* Cutting edge: generation of IL-18 receptor-deficient mice: evidence for IL-1 receptor-related protein as an essential IL-18 binding receptor. *J. Immunol.* **162**, 5041–4 (1999).
87. Gross, O. *et al.* Multiple ITAM-coupled NK-cell receptors engage the Bcl10/Malt1 complex via Carma1 for NF-kappaB and MAPK activation to selectively control cytokine production. *Blood* **112**, 2421–8 (2008).
88. Kwon, H.-J. *et al.* Stepwise phosphorylation of p65 promotes NF- $\kappa$ B activation and NK cell responses during target cell recognition. *Nat. Commun.* **7**, 11686 (2016).
89. Hibbert, L., Pflanz, S., de Waal Malefyt, R. & Kastelein, R. A. IL-27 and IFN- $\alpha$  Signal via Stat1 and Stat3 and Induce T-Bet and IL-12R  $\beta$  2 in Naive T Cells. *J. Interf. Cytokine Res.* **23**, 513–522 (2003).
90. Lighvani, A. A. *et al.* T-bet is rapidly induced by interferon-gamma in lymphoid and myeloid cells. *Proc. Natl. Acad. Sci. U. S. A.* **98**, 15137–42 (2001).
91. Hollneder, G. A. *et al.* Monoallelic Expression of the Interleukin-2 Locus. *Science (80-. )*. **279**, 2118–2121 (1998).
92. Afkarian, M. *et al.* T-bet is a STAT1-induced regulator of IL-12R expression in naïve CD4+ T cells. *Nat. Immunol.* **3**, 549–557 (2002).
93. Kaplan, M. H., Sun, Y.-L., Hoey, T. & Grusby, M. J. Impaired IL-12 responses and enhanced development of Th2 cells in Stat4-deficient mice. *Nature* **382**, 174–177 (1996).
94. Liao, W., Lin, J.-X. & Leonard, W. J. IL-2 family cytokines: new insights into the complex roles of IL-2 as a broad regulator of T helper cell differentiation. *Curr. Opin. Immunol.* **23**, 598–604 (2011).
95. Oh, H. & Ghosh, S. NF- $\kappa$ B: roles and regulation in different CD4(+) T-cell subsets. *Immunol. Rev.* **252**, 41–51 (2013).
96. Aronica, M. A. *et al.* Preferential Role for NF- $\kappa$ B/Rel Signaling in the Type 1 But Not Type

- 2 T Cell-Dependent Immune Response In Vivo. *J. Immunol.* **163**, 5116–5124 (1999).
97. Corn, R. A., Hunter, C., Liou, H.-C., Siebenlist, U. & Boothby, M. R. Opposing Roles for RelB and Bcl-3 in Regulation of T-Box Expressed in T Cells, GATA-3, and Th Effector Differentiation. *J. Immunol.* **175**, 2102–2110 (2005).
  98. Hilliard, B. A. *et al.* Critical roles of c-Rel in autoimmune inflammation and helper T cell differentiation. *J. Clin. Invest.* **110**, 843–50 (2002).
  99. Balasubramani, A. *et al.* Modular utilization of distal cis-regulatory elements controls Ifng gene expression in T cells activated by distinct stimuli. *Immunity* **33**, 35–47 (2010).
  100. Ruan, Q. *et al.* Development of Foxp3(+) regulatory t cells is driven by the c-Rel enhanceosome. *Immunity* **31**, 932–40 (2009).
  101. Long, M., Park, S.-G., Strickland, I., Hayden, M. S. & Ghosh, S. Nuclear factor-kappaB modulates regulatory T cell development by directly regulating expression of Foxp3 transcription factor. *Immunity* **31**, 921–31 (2009).
  102. Zheng, Y. *et al.* Role of conserved non-coding DNA elements in the Foxp3 gene in regulatory T-cell fate. *Nature* **463**, 808–812 (2010).
  103. Isomura, I. *et al.* c-Rel is required for the development of thymic Foxp3+ CD4 regulatory T cells. *J. Exp. Med.* **206**, 3001–3014 (2009).
  104. Polesso, F., Sarker, M., Anderson, A., Parker, D. C. & Murray, S. E. Constitutive expression of NF-κB inducing kinase in regulatory T cells impairs suppressive function and promotes instability and pro-inflammatory cytokine production. *Sci. Rep.* **7**, 14779 (2017).
  105. Vasanthakumar, A. *et al.* The TNF Receptor Superfamily-NF-κB Axis Is Critical to Maintain Effector Regulatory T Cells in Lymphoid and Non-lymphoid Tissues. *Cell Rep.* **20**, 2906–2920 (2017).
  106. Oh, H. *et al.* An NF-κB Transcription-Factor-Dependent Lineage-Specific Transcriptional Program Promotes Regulatory T Cell Identity and Function. *Immunity* **47**, 450–465.e5 (2017).
  107. Annemann, M. *et al.* Atypical IκB proteins in immune cell differentiation and function. *Immunol. Lett.* **171**, 26–35 (2016).
  108. Schuster, M., Annemann, M., Plaza-sirvent, C. & Schmitz, I. Atypical I κ B proteins – nuclear modulators of NF- κ B signaling. *Cell Comun. Signal.* **11**, 1–11 (2013).
  109. Sun, S.-C. The non-canonical NF-κB pathway in immunity and inflammation. *Nat. Rev. Immunol.* **17**, 545–558 (2017).
  110. Fiorini, E. *et al.* Peptide-induced negative selection of thymocytes activates transcription of an NF-kappa B inhibitor. *Mol. Cell* **9**, 637–48 (2002).
  111. Hirotani, T. *et al.* The nuclear IκappaB protein IκappaBNS selectively inhibits lipopolysaccharide-induced IL-6 production in macrophages of the colonic lamina propria. *J. Immunol.* **174**, 3650–7 (2005).
  112. Schuster, M. *et al.* IκBNS Protein Mediates Regulatory T Cell Development via Induction of the Foxp3 Transcription Factor. *Immunity* **37**, 998–1008 (2012).
  113. Kuwata, H. *et al.* IκappaBNS inhibits induction of a subset of Toll-like receptor-dependent genes and limits inflammation. *Immunity* **24**, 41–51 (2006).
  114. Touma, M. *et al.* Functional role for I kappa BNS in T cell cytokine regulation as revealed by targeted gene disruption. *J. Immunol.* **179**, 1681–92 (2007).

115. Touma, M. *et al.* Impaired B cell development and function in the absence of I $\kappa$ BNS. *J. Immunol.* **187**, 3942–52 (2011).
116. Annemann, M. *et al.* I $\kappa$ BNS regulates murine Th17 differentiation during gut inflammation and infection. *J. Immunol.* **194**, 2888–98 (2015).
117. Kobayashi, S. *et al.* The Nuclear I $\kappa$ B Family Protein I $\kappa$ BNS Influences the Susceptibility to Experimental Autoimmune Encephalomyelitis in a Murine Model. *PLoS One* **9**, e110838 (2014).
118. Hosokawa, J. *et al.* I $\kappa$ BNS enhances follicular helper T-cell differentiation and function downstream of ASC12. *J. Allergy Clin. Immunol.* **140**, 288–291.e8 (2017).
119. Arnold, C. N. *et al.* A forward genetic screen reveals roles for Nfkbid, Zeb1, and Ruvbl2 in humoral immunity. *Proc. Natl. Acad. Sci. U. S. A.* **109**, 12286–93 (2012).
120. Killick-Kendrick, R. The life-cycle of *Leishmania* in the sandfly with special reference to the form infective to the vertebrate host. *Ann. Parasitol. Hum. Comparée* **65**, 37–42 (1990).
121. Sacks, D. & Noben-Trauth, N. The immunology of susceptibility and resistance to *Leishmania major* in mice. *Nat. Rev. Immunol.* **2**, 845–858 (2002).
122. Rossi, M. & Fasel, N. How to master the host immune system? *Leishmania* parasites have the solutions! *Int. Immunol.* **30**, 103–111 (2018).
123. Scott, P. & Novais, F. O. Cutaneous leishmaniasis: immune responses in protection and pathogenesis. *Nat. Rev. Immunol.* **16**, 581–592 (2016).
124. Belkaid, Y., Piccirillo, C. A., Mendez, S., Shevach, E. M. & Sacks, D. L. CD4+CD25+ regulatory T cells control *Leishmania major* persistence and immunity. *Nature* **420**, 502–507 (2002).
125. Mendez, S., Reckling, S. K., Piccirillo, C. A., Sacks, D. & Belkaid, Y. Role for CD4+ CD25+ Regulatory T Cells in Reactivation of Persistent Leishmaniasis and Control of Concomitant Immunity. *J. Exp. Med.* **200**, 201–210 (2004).
126. Titus, R., Gueiros-Filho, F., Freitas, L. de & Beverley, S. Development of a safe live *Leishmania* vaccine line by gene replacement. *PNAS* **92**, 10267–10271 (2009).
127. Ventura, A. *et al.* Restoration of p53 function leads to tumour regression in vivo. *Nature* **445**, 661–665 (2007).
128. Eckelhart, E. *et al.* A novel Ncr1-Cre mouse reveals the essential role of STAT5 for NK-cell survival and development. *Blood* **117**, 1565–1573 (2011).
129. Rubtsov, Y. P. *et al.* Regulatory T Cell-Derived Interleukin-10 Limits Inflammation at Environmental Interfaces. *Immunity* **28**, 546–558 (2008).
130. Sawada, S., Scarborough, J. D., Killeen, N. & Littman, D. R. A lineage-specific transcriptional silencer regulates CD4 gene expression during T lymphocyte development. *Cell* **77**, 917–929 (1994).
131. Kamphuis, E., Junt, T., Waibler, Z., Forster, R. & Kalinke, U. Type I interferons directly regulate lymphocyte recirculation and cause transient blood lymphopenia. *Blood* **108**, 3253–61 (2006).
132. Kiessling, R., Klein, E. & Wigzell, H. „Natural” killer cells in the mouse. I. Cytotoxic cells with specificity for mouse Moloney leukemia cells. Specificity and distribution according to genotype. *Eur. J. Immunol.* **5**, 112–117 (1975).
133. Chung, S., Kim, S.-H., Seo, Y., Kim, S.-K. & Lee, J. Y. Quantitative analysis of cell proliferation by a dye dilution assay: Application to cell lines and cocultures. *Cytom. Part A* **91**, 704–712

- (2017).
134. Chamakh-Ayari, R. *et al.* In vitro evaluation of a soluble Leishmania promastigote surface antigen as a potential vaccine candidate against human leishmaniasis. *PLoS One* **9**, 1–12 (2014).
  135. Dobin, A. *et al.* STAR: ultrafast universal RNA-seq aligner. *Bioinformatics* **29**, 15–21 (2013).
  136. Durinck, S. *et al.* BioMart and Bioconductor: a powerful link between biological databases and microarray data analysis. *Bioinformatics* **21**, 3439–3440 (2005).
  137. Liao, Y., Smyth, G. K. & Shi, W. featureCounts: an efficient general purpose program for assigning sequence reads to genomic features. *Bioinformatics* **30**, 923–930 (2014).
  138. Ádori, M. *et al.* Altered Marginal Zone B Cell Selection in the Absence of IκBNS. *J. Immunol.* [doi:10.4049/jimmunol.1700791](https://doi.org/10.4049/jimmunol.1700791) (2017).
  139. Sharma, R. & Das, A. IL-2 mediates NK cell proliferation but not hyperactivity. *Immunol. Res.* **66**, 151–157 (2018).
  140. Gotthardt, D. *et al.* NK cell development in bone marrow and liver: site matters. *Genes Immun.* **15**, 584–587 (2014).
  141. Deng, W. *et al.* Antitumor immunity. A shed NKG2D ligand that promotes natural killer cell activation and tumor rejection. *Science* **348**, 136–9 (2015).
  142. Shabrish, S., Gupta, M. & Madkaikar, M. A Modified NK Cell Degranulation Assay Applicable for Routine Evaluation of NK Cell Function. *J. Immunol. Res.* **2016**, 3769590 (2016).
  143. Eskelinen, E. L. Roles of LAMP-1 and LAMP-2 in lysosome biogenesis and autophagy. *Mol. Aspects Med.* **27**, 495–502 (2006).
  144. López-Soto, A., Bravo-San Pedro, J. M., Kroemer, G., Galluzzi, L. & Gonzalez, S. Involvement of autophagy in NK cell development and function. *Autophagy* **13**, 633–636 (2017).
  145. Mehlhop-Williams, E. R. & Bevan, M. J. Memory CD8+ T cells exhibit increased antigen threshold requirements for recall proliferation. *J. Exp. Med.* **211**, 345–56 (2014).
  146. Nechanitzky, R. *et al.* Transcription factor EBF1 is essential for the maintenance of B cell identity and prevention of alternative fates in committed cells. *Nat. Immunol.* **14**, 867–875 (2013).
  147. Chen, S., Liang, M. C., Chia, J. N., Ngsee, J. K. & Ting, A. E. Rab8b and its interacting partner TRIP8b are involved in regulated secretion in AtT20 cells. *J. Biol. Chem.* **276**, 13209–16 (2001).
  148. Yong, X. *et al.* Expression and purification of the SNX1/SNX6 complex. *Protein Expr. Purif.* **151**, 93–98 (2018).
  149. Belkaid, Y. *et al.* The role of interleukin (IL)-10 in the persistence of Leishmania major in the skin after healing and the therapeutic potential of anti-IL-10 receptor antibody for sterile cure. *J. Exp. Med.* **194**, 1497–506 (2001).
  150. Shih, Y. P., Sun, P., Wang, A. & Lo, S. H. Tensin1 positively regulates RhoA activity through its interaction with DLC1. *Biochim. Biophys. Acta - Mol. Cell Res.* **1853**, 3258–3265 (2015).
  151. Saoudi, A., Kassem, S., Dejean, A. & Gaud, G. Rho-GTPases as key regulators of T lymphocyte biology. *Small GTPases* **5**, (2014).
  152. Mercier, B. C. *et al.* NOD1 cooperates with TLR2 to enhance T cell receptor-mediated activation in CD8 T cells. *PLoS One* **7**, e42170 (2012).

153. Ghosh, S., Roy-Chowdhuri, S., Kang, K., Im, S.-H. & Rudra, D. The transcription factor Foxp1 preserves integrity of an active Foxp3 locus in extrathymic Treg cells. *Nat. Commun.* **9**, 4473 (2018).
154. Cadigan, K. M. & Waterman, M. L. TCF/LEFs and Wnt signaling in the nucleus. *Cold Spring Harb. Perspect. Biol.* **4**, (2012).
155. Li, Y. *et al.* Nucleo-cytoplasmic shuttling of PAK4 modulates  $\beta$ -catenin intracellular translocation and signaling. *Biochim. Biophys. Acta - Mol. Cell Res.* **1823**, 465–475 (2012).
156. van Loosdregt, J. *et al.* Canonical Wnt Signaling Negatively Modulates Regulatory T Cell Function. *Immunity* **39**, 298–310 (2013).
157. Hopf, F. W., Turner, P. R. & Steinhardt, R. A. Calcium misregulation and the pathogenesis of muscular dystrophy. *Subcell. Biochem.* **45**, 429–64 (2007).
158. Hosoi, E. *et al.* Expression of the ryanodine receptor isoforms in immune cells. *J. Immunol.* **167**, 4887–94 (2001).
159. Conrad, D. M., Hanniman, E. A., Watson, C. L., Mader, J. S. & Hoskin, D. W. Ryanodine receptor signaling is required for anti-CD3-induced T cell proliferation, interleukin-2 synthesis, and interleukin-2 receptor signaling. *J. Cell. Biochem.* **92**, 387–399 (2004).
160. Wiel, C. *et al.* Endoplasmic reticulum calcium release through ITPR2 channels leads to mitochondrial calcium accumulation and senescence. *Nat. Commun.* **5**, 3792 (2014).
161. Walker, L. S. K. Treg and CTLA-4: two intertwining pathways to immune tolerance. *J. Autoimmun.* **45**, 49–57 (2013).
162. Yamazaki, T. *et al.* CCR6 regulates the migration of inflammatory and regulatory T cells. *J. Immunol.* **181**, 8391–401 (2008).
163. Jones, B. A., Beamer, M. & Ahmed, S. Fractalkine/CX3CL1: a potential new target for inflammatory diseases. *Mol. Interv.* **10**, 263–70 (2010).
164. Wojdasiewicz, P. *et al.* The chemokine CX3CL1 (fractalkine) and its receptor CX3CR1: occurrence and potential role in osteoarthritis. *Arch. Immunol. Ther. Exp. (Warsz.)* **62**, 395–403 (2014).
165. Smith, S. L. *et al.* Overexpression of aurora B kinase (AURKB) in primary non-small cell lung carcinoma is frequent, generally driven from one allele and correlates with the level of genetic instability. *Br. J. Cancer* **93**, 719–729 (2005).
166. Kõivomägi, M. *et al.* Dynamics of Cdk1 substrate specificity during the cell cycle. *Mol. Cell* **42**, 610–23 (2011).
167. Draney, C., Hobson, A. E., Grover, S. G., Jack, B. O. & Tessem, J. S. Cdk5r1 Overexpression Induces Primary  $\beta$ -Cell Proliferation. *J. Diabetes Res.* **2016**, 6375804 (2016).
168. Mebarki, S. *et al.* De novo HAPLN1 expression hallmarks Wnt-induced stem cell and fibrogenic networks leading to aggressive human hepatocellular carcinomas. *Oncotarget* **7**, 39026–39043 (2016).
169. Klunker, S. *et al.* Transcription factors RUNX1 and RUNX3 in the induction and suppressive function of Foxp3+ inducible regulatory T cells. *J. Exp. Med.* **206**, 2701–15 (2009).
170. Olesin, E., Nayar, R., Saikumar-Lakshmi, P. & Berg, L. J. The Transcription Factor Runx2 Is Required for Long-Term Persistence of Antiviral CD8<sup>+</sup> Memory T Cells. *ImmunoHorizons* **2**, 251–261 (2018).

171. Stewart, M. P., Cabanas, C. & Hogg, N. T cell adhesion to intercellular adhesion molecule-1 (ICAM-1) is controlled by cell spreading and the activation of integrin LFA-1. *J. Immunol.* **156**, 1810–7 (1996).
172. Pallmer, K. & Oxenius, A. Recognition and Regulation of T Cells by NK Cells. *Front. Immunol.* **7**, 251 (2016).
173. Gerosa, F. *et al.* Reciprocal activating interaction between natural killer cells and dendritic cells. *J. Exp. Med.* **195**, 327–33 (2002).
174. Piccioli, D., Sbrana, S., Melandri, E. & Valiante, N. M. Contact-dependent Stimulation and Inhibition of Dendritic Cells by Natural Killer Cells. *J. Exp. Med.* **195**, 335–341 (2002).
175. Vitale, M. *et al.* NK-dependent DC maturation is mediated by TNFalpha and IFNgamma released upon engagement of the Nkp30 triggering receptor. *Blood* **106**, 566–71 (2005).
176. Martín-Fontecha, A. *et al.* Induced recruitment of NK cells to lymph nodes provides IFN-γ for TH1 priming. *Nat. Immunol.* **5**, 1260–1265 (2004).
177. Rabinovich, B. A. *et al.* Activated, But Not Resting, T Cells Can Be Recognized and Killed by Syngeneic NK Cells. *J. Immunol.* **170**, 3572–3576 (2003).
178. Waggoner, S. N., Cornberg, M., Selin, L. K. & Welsh, R. M. Natural killer cells act as rheostats modulating antiviral T cells. *Nature* **481**, 394–398 (2012).
179. Lang, P. A. *et al.* Natural killer cell activation enhances immune pathology and promotes chronic infection by limiting CD8+ T-cell immunity. *Proc. Natl. Acad. Sci. U. S. A.* **109**, 1210–5 (2012).
180. Soderquest, K. *et al.* Monocytes control natural killer cell differentiation to effector phenotypes. *Blood* **117**, 4511–4518 (2011).
181. Crouse, J. *et al.* Type I interferons protect T cells against NK cell attack mediated by the activating receptor NCR1. *Immunity* **40**, 961–73 (2014).
182. Xu, H. C. *et al.* Type I interferon protects antiviral CD8+ T cells from NK cell cytotoxicity. *Immunity* **40**, 949–60 (2014).
183. Chiang, S. C. *et al.* Surface CD107a / LAMP-1 protects natural killer cells from degranulation-associated damage. **122**, 1411–1419 (2016).
184. Thompson, T. W. *et al.* Endothelial cells express NKG2D ligands and desensitize antitumor NK responses. *Elife* **6**, (2017).
185. Male, V. & Brady, H. J. M. Murine thymic NK cells: A case of identity. *Eur. J. Immunol.* **47**, 797–799 (2017).
186. Ribeiro, V. S. G. *et al.* Cutting edge: Thymic NK cells develop independently from T cell precursors. *J. Immunol.* **185**, 4993–7 (2010).
187. Sitnicka, E. Early cellular pathways of mouse natural killer cell development. *J. Innate Immun.* **3**, 329–336 (2011).
188. Adli, M. The CRISPR tool kit for genome editing and beyond. *Nat. Commun.* **9**, 1911 (2018).
189. Abel, A. M., Yang, C., Thakar, M. S. & Malarkannan, S. Natural Killer Cells: Development, Maturation, and Clinical Utilization. *Front. Immunol.* **9**, 1869 (2018).
190. Narni-Mancinelli, E., Vivier, E. & Kerdiles, Y. M. The ‘T-cell-ness’ of NK cells: unexpected similarities between NK cells and T cells. *Int. Immunol.* **23**, 427–431 (2011).

191. Bennisstein, S. B. Unraveling Natural Killer T-Cells Development. *Front. Immunol.* **8**, 1950 (2017).
192. Crinier, A. *et al.* High-Dimensional Single-Cell Analysis Identifies Organ-Specific Signatures and Conserved NK Cell Subsets in Humans and Mice. *Immunity* **0**, 971–986 (2018).
193. LeBien, T. W. & Tedder, T. F. B lymphocytes: how they develop and function. *Blood* **112**, 1570–80 (2008).
194. Medvedovic, J., Ebert, A., Tagoh, H. & Busslinger, M. Pax5: A Master Regulator of B Cell Development and Leukemogenesis. *Adv. Immunol.* **111**, 179–206 (2011).
195. Li, R. *et al.* Dynamic EBF1 occupancy directs sequential epigenetic and transcriptional events in B-cell programming. *Genes Dev.* **32**, 96–111 (2018).
196. Vilagos, B. *et al.* Essential role of EBF1 in the generation and function of distinct mature B cell types. *J. Exp. Med.* **209**, 775–92 (2012).
197. Treiber, N., Treiber, T., Zocher, G. & Grosschedl, R. Structure of an Ebf1:DNA complex reveals unusual DNA recognition and structural homology with Rel proteins. *Genes Dev.* **24**, 2270–5 (2010).
198. Das, J. *et al.* A critical role for NF-kappa B in GATA3 expression and TH2 differentiation in allergic airway inflammation. *Nat. Immunol.* **2**, 45–50 (2001).
199. MaruYama, T. *et al.* Control of IFN- $\gamma$  production and regulatory function by the inducible nuclear protein I $\kappa$ B- $\zeta$  in T cells. *J. Leukoc. Biol.* **98**, 385–393 (2015).
200. Totzke, G. *et al.* A novel member of the I $\kappa$ B family, human I $\kappa$ B-zeta, inhibits transactivation of p65 and its DNA binding. *J. Biol. Chem.* **281**, 12645–54 (2006).
201. Zeng, H., Zhang, R., Jin, B. & Chen, L. Type 1 regulatory T cells: a new mechanism of peripheral immune tolerance. *Cell. Mol. Immunol.* **12**, 566–571 (2015).
202. Dechend, R. *et al.* The Bcl-3 oncoprotein acts as a bridging factor between NF- $\kappa$ B/Rel and nuclear co-regulators. *Oncogene* **18**, 3316–3323 (1999).
203. Wang, V. Y.-F. *et al.* The transcriptional specificity of NF- $\kappa$ B dimers is coded within the  $\kappa$ B DNA response elements. *Cell Rep.* **2**, 824–39 (2012).
204. Franzoso, G. *et al.* Critical roles for the Bcl-3 oncoprotein in T cell-mediated immunity, splenic microarchitecture, and germinal center reactions. *Immunity* **6**, 479–90 (1997).
205. Schwarz, E. M., Krimpenfort, P., Berns, A. & Verma, I. M. Immunological defects in mice with a targeted disruption in Bcl-3. *Genes Dev.* **11**, 187–97 (1997).
206. Szabo, S. J. *et al.* A novel transcription factor, T-bet, directs Th1 lineage commitment. *Cell* **100**, 655–69 (2000).
207. Liao, W., Lin, J.-X., Wang, L., Li, P. & Leonard, W. J. Modulation of cytokine receptors by IL-2 broadly regulates differentiation into helper T cell lineages. *Nat. Immunol.* **12**, 551–9 (2011).
208. Boyman, O. & Sprent, J. The role of interleukin-2 during homeostasis and activation of the immune system. *Nat. Rev. Immunol.* **12**, 180–190 (2012).
209. Scott, P., Natovitz, P., Coffman, R. L., Pearce, E. & Sher, A. Immunoregulation of cutaneous leishmaniasis. T cell lines that transfer protective immunity or exacerbation belong to different T helper subsets and respond to distinct parasite antigens. *J. Exp. Med.* **168**, 1675–84 (1988).

210. Heinzl, F. P., Sadick, M. D., Holaday, B. J., Coffman, R. L. & Locksley, R. M. Reciprocal expression of interferon gamma or interleukin 4 during the resolution or progression of murine leishmaniasis. Evidence for expansion of distinct helper T cell subsets. *J. Exp. Med.* **169**, 59–72 (1989).
211. Müller, A. J. *et al.* CD4+ T cells rely on a cytokine gradient to control intracellular pathogens beyond sites of antigen presentation. *Immunity* **37**, 147–57 (2012).
212. Liew, F. Y., Hale, C. & Howard, J. G. Immunologic regulation of experimental cutaneous leishmaniasis. V. Characterization of effector and specific suppressor T cells. *J. Immunol.* **128**, 1917–22 (1982).
213. Peters, N. C. *et al.* Chronic Parasitic Infection Maintains High Frequencies of Short-Lived Ly6C+CD4+ Effector T Cells That Are Required for Protection against Re-infection. *PLoS Pathog.* **10**, e1004538 (2014).
214. Miles, S. A., Conrad, S. M., Alves, R. G., Jeronimo, S. M. B. & Mosser, D. M. A role for IgG immune complexes during infection with the intracellular pathogen *Leishmania*. *J. Exp. Med.* **201**, 747–754 (2005).
215. Anderson, C. F., Oukka, M., Kuchroo, V. J. & Sacks, D. CD4+CD25–Foxp3– Th1 cells are the source of IL-10–mediated immune suppression in chronic cutaneous leishmaniasis. *J. Exp. Med.* **204**, 285–297 (2007).
216. Kane, M. M. & Mosser, D. M. The role of IL-10 in promoting disease progression in leishmaniasis. *J. Immunol.* **166**, 1141–7 (2001).
217. Bourreau, E. *et al.* Intralesional regulatory T-cell suppressive function during human acute and chronic cutaneous leishmaniasis due to *Leishmania guyanensis*. *Infect. Immun.* **77**, 1465–74 (2009).
218. Campanelli, A. P. *et al.* CD4<sup>+</sup> CD25<sup>+</sup> T Cells in Skin Lesions of Patients with Cutaneous Leishmaniasis Exhibit Phenotypic and Functional Characteristics of Natural Regulatory T Cells. *J. Infect. Dis.* **193**, 1313–1322 (2006).
219. Yurchenko, E. *et al.* CCR5-dependent homing of naturally occurring CD4+ regulatory T cells to sites of *Leishmania major* infection favors pathogen persistence. *J. Exp. Med.* **203**, 2451–2460 (2006).
220. Suffia, I. J., Reckling, S. K., Piccirillo, C. A., Goldszmid, R. S. & Belkaid, Y. Infected site-restricted Foxp3+ natural regulatory T cells are specific for microbial antigens. *J. Exp. Med.* **203**, 777–788 (2006).
221. Li, J., Tan, J., Martino, M. M. & Lui, K. O. Regulatory T-Cells: Potential Regulator of Tissue Repair and Regeneration. *Front. Immunol.* **9**, 585 (2018).
222. Stebut, E. von, Belkaid, Y., Jakob, T., Sacks, D. L. & Udey, M. C. Uptake of *Leishmania major* Amastigotes Results in Activation and Interleukin 12 Release from Murine Skin–derived Dendritic Cells: Implications for the Initiation of Anti-*Leishmania* Immunity. *J. Exp. Med.* **188**, 1547–1552 (1998).
223. Iezzi, G. *et al.* Lymph node resident rather than skin-derived dendritic cells initiate specific T cell responses after *Leishmania major* infection. *J. Immunol.* **177**, 1250–6 (2006).
224. Arpaia, N. *et al.* A Distinct Function of Regulatory T Cells in Tissue Protection. *Cell* **162**, 1078–1089 (2015).
225. Li, M. O. & Rudensky, A. Y. T cell receptor signalling in the control of regulatory T cell

- differentiation and function. *Nat. Rev. Immunol.* **16**, 220–33 (2016).
226. Dolmetsch, R. E., Lewis, R. S., Goodnow, C. C. & Healy, J. I. Differential activation of transcription factors induced by Ca<sup>2+</sup> response amplitude and duration. *Nature* **386**, 855–858 (1997).
227. Konopacki, C., Pritykin, Y., Rubtsov, Y., Leslie, C. S. & Rudensky, A. Y. Transcription factor Foxp1 regulates Foxp3 chromatin binding and coordinates regulatory T cell function. *Nat. Immunol.* **20**, (2019).
228. Mesquita, I. *et al.* The impact of IL-10 dynamic modulation on host immune response against visceral leishmaniasis. *Cytokine* **112**, 16–20 (2018).

## 9. Declaration of originality

### Ehrenerklärung

Ich versichere hiermit, dass ich die vorliegende Arbeit ohne unzulässige Hilfe Dritter und ohne Benutzung anderer als der angegebenen Hilfsmittel angefertigt habe; verwendete fremde und eigene Quellen sind als solche kenntlich gemacht.

Ich habe insbesondere nicht wissentlich:

- Ergebnisse erfunden oder widersprüchlich Ergebnisse verschwiegen,
- statistische Verfahren absichtlich missbraucht, um Daten in ungerechtfertigter Weise zu interpretieren,
- fremde Ergebnisse oder Veröffentlichungen plagiiert,
- fremde Forschungsergebnisse verzerrt wiedergegeben.

Mir ist bekannt, dass Verstöße gegen das Urheberrecht Unterlassungs- und Schadensersatzansprüche des Urhebers sowie eine strafrechtliche Ahndung durch die Strafverfolgungsbehörden begründen kann.

Ich erkläre mich damit einverstanden, dass die Arbeit ggf. mit Mitteln der elektronischen Datenverarbeitung auf Plagiate überprüft werden kann.

Die Arbeit wurde bisher weder im Inland noch im Ausland in gleicher oder ähnlicher Form als Dissertation eingereicht und ist als Ganzes auch noch nicht veröffentlicht.

Magdeburg 19.02.2019

(Unterschrift)